ON TREADMILL AUTOMATION AND PHYSIOLOGICAL CONTROL SYSTEMS

A DISSERTATION
SUBMITTED TO THE DEPARTMENT OF MECHANICAL ENGINEERING
OF THE UNIVERSITY OF GLASGOW
FOR THE DEGREE OF
DOCTOR OF PHILOSOPHY

By
Olatunbosun Oluwatoyin Ajayi
November 2005

ABSTRACT

This thesis deals with a new approach to Treadmill Automation and Physiological Control Systems that will serve as a platform for enhanced rehabilitation therapy, and will open up and facilitate a major new area of research in physiological control systems.

On treadmill automation, the investigation focussed on the feasibility of a low-cost non-contact position control system with the aim of maintaining a subject at a prescribed position during a treadmill training exercise in order to ensure safety at all times. The development of an automatic speed control for the treadmill was first carried out using an identified model for the treadmill motor dynamics (response from speed command to actual belt speed). Subsequently, the positioning control system was designed and tested. The fundamental limitations to treadmill automation performance include low bandwidth and long time delays of the hardware (treadmill and ultrasonic sensor). Interactions between natural human control and the position controller, and spontaneous variability of human movement due to body oscillations and swaying, are discussed.

On physiological control systems, we considered two key variables - the heart rate and oxygen uptake. The purpose of this is to develop a means of controlling exercise intensity during treadmill exercise. On the control of heart rate, a model of heart rate response to changes in speed was obtained via the system identification method. Thereafter, a heart rate controller was developed, tested, and evaluated on three healthy subjects during treadmill exercise. The results of the experiments demonstrated that the developed heart rate controller is superior to the in-built treadmill heart rate controller.

A novel system is developed for the control of oxygen uptake, and is thus presented. The system proved that it is possible to control exercise intensity using the level of oxygen uptake during moderate exercise. The results of this work demonstrate that a linear first order model is able to sufficiently capture the complex dynamics of oxygen uptake during treadmill exercise. A controller was developed using this model and tested on healthy subjects. Six healthy active subjects participated completely in the tests. The results of the tests with these subjects establish the robustness of the controllers to inter-subject variability. Furthermore, the controller was refined and tuned to improve the performance of the control signal (treadmill speed). This was achieved by designing a controller that incorporated a pre-filter in the system. The results of the experiments using this set-up with the same set of healthy subjects show a significant improvement on the control signal (smoother treadmill speed).

ACKNOWLEDGEMENTS

I owe a great debt to all the people who have helped me during my PhD studies some of whom I may not mention their names categorically, but their contributions are immense.

First and foremost, I wish to thank my supervisor Prof Ken Hunt for his numerous support, advice, unique guidance and motivation during my PhD. My sincere thanks also goes to Dr Henrik Gollee for his help and assistance at most times and most especially during system development stages. Sincere appreciation goes to my colleagues (Lindsay, Sylvie, Chiara, ...) and my subjects whose participation are mostly valued. I used to call them my dear valued subjects!

Without the support of the Universities UK and the Faculty of Engineering, of the University of Glasgow through their ORS Award and Faculty Scholarship respectively, this research would not have been carried out. I also acknowledge the contributions of the members of the CRE group and the Department.

Finally, to my family and friends and the ones I met while doing this research work I say a big thank you to you all; and of course to God be all the glory forever ad maiorem Dei gloriam.

Contents

List of Tables

List of Figures

1 INTRODUCTION

Rehabilitation therapy is a means of improving the health and quality of life of a disabled or impaired person because there is currently no cure for disability or impairment. Furthermore, a disabled person has limited physical activity, and this could put them at risk of other medical conditions. Thus, an optimal (or valid) exercise intensity that could maintain or increase physical activity is essential.

Treadmill exercise training is commonly used for rehabilitation therapy ([41], [31] and [38]). When used as rehabilitation therapy, it generally requires two or more therapists to provide assistance and to ensure the safety of the patient. This is necessary because a treadmill can lead to injury without certain safety precautions [2]. The latter paper further discusses the potential risks for a patient to lose balance and fall when using treadmills. Furthermore, the time and effort of the therapist have cost implications (health costs). However, there is no such system in place for rehabilitation. Thus, an automatic treadmill system may provide a means of solving the problems of safety, labour and time costs, and reduces the variability of therapy provided by different therapists. This system will involve the use of a comparatively low-cost non-contact sensor which measures the relative position of the subject and provide a means of controlling the position of a person during treadmill exercise and therapy.

In addition, there is interplay between exercise and physiological state of a person, and the need to provide a secondary benefit in the form of cardiopulmonary fitness, or to enhance the level of fitness of treadmill users. Similarly, muscles require energy during exercise and even at rest, and the energy requirement depends on the intensity of the exercise and on each individual's state and capacity. To measure exercise intensity the heart rate is commonly used while maximal oxygen uptake is a fundamental measure of

exercise physiology and represents a measure of aerobic fitness. Therefore, the control of these physiological variables (heart rate and oxygen uptake) may provide a means of specifying an unambiguous level of exercise intensity that is most appropriate for each individual. This would enable the level of the activity to be measured as a proportion of the user/subject's fitness. Thus, a physiological control system can provide a platform for improved fitness, therapy for patients (spinal cord injury, stroke, paraplegic, hemiplegics, etc) and also for recreational exercise and sports (i.e. for increasing activity levels in daily life, improving the quality of life, and also enhancing the conditions of well-being).

At present there is no low-cost non-contact automatic position control system. Similarly, there is no closed-loop feedback control system for oxygen uptake ($\dot{V}O_2$) even though there are existing heart rate (HR) controllers. However, most commercially available HR control systems are slow. Therefore, this thesis focuses on investigating the feasibility of treadmill automation and physiological control systems (real-time closed-loop control of HR and $\dot{V}O_2$) using a model-based (analytical) feedback control approach.

The key benefits of this research are to:

1. Enhance rehabilitation therapy by improving patient safety and confidence during therapy.
2. Improve the efficiency of rehabilitation by reducing the load on therapy staff, thus reducing overall costs.
3. Patients may be trained in a more reproducible and reliable way than with current approaches.
4. More patients may be more likely to reach higher levels of mobility.
5. Improved mobility and training by providing secondary benefits to the patient's cardiopulmonary fitness and general health.
6. Provide understanding of physiological control systems and their benefits and possible applications.

1.1 Aims and Objectives

The main aim of my thesis is to investigate the feasibility of novel feedback controllers for treadmill automation (a non-contact position system), and real-time control of HR and $\dot{V}O_2$.

The objectives of this thesis are to investigate:

1. the potential of a novel control of position and thus speed;
2. the accurate control of heart rate and to further compare it with an in-built controller;
3. the feasibility of accurate control of $\dot{V}O_2$

during treadmill exercise and training.

All these involve:

- System development: using a non-contact position measuring sensor and other instruments (e.g., a breath-by-breath measuring device), and interfacing it with a treadmill system, and to a computer;
- Modelling, simulation, analysis, and control: using the system identification method for modelling, and analytical (model-based) feedback control techniques to control the identified variables during treadmill exercise training;
- Experimental verification, validation, implementing and testing in a real-time environment.

The experimental work described in this thesis was carried out with healthy volunteer subjects. These experiments were reviewed and approved by the ethics committee of the Faculty of Biomedical and Life Sciences, University of Glasgow. Subjects read and signed the subject consent form and completed the medical history questionnaire before the experiment.

The goal of each controller is to ensure that the system is maintained at a pre-specified level, position or profile, despite disturbances acting on the system. The requirement of the control law is therefore firstly to stabilise the system and secondly to achieve the required performance.

1.2 Thesis Contributions

The novelty and originality of this thesis consist of the following:

- Provide an understanding of treadmill position control and its limitations.
- A faster response of the heart rate controller compared with the in-built controller is achieved.
- A novel and original contribution to real-time control of oxygen uptake during exercise is achieved. This extends the use of the empirical model often developed in the realm of physiology for a feedback control system.
- The model identification/validation approach is novel for the selection of an appropriate model that captures $\dot{V}O_2$ dynamics and this is a distinct contribution to knowledge in exercise physiology.
- Accurately control $\dot{V}O_2$ levels during moderate treadmill exercise.
- Serve as a translational feasibility study that could be deployed, applied and developed into potential therapies in clinical sciences.

The overall structure of the thesis will follow.

1.3 The Scope of this Thesis

The thesis is in seven chapters and is organized as follows:

In the first chapter, the background to the work is described and the objectives introduced. The second chapter gives a detailed survey of relevant literature covering the background theories and research context as it relates to treadmill automation, heart rate and oxygen uptake. The next chapter describes the experimental set-up and the measuring equipment used, the choice of a position measuring sensor and the software utilised. This chapter also consists of the methodology (i.e., modelling techniques and controller design method) applied during the experimental studies.

In chapter 4, an investigation of the feasibility of treadmill automation is presented. This study covers the treadmill dynamics identification and modelling which was used to develop a speed controller, and which was cascaded into the position control system in order to achieve treadmill automation. The chapter further presents the results of the experiments and discusses the results. Furthermore, the chapter concludes with discussions on the limitations of the system.

Chapter 5 describes experiments that were undertaken to build a heart rate control for normal subjects. This chapter also gives details of core approaches for manipulating the HR data for a linear model. It builds on the model to design and develop the HR controller which was implemented on normal subjects. The controller was then compared with the in-built treadmill controller for a constant, step and a series of step reference HR inputs, and the results were presented. The chapter finishes with discussion and conclusions.

Chapter 6 presents the experiments on the control of oxygen uptake. A review of the experimental procedure and measurement is given as is the processing of raw data. It also focuses on algorithm design. A linear model was derived from the open loop identification experiments. The model was used for designing a controller which was implemented on a group of healthy subjects over a series of experiments. The $\dot{V}O_2$ controller was further

refined and improved by designing a controller that incorporates a pre-filter. The results of experiments on control of $\dot{V}O_2$ are presented and discussed, and conclusions are drawn.

General discussion, conclusions and outlook are covered in the last chapter.

2 LITERATURE REVIEW

This chapter covers the background theory, relevant literature and publication on treadmill automation, heart rate and $\dot{V}O_2$. It also contains the literature survey and review on treadmill automation and control, and on control of physiological variables which comprises of HR and $\dot{V}O_2$ control systems.

2.1 Background Theories

Here, consideration is given to the relevant theories and issues that could affect our methodology, control design and results of this research. The discussion covers human locomotion and biomechanics, i.e., walking, running, transition between walking and running, running economy, and spontaneity in human locomotion. In addition, cardio-respiratory responses to exercise comprising $\dot{V}O_2$ and its dynamics and components, maximum oxygen uptake, variability during exercises, heart rate variability and breath-by-breath variability, and finally the relationship between oxygen uptake, heart rate and work-rate/speed were considered.

2.1.1 Human Locomotion and Biomechanics

Locomotion is a primary form of exercise [73] and could be in the form of walking and running. It has proved useful for both healthy and disabled people.

The relationship between human locomotion and biomechanics have been widely researched [72]; for a comprehensive review and understanding of the biomechanics of

running see Novacheck [87]. This paper compares walking and sprinting, discusses gait cycle and the impact of changes in velocity on running, and the alteration in movement strategies. It also examines economy of motion, the effect of inter-individual variability in walking and running and its impact on aerobic demand. The paper stated that each individual walks at his/her most economic speed. It also identified that a speed of 1.3 m/s results in minimum aerobic demand and also that a speed range of 1.1 - 1.4 m/s results in variability of approximately 15% difference in walking speed without compromising efficiency. It went on further to say that the economy of movement is still not well understood except that the choice of stride length and cadence, muscle shortening velocity and mechanical powers relationships are involved. The paper concludes that it is uneconomical to walk at speeds exceeding 3 m/s.

Walking

Walking is fundamental to life and living and is also a natural part of life [73], [69]. It involves shoulders and pelvis rotation in opposite directions while the trunk motion contributes significantly to this movement function [69]. Thus, during walking and also running there is a whole body movement involving the co-ordination of arms and legs, and the upper and lower extremities. The extremities also contribute to the linear and angular momentum during running.

Furthermore, there is also intra-subject variability during walking and also running, while the ground reaction and movement of centre of gravity caused by body weight and its distribution during motion [49], [20] have implications on walking and running.

Transition between walking and running

There is a preferred walking speed above which individuals normally switch to a running gait [73], [64]. This transition to running represents a bifurcation and has been identified by different researchers.

Furthermore, the extension of the gait beyond the normal transition speed leads to a higher metabolic rate than in the normal gait [116], [76], [80].

The existence of a transition between different speeds implies that there is a fundamental decision to be considered in this research so as to avoid mode confusion, interaction and coupling.

Running

Running is a type of locomotion consisting of alternating support and non-support phases [57]. The lower extremity supports the body against gravity during running and also provides a means to overcome inertia, and accelerates the centre of gravity against resistance [57], [3].

During running both stride length and stride frequency are adjusted to compensate for an increase in running speed [119]. Cavanagh and Kram [19] reported that humans' stride frequency increases more at higher speed and that stride length reaches its maximum at a higher speed of running. The paper also stated that there is a linear relationship between stride length and running speed at 3.2 - 4.2 m/s. Furthermore, the paper explains that the exact combination of stride length and stride frequency at a certain speed may be accounted for by differences in leg length, hip flexion, breathing rate and state of fatigue. These may have interesting implications in our research.

Running economy

Running economy is the aerobic $\dot{V}O_2$ demand of running at a given sub-maximal running speed in individuals with comparable value of maximal $\dot{V}O_2$ [80]. Williams and Cavanagh [118] suggested that the variation in running economy is due to biomechanical features of the running pattern. Other possible explanations for running efficiency is the running stride, muscle contraction or the biomechanical factors such as differences in limb lengths, body weight distributions etc. Running economy involves a combination

of stride length, stride frequency and the speed; Billat et al [14] hypothesised that a stride frequency lower than optimal may affect $\dot{V}O_2$.

As running speed increases, $\dot{V}O_2$ per stride length remains independent of body mass while on the contrary, a mass-specific $\dot{V}O_2$ remains proportional to stride frequency [40]. Thus, the primary factor determining running economy is the energetic cost of generating muscle force needed to raise and support the body against gravity during running [102].

In addition, various physiological factors (age, gender, body weight, maximal aerobic power and muscle fibre distribution) and environmental factors (air resistance and body temperature) influence the running economy [65].

There is also a coupling between respiration and running, which implies that stride length and breathing frequency may affect running economy, and this raises some interesting implications. Therefore, running economy and efficiency may have implications on HR and $\dot{V}O_2$ control because of the effect of stride length (different stride lengths at different speed conditions), different running strategy and individual differences.

Spontaneity

Adjusting to speed fluctuation may result in spontaneity in running, because each person/user accelerates or decelerates depending on the magnitude of the change in speed. This may be compounded when one accelerates from walking to running or decelerates from running to walking. In addition, there is also the effect of inertia force due to acceleration/deceleration on this reaction.

The impulse or change to acceleration is often more important than sustained acceleration during human motion and this normally requires the use of one's visual and vestibular systems, with some contribution to the forces by the rest of the human body. The study conducted by Varraine et al [104] focuses on the co-ordination of stride length

and the mechanism underlying intentional stride length during different walking speeds.

Furthermore, treadmills cannot distinguish between constant velocity locomotion and constant velocity motion on a stationary surface because they both have similar characteristics [79]. However, when a person/user accelerates to run, the physics of treadmill locomotion is different [79]. When the user moves forward, the belt moves in the opposite direction, i.e. backward. Hence the belt motion imparts an inertia force on the user.

2.1.2 Cadiorespiratory Response to Exercise

As exercise begins, the blood flow to the muscles increases, and as the intensity of the exercise increases, the body pumps more blood to the muscles to maintain the increase in energy, thus maintaining a state of homeostasis balance [106].

During exercise, the body's physiological mechanisms respond to the interaction of physiological mechanisms that enable the cardiovascular and respiratory systems to support the increased energy demands of contracting muscles. This results in an instantaneous increase in the requirement of oxygen consumption by the active muscles.

Oxygen uptake, $\dot{V}O_2$, is the amount of oxygen utilized by the body's metabolic process in a given time, and it is expressed in litres per minute at standard conditions of temperature, pressure and free water vapour (STPD) [106]. At rest $\dot{V}O_2$ is approximately 0.3L/min and could reach about 3-5L/min during aerobic exercise.

$\dot{V}O_2$ kinetics :

This depends on the work rate of an exercise for each person/individual and it follows a time course. Generally, it takes about 3 minutes to reach a steady state of $\dot{V}O_2$ for a normal individual at a constant work rate, if the exercise is below the Anaerobic Threshold (AT) [9], [114][1].

As work rates increase during exercise tests, the rate of $\dot{V}O_2$ also increases [107]. If the subject is not limited by disease or fatigue, the $\dot{V}O_2$ continues to increase with a growing work rate until it plateaus. At that time, if a further increase in work rate does not result in increased $\dot{V}O_2$, then the maximal $\dot{V}O_2$ is reached. The term $\dot{V}O_2$ peak occurs mostly in subjects with disability.

Phases :

There are three time-related phases (Figure 2.1) for $\dot{V}O_2$, carbon-dioxide output, $\dot{V}CO_2$, and ventilation, $\dot{V}_E$, responses following the start of constant work exercise from rest [113], [106], [34], [89]:

Phase I (Cardiodynamic Phase): Is the immediate increase in gas exchange at the start of exercise and lasts for about 15 seconds. It is coupled by the immediate increase in cardiac output, CO, due to the increase in pulmonary blood flow at the onset of exercise.

Phase II (Cell Respiration): Starts about fifteen seconds after the onset of exercise until the third minute of exercise. If the exercise is below AT, the steady state in $\dot{V}O_2$ is achieved within three minutes. On the contrary, if the exercise is above the AT, the steady state in $\dot{V}O_2$ is delayed before the subject starts to fatigue.

Phase III (Steady-State): Starts three minutes after exercise begins, and reflects the start of $\dot{V}O_2$ steady state period if the work rate is below AT. In this third phase, a steady state is reached between internal and external respiration [111].

[1] AT is defined as the level of exercise $\dot{V}O_2$ above which aerobic energy production is supplemented by anaerobic mechanisms (i.e. the $\dot{V}O_2$ at which the anaerobic supplement of the aerobic energy exchange begins by production of blood lactate) [103].

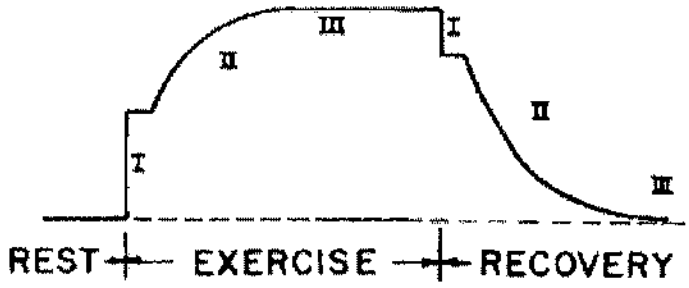

Figure 2.1: Exercise phases at constant work load, source: [106]

$\dot{V}O_2$ time delay :
At the start of exercise, there is normally a steep increase in both $\dot{V}O_2$ and $\dot{V}CO_2$ responses following an abrupt increase in pulmonary blood flow and this is due to an immediate increase in HR and Stroke Volume (SV). The delay for $\dot{V}O_2$ and $\dot{V}CO_2$ to respond to a step input is approximately fifteen seconds [106]. After this fifteen seconds delay, $\dot{V}O_2$ and $\dot{V}CO_2$ increase further with $\dot{V}CO_2$ increasing more slowly than $\dot{V}O_2$ [106].

Similarly, when a progressive increase in work rate is initiated, a delay occurs before $\dot{V}O_2$ begins to increase in a linear fashion. These delays will be considered in the controller design. Wasserman et al [106] assert that this kinetic delay is equal to the time constant of $\dot{V}O_2$ following a stepwise increase and is between half and three quarters of a minute. Furthermore, the time constant for $\dot{V}O_2$ at work intensities below the AT is thirty-five to forty-five seconds in healthy subjects [106].

$\dot{V}O_2$ response to different exercise intensities :
Different exercise intensities elicit different oxygen uptake profiles [114].

HR stability :

HR increases from rest (rest value) as the level of exercise intensity increases with time, and the relationship between HR and exercise duration for a specific level of exercise intensity can be found in [92]. Power & Howley [92] also indicated that HR reaches a steady state within three to five minutes at a specific exercise intensity if the exercise is aerobic (below the lactate threshold). With a further increase in work rate, it takes the heart rate about one to three minutes to reach a new steady state. Furthermore, the more intense the exercise the greater the time it takes to attain a new steady state.

Anaerobic Threshold :

Actively contracting muscles obtain adenosine triphosphate (ATP) from glucose stored in the blood stream and the breakdown of glycogen stored in the muscles. Lactic acid starts to accumulate in the muscles once you start operating above your anaerobic threshold. Thus, the lactate (or anaerobic) threshold, LT, is the highest exercise oxygen uptake that can be achieved without a sustained increase in blood and muscle lactate concentration [108], [13], [101] and [12]. At heavy exercise which is above LT, there is a linear and nonlinear characteristic of oxygen uptake kinetics [9], while exercise at below the LT level is regarded as a moderate, or aerobic exercise. Exercising at this moderate level is safe and effective for exercise training and could be sustained for a prolonged exercise period.

Maximal oxygen uptake, $\dot{V}O_{2_{max}}$:

Maximal oxygen uptake or consumption is the maximal rate at which oxygen can be taken up, distributed, and used by the body in the performance of work [10], [109]. Graphically and mathematically, it is seen as the point at which oxygen consumption plateaus, and shows only minimal or no further increases with additional workload. It has also been referred to as maximal aerobic power. It is frequently used as an indicator of an individual's cardio-respiratory fitness [10], [84], [110], [5], [32], [68] and it reflects a person's capacity to aerobically use ATP. $\dot{V}O_{2_{max}}$, thus varies between individuals [73].

$\dot{V}O_{2_{max}}$ is dependent upon the proper functioning of three important systems within the body:

1. The respiratory system, which takes up oxygen from inspired air and transports it into the blood;

2. The cardiovascular system, that pumps and distributes this oxygenated blood throughout the body tissues, and;

3. The musculoskeletal system, which uses this oxygen to convert stored substrates into work and heat during physical activity [107].

Maximal aerobic power is assessed for many reasons, ranging from an assessment of cardiovascular function in people (e.g. cardiac patient) to the prediction of performance of sporting people (e.g. athletes) and for exercise prescription [10]. However, it is desirable to have an accurate measurement of $\dot{V}O_2$ in clinical evaluations rather than an estimate, thus, an actual measurement of $\dot{V}O_{2_{max}}$ is necessary. In addition, exercise intensity is normally prescribed as a proportion of $\dot{V}O_{2_{max}}$.

Various researchers have argued about the existence of $\dot{V}O_{2_{max}}$ and what determines it [84], [10]. Notwithstanding, it has also been argued that in order to accept a $\dot{V}O_2$ level as maximum several other criteria should also be met [10], [4], [73]. Age, gender, training and altitude also affect $\dot{V}O_{2_{max}}$ [83]. It is also interesting to note that different values have been obtained for the same individual when the different protocols have been used [73]. Peak $\dot{V}O_2$ occurs if a person's predicted $\dot{V}O_{2_{max}}$ is limited by the subject's muscle and not its heart and lungs.

$\dot{V}O_2$ transport components :
The dynamics of $\dot{V}O_2$ are determined by the complex interaction of pulmonary gas exchange, cardiac output, limb blood flow, oxygen diffusion and rates of mitochondrial oxygen consumption. The $\dot{V}O_2$ components include heart rate, stroke volume, arteriovenuous oxygen difference and cardiac output.

Heart Rate, HR :

The heart rate is an involuntary action controlled by the balance of stimulation coming from the sympathetic and parasympathetic actions of the autonomic nervous system. Both nervous (sympathetic and parasympathetic) inputs to the heart converge at the right atrium called the sinoatrial node, which is the pacemaker of the human heart.

Parasympathetic stimulation tends to slow down the heart rate, while sympathetic impulse increases the heart rate. Normally, there is a balance between the nervous actions leaning toward the parasympathetic action. However, even without any nervous impulse, the heart will beat automatically due to some unique features of its membrane physiology.

The HR cycle takes about 0.8 seconds at rest (1/(0.8 sec) *60 sec/min=75bpm)

Maximum heart rate is given empirically by:

$$MaxHR = 220 - Age \tag{2.1}$$

Stroke Volume, SV :

This is the difference between the ventricular end-diastolic volume (EDV) and the end-systolic volume (ESV). EDV is the volume available to be pumped in the left ventricle.

In a typical heart, the EDV is about 120 ml of blood and the ESV about 50 ml of blood.

$$SV = EDV - ESV \tag{2.2}$$

The difference in these two volumes, 70 ml, represents the SV. Therefore, any factor that alters either the EDV or the ESV will change SV.

Maximum SV, ($SVmax$), is 100 - 115 ml/beat (this corresponds to 50-60% $\dot{V}O_{2max}$).

Stroke volume, depends on several factors:

- the rate at which blood returns to the heart through the veins;

- how vigorously the heart contracts;
- the pressure of blood in the arteries, which affects how hard the heart must work to propel blood into them.

The magnitude of increase in SV is dependent upon the relative degree of the person/individual's fitness, age and size [106].

Arteriovenous oxygen difference, $a - vO2_{difference}$:
The arteriovenous oxygen difference is the amount of oxygen extracted as blood travels through the body, i.e., it refers to the extraction of oxygen from the blood and is calculated as the difference between the oxygen content of arterial and mixed-venous blood. Arteriovenous oxygen difference increases with an increasing rate of exercise because more oxygen is taken from the blood. Furthermore, arteriovenous oxygen difference has a unique relationship with oxygen consumption and coronary blood flow, which is described by the Fick Equation [73].

Cardiac Output, CO :
Cardiac Output increases rapidly at the start of exercise or during transition from rest to steady-state exercise level by increasing SV and HR in order to provide the flow to serve the muscles. HR increases as vagal tone decreases while SV increases due to increased cardiac inotropy and increased venous return resulting from pressure gradients. This is caused by the compression of veins by contracting muscles, and decreased intrathoracic pressure accompanying increased depth of breathing [106].

As exercise continues, CO rises gradually until it reaches a plateau when blood flow meets the exercise metabolic requirements. Then further increases in CO are predominantly achieved by increasing HR, with SV remaining relatively constant especially at a work rate of approximately 30% of peak $\dot{V}O_2$ [106].

Nevertheless, CO still varies considerably at rest due to emotional conditions that alter the cortical outflow to the cardio accelerator nerves and to nerves that modulate the arterial resistance vessels [73]. McArdle et al [73] also infer that the maximal cardiac output reflects the functional capacity of the cardiovascular system.

The amount of blood pumped by the heart and is given by:

$$CO = SV * HR \tag{2.3}$$

At rest, it is about 5L/min.

Maximum CO is about 20-22L/min (but for elite athletes it could reach up to 40L/min).

CO increases due to:

- Increased HR, which has a linear increase to Maximum HR, (MaxHR)
- Increased stroke volume which plateaus at 40% $\dot{V}O_{2_{max}}$

Since $\dot{V}O_2$ is given by:

$$\dot{V}O_2 = CO * a - vO2_{difference} \tag{2.4}$$

Substituting eqn. (2.3) in eqn. (2.4) becomes:

$$\dot{V}O_2 = HR * SV * a - vO2_{difference} \tag{2.5}$$

This equation is called the Fick equation.

Therefore, the relationship between $\dot{V}O_{2_{max}}$, HR, SV and arteriovenous oxygen difference is:

$$\dot{V}O_{2_{max}} = MaxHR * SVmax * a - vO2_{difference} \tag{2.6}$$

Ventilation, $\dot{V}_E$:
Ventilation is coupled by physiological control mechanisms to CO_2 exchange during exercise [106] and can be expressed as

$$\dot{V}_E = fb * VT \tag{2.7}$$

where fb = breathing frequency and VT = tidal volume

VT is the amount of air volume moved during either inspiratory/expiratory phase of each breathing cycle, i.e. the volume inspired or expired per breath. It increases during exercise by encroachment into inspiratory and expiratory reserve volumes. As exercise becomes more intense, VT begins to plateau at approximately 60% of vital capacity. However, $\dot{V}_E$ increases further through increase in breathing rate.

In a 70-kg man, the $\dot{V}_E$ at rest is generally around 7.5L/min, with a tidal volume, VT of 0.5L and a breathing frequency of 15(1/min) [92]. However, during maximal exercise, $\dot{V}_E$ may reach 120-175L/min with a fb of 40-50(1/min) and a VT of approximately 3-3.5L [92].

Variability during exercise :
The variability in breath (e.g., quiet, shallow, deep and normal breathing) affects the physiological dynamics and is normally evident in breath-by-breath data [88]. There is also the possibility that coughing, breath-holding, hyperventilation, breathing pattern, shortness of breath and periodic breathing could affect variability of physiological parameters during exercise. There are also beat-to-beat fluctuations in the duration of the cardiac cycle, arterial blood pressure, cardiac output, etc. which are well-known phenomena. Moreover, the ventilatory variability is induced by spontaneous variation in arterial CO_2 partial pressure [78].

Khoo [62] reviews the major mechanisms that can give rise to various forms of variability in the ventilatory patterns. This paper reveals that though instability and variability are frequently used interchangeably as having the same implication, that they can be

very different. It also discussed the possible causes of breath-to-breath variability in the pattern of breathing.

HR variability :

Even in the absence of external perturbation to the human cardiovascular system, the heart rate still varies with time in normal physiology [100]. The primary source of the variation is possibly due to a complex regulation and control system which modulates cardiac function through the autonomic nervous system.

HR variability is influenced by several factors:

- Hormonal influence - Under conditions of stress, adrenaline and noradrenaline are released from the tissues of the adrenal medulla into the general circulation. Each of these hormones produces an increase in heart rate.
- Temperature - Elevation of the body temperature markedly increases the heart rate.

High-frequency (0.15 - 0.5Hz) heart rate (HR) variability [18] is frequently employed as an index of cardiac parasympathetic (vagal) control and is related to risk or severity of cardiovascular disease. The variability associated with low frequency bands (0.06 - 0.15Hz) is believed to be induced by both sympathetic and parasympathetic nervous systems [29].

HR varies independently of $\dot{V}O_2$. In addition, HR is affected by emotional state, time after meal, total circulating haemoglobin, degree of dehydration or ambient temperature. Thus, the assumption of the linearity between HR and $\dot{V}O_2$ throughout the range of work-rate to its maximum can under or over estimate $\dot{V}O_{2_{max}}$ and thereby affect an HR controlled system. HR reaches a maximum at slightly lower work-rate than $\dot{V}O_2$ [71].

Similarly, age related HR varies considerably to interpersonal variation and daily fluctuations. Furthermore, HR may be influenced by a number of factors other than exercise,

such as training status, genes, respiratory sinus arrhythmia [39], emotional changes, temperature and food intake.

Respiration affects the heart rate [100]. Furthermore, respirating frequency was shown to have a significant effect on the HR variability [117]. In addition, tidal volume may also have implications for the variability of HR.

Breath-by-Breath variability :
Humans breathe at approximately every 3 to 6 seconds at rest while under strenuous conditions at about 1 to 1.5s unless there is a heart/lung disease or disability. This corresponds to a breathing rate of 10 - 20 breaths/minute at rest, and 40 - 60 breaths at maximum exercise in adults [33], [115].

The breathing rate thus affects the sampling rate selection for accurate control of $\dot{V}O_2$ [46]. Similarly, the impact of inter-breath variability and the role of breath-to-breath variability in gas exchange and $\dot{V}O_2$ have been discussed by [82] and [113]. Furthermore, the time delay in most normal subjects is generally 6 to 12 seconds [63]. Thus, a reasonable delay in the number of breaths might be 1 to 4. This variability of each breath-by-breath measurement introduces noise and random errors.

Busso et al [15] observed a correlation between breaths and tidal volume and the paper also stated that the breath-by-breath fluctuations in the respiratory cycle are not random.

Other considerations :
Pollack et al [91] state that a significant reduction in cardiorespiratory fitness occurs after two weeks of detraining, with participants returning to near pre-training levels of fitness after 12 weeks to eight months. In the course of a long-time exercise, optimal exercise intensities may change even within an individual due to physical conditioning effects. Thus, a recalibration mechanism, such as the use of a $\dot{V}O_2$ control system, may

be required to validate the appropriate exercise regimes.

The control of breathing results from a complex interaction involving the respiratory centres and the muscles [16], [74]. In addition, there are various factors influencing variation in the rate and depth of breathing, both at rest and under a range of exercise conditions. Moreover, it is also known that breathing is periodic and normally characterised by the dynamic behaviour observed in physiological oscillators, such as HR.

Linearity relationship

Astrand and Rodahl [6], and Imbeau et al [53] show that $\dot{V}O_2$ increases as a linear function of increasing work output/speed. This linear relationship concept holds at aerobic exercise, that is when exercise is below the AT. Above the AT, a non-linearity exists between $\dot{V}O_2$ and the work output/speed.

The slope of $\dot{V}O_2$ as a function of work rate is important because it measures the aerobic work efficiency. In addition, this slope is not necessarily constant as work rate is increased above the AT. Even though $\dot{V}O_2$ often increases linearly with increasing work rate, this may not necessarily be true for people with cardiovascular disease. However, both cardiac output and heart rate normally increase linearly with $\dot{V}O_2$ during increasing work rate exercise. The effect of body weight is more pronounced on the treadmill since an even greater work rate is required to support the movement of the entire body through space [106].

In a given individual, a consistent relationship exists between $\dot{V}O_2$ and HR during exercise. The quotient of $\dot{V}O_2$ and HR is the O_2 pulse; its values are dependent on the stroke volume and the difference between the arterial and mixed venous blood O_2 content. This arterial-venous O_2 difference is in turn dependent on the availability of haemoglobin, blood oxygenation in the lung, and the extraction of oxygen in the periphery [106]. Research suggests a linear relationship between $\dot{V}O_2$ and cardiac output over a wide range of submaximal exercise exist [73]. Bassett and Howley [10] estimated that 70-85% of the limitation in $\dot{V}O_{2_{max}}$ is attributable to maximal cardiac output. A linear

relationship exists between $\dot{V}O_2$ and speed [92]. Similarly, there is a linear relationship between $\dot{V}O_2$ and HR [92], and this can be used for estimating $\dot{V}O_2$. However, the limitation of this method is that though the slope of HR and $\dot{V}O_2$ is linear, it can differ for each individual based on large variation caused predominantly by stroke volume. Other limitations include the assumed maximum HR, variability in exercise economy and day-to-day variation of HR in individuals. All these limitations can lead to under or overstating $\dot{V}O_2$ values. Nevertheless, HR is easy to measure.

2.2 Research Context

To date no research on the real-time control of oxygen uptake during exercise-based treadmill rehabilitation appears to have been done, although it is generally believed that oxygen uptake is the best measure of fitness [92]. Furthermore, HR is liable to daily variation, blood flow, emotion (stress and anxiety), and body temperature as previously discussed. Thus, this research will attempt to fill that gap by using $\dot{V}O_2$ control to influence work rate as an alternative to HR control. Here, a detailed review of the existing literature on treadmill automation and control, HR control and $\dot{V}O_2$ control is given.

2.2.1 Treadmill and Automation

Work cannot be clearly defined for horizontal walking or running on the treadmill, even though energy is required for the work. Although a treadmill is not the best device to measure work, it is the most commonly used for exercise because it uses a large muscle mass and because performance is generally limited by aerobic capacity, not by skill or local leg strength.

Treadmill rehabilitation therapy

Stroke affects about 2 million people in US while over 500,000 people in the US suffer from stroke each year [59]. Treadmill training has been used for ambulation training for paraplegic patients, for neurologically impaired patients, for nonambulatory patients with cerebral palsy, for hemiparetic patients, for walking after stroke and for spinal cord injury [43], [8], [23], [30], [35], [96], [42] and [81]. It is used because it has the capability to improve walking abilities in incomplete spinal cord-injured patients [44], [1], [90], [26]. It also has the potential to improve the daily living activities, motor performance and ambulation more than physical therapy for persons with Parkinson's disease [77].

Treadmill training has been used with body weight support [96], [43], [77], [35] and [42] most especially when patients cannot work independently. Visintin et al [105] compared the effect of using a treadmill with and without body weight support. Furthermore, treadmill training has also been combined with electrical stimulation [45], [66] and with robotic devices [23].

Recently, consideration has been given to the fact that treadmill training can also provide cardiovascular fitness in ambulatory hemiparetic patients after stroke [90]. Danielsson and Sunnerhagen, [24] compared oxygen consumption during walking with body weight support and during unsupported treadmill walking in patients with hemiparesis stroke.

When a treadmill is used with patients that lack sufficient motor competencies, it normally requires therapists to guide gait motion and provide support, which can limit the usage of treadmill therapy. Most often two therapists are needed; however, it may sometimes require three therapists. When three therapist are needed, there will be one for each leg manipulation and the last one to stabilise the hips. This thus increases the work load of the therapists. Moreover, the number of therapists that are available may be insufficient for the tasks at hand, or compared with the number of patients that require therapy.

Secondly, the therapy provided by different therapists will vary and this may not be

optimum for each patient. Thus, manual assistance may lead to the need for mechanical/robotic systems. However, these kinds of systems are expensive, immobile and complex to setup and be utilized by therapists. Therefore, treadmill automation may be feasible and preferable.

Treadmill automation

The whole essence of treadmill automation is firstly to serve as a rehabilitation platform for enhancing the quality of life of disabled patients during gait retraining, and secondly to prevent falls due to the limit of the active surface of the treadmill, and thus act as a safety mechanism. These purposes also make it suitable for exercise and recreational usage. The system is also envisaged to be labour and cost effective when used for rehabilitation therapy.

All previous work on treadmill automation has been focused on locomotive interfaces in virtual environments [21], [48], [85], [25], [86], [55], [47], [93] and [22], and they mostly use treadmill devices. They mostly focus on the virtual reality, VR.

The difference between virtual and real-world locomotion is the inertia force due to the acceleration of a locomotion system [22]. In addition, these locomotion systems require self propulsion by the user to move through a virtual environment. Furthermore, linear and turning motion controls were achieved by either leg-based tracking [85] or body -based tracking [21], [25] for the treadmill locomotion system.

In the Omni-Directional Treadmill [25], the user is tethered to a device via an overhead tracking arm which is used to locate position and orientation. The SARCOS Treadport ([21] and [48]) also uses a mechanical tether as a position tracker, while the ATLAS system [121], is based upon a high-cost optical and magnetic position tracking system. In this ATLAS system, the user wears a magnetic sensor on the head to track head motion and wears optical sensors on the feet and legs in order to determine the gait pattern. Thus, each of the treadmill automation systems control belt speed by measuring the

subject's position by mechanical or optical means. Furthermore, the subject is either tethered to the device or must wear an array of sensors. While this may be acceptable for healthy users, such constraint are undesirable in rehabilitation therapy.

In contrast to all the available treadmill automation systems, this research will be exploring and exploiting a safe, low-cost and non-contact positioning control system that is practical and workable for use on a practical treadmill by both healthy and disabled people.

2.2.2 Heart Rate Control

The earlier work on modelling of the human heart rate control system was done by using a time-domain model [28] to model the natural heart rate control. In their two papers ([28] and [27]), they compared two models using two different methods [27]. These two papers emphasized the non-linearity, time-varying and complex nature of the natural HR control system. Similarly, [37] also asserted that HR is non-linear, chaotic/rhythm system and that time-delay must be incorporated in the HR structure because it is inherent in the nonlinear dynamic analysis of the HR system.

In recent times, the conventional HR adjustment is achieved by either fixing the exercise load or fixing the HR, and this is an artificial method of HR control. If the load is allowed to vary unabated, the HR will also vary. However if the HR is not limited or controlled automatically, the HR will continue to increase and may increase beyond the limit of the safety of the user. This could result in potential health problems. Therefore, HR has to be controlled for safety reasons and for fitness.

Jacobsen and Johansen [56] constructed a HR-controlled bicycle ergometer based on physiological theory using a modified Fick equation (see Equation 2.5 on page 18). They used the linearity between HR and $\dot{V}O_2$ as the basis for controlling the work rate via heart rate. They observed that there are inter-individual variations in HR and that physiological factors can cause fluctuations in HR. In their work they took the delay

time constant to be approximately 60 seconds and time constant for the controller to effect change was postulated to be more than 5 seconds (i.e. the delay time for the body to adjust to HR due to involuntary actions). They justified that the delay time constant is caused by psychological factors, mental activity and emotion, outside environment or noise, stress and sense impression. They stated that those physiological factors are negligible at HR greater than 120 bpm. The control sample interval is at every minute and HR was picked up through an ear sensor. The control experiments lasted for about 10 min with only 6 min for a fixed HR level/mark. The controller showed instability at low HR levels and the authors explained that it was caused by the physiological factors. Nevertheless, the conclusion is that HR can be kept very constant during ergometer bicycle exercise.

However, the Fick equation (Equation 2.5 on page 18) is a labile relationship that may be unreliable, inconsistent and unpredictable [97] and thus may not be suitable for routine monitoring and control because of the limitation inherent in the determination of the dynamic and physiological parameters.

Goldstein et al [36] investigated whether heart rate biofeedback influences the cardiovascular responses to exercise. 18 healthy people participated in that experiment for a duration of 10 weekly sessions. They provided feedback to the subjects through different illuminated light signals indicating if a preset value had been reached and secondly by electronic display. The results of the experiment showed that the HR can be decreased through learning and/or motivation under certain conditions.

Sada et al [94] developed a self-biofeedback HR control for improving cardiac adjustment to exercise. Their study focuses on changes in HR, running speed, stride and pitch of gait in response to various preset HR levels during exercise in healthy human subjects. They developed a system that allows the subjects to be aware of whether their own HR exceeded their preset level during the exercise by producing a photo and sound alarm signals whenever their actual HR had exceeded the preset value. This enabled the subjects to externally control their actual HR to the preset HR value by either changing

their running or walking speed. 7 subjects participated in the experimental testing, with a preset HR to five different HR levels (80, 100, 120, 140, 160 bpm). The experiment lasted for 6min while HR was measured by ECG. The paper concluded that HR could be controlled by a change in running speed due to pitch and stride length. The self-biofeedback control method is in the category of making HR constant while varying the load.

However, this method is not automatic because it requires the user's direct effort or manual intervention to adjust the speed. The method cannot achieve a precise and accurate control of HR because of the possibility of human errors.

Kawada et al [60] developed a HR controller using a computer-controlled cycle ergometer. They estimated transfer functions from work rate (WR) to HR by averaging 10 healthy subjects' data obtained from experimental WR - HR data, and then developed a Proportional-Integral, PI feedback controller based on the transfer function. The controller was validated with 55 healthy volunteers. The desired HR was set at 60 -75% of the age predicted maximum HR. The experimental duration was 10 minutes. The controller's major limitation is that if a set target is not reached, the controller continues to increase the work rate and this may be unsafe.

Kawada et al [61] also developed a HR controller using a treadmill. Similarly to their HR controller cycle ergometer, the feedback controller incorporated a PI controller. 10 subjects participated in the experiment. HR was measured by electrocardiogram, ECG sampled at 1 kHz while the HR and speed command signals were recorded at a sampling rate of 4Hz. The target HR was set at about 40 bpm above the baseline HR while for ramped tests it was set to 80% of age predicted maximum HR (as peak HR). The control test lasted for 8 minutes. The controller's limitation is similar to the HR controlled cycle ergometry previously discussed.

Most commercially controlled HR equipment (in-built HR control system) uses a proportional controller with variable gains. Such a system may be population biased and

may not take into account inter-individual variability.

This research will therefore focus on the use of a feedback control system that would be dynamic and robust to automatically adjust to individual differences. The outcome is expected to be reliable, faster and responsive, effective, consistent and stable compared with a commercially available HR-controlled treadmill system.

2.2.3 Control of Oxygen Uptake

A $\dot{V}O_2$ controller can be used in training programmes, especially when it is important to restrict $\dot{V}O_2$ within certain levels (for safety, etc). After a thorough and extensive survey of existing literature, the research akin to automatic control of oxygen concentration or oxygen consumption was found in the field of anaesthesia ([98], [99], [97]). Here those relevant papers and publications are reviewed.

Sieber et al [98] studied the clinical use of a model-based automatic control system to adjust the end-tidal anaesthetic concentration, and also compared the results with human/manual control; while Stadler et al [99] developed an automatic feedback control system to regulate the end-tidal CO_2 concentration during general anaesthesia using a model-based approach. In addition, Schindler et al [97] assessed the accuracy of feedback-controlled oxygen delivery into a closed anaesthesia circuit for the measurement of $\dot{V}O_2$ in vitro and in vivo.

Inbar et al [54] developed a closed-loop pacemaker controller for regulating a mixed venous oxygen saturation level using HR as input. The model uses the linear relationship between the mixed venous oxygen saturation level to HR and work rate obtained from existing data in literature, and from experiments using a venous oxygen saturation (SO_2) sensor. The study discussed that there is a nonlinear relationship between CO and HR as a result of optimal heart rate phenomenon (i.e., at a certain frequency, an increase in HR causes a decrease in CO and the implication is that the controller will continue to increase HR with a decrease in SO_2 level because the model is based on the

linearity assumption which is not the case since there is nonlinearity at this frequency). The experiments were performed with healthy young volunteers, while SO_2, HR and other parameters were measured as the subjects were performing controlled work. The controller was of the proportional-Derivative, PD form. Determination of the cardiovascular parameters for each patient may be difficult. The results showed a time delay in the closed-loop system response as 5 - 8 seconds and the recover time as 5 - 15 seconds depending on work rate/load and patients. It concluded that a more complex model is needed; nevertheless, that the model can be used under certain conditions (where linearity assumption is valid) and by certain patients.

Sasaki et al [95] use an indirect method for estimation of $\dot{V}O_2$. Even though no control system was developed, the approach of indirectly estimating $\dot{V}O_2$ from HR using mathematical method, and using this for control, is faulted with potential errors because HR can over or under estimate $\dot{V}O_2$ if one of the components of $\dot{V}O_2$ changes quicker or slower than HR movement [97]. These components were discussed earlier in this thesis (on page 15).

Yamamoto et al. [120] developed a computer software to produce a ramp protocol for treadmill by increasing $\dot{V}O_2$ in a linear fashion. This system increases $\dot{V}O_2$ arbitrarily by determining the necessary variables from a mathematical formula that increases the speed and grade of the treadmill. The ramping protocol was applied to 10 healthy subjects and the paper disclosed that a similar relationship existed between predicted $\dot{V}O_2$ and measured $\dot{V}O_2$. The limitation is that one cannot control $\dot{V}O_2$ with this system because the method continuously increases the $\dot{V}O_2$ until the end of the exercise. If $\dot{V}O_2$ is continuously increased without limitation it can be detrimental to the health of individuals if their tolerable $\dot{V}O_2$ limits are exceeded. Thus, a dynamic regulation of $\dot{V}O_2$ is required that will match the targeted exercise $\dot{V}O_2$ to measured exercise $\dot{V}O_2$, by adjusting the speed or gradient while also compensating for individual differences.

Therefore, a precise control of $\dot{V}O_2$ is important in rehabilitation and exercise training to maximize the outcome of training, and to minimize the associated risks. This is one

of this thesis' objectives, i.e., to automatically control $\dot{V}O_2$ during moderate treadmill exercise.

3 MATERIALS AND METHODS

This chapter describes the experimental apparatus used and the methods adopted throughout the experimental studies.

3.1 Experimental Apparatus

Experiments were performed using the following commercially available equipment (which were integrated to a computer for computer controlled system) at the Rehabilitation Engineering Lab. The experimental set-up is shown in Figure 3.1. A brief description of hardware and software systems used are discussed in this section.

3.1.1 Treadmill Device

A commercial motor driven treadmill (T-Track Tunturi Model Gamma 300)[1] was utilised in this research. The treadmill running surface is 150 cm long by 50 cm. The treadmill features speeds of 0.5 - 16km/hr with 0.1km/hr increments and gradients (or slope) of 0 - 10% with 1% increments. Parallel handrails are attached to the treadmill's front vertical beam, on which a digital control panel is located.

The treadmill is equipped with an RS-232C serial port interface through which connection to the personal computer (PC) is integrated for the computer controlled system. All experiments were performed using this treadmill.

[1] http://www.tunturi.com/fitness/product.cfm?id=36

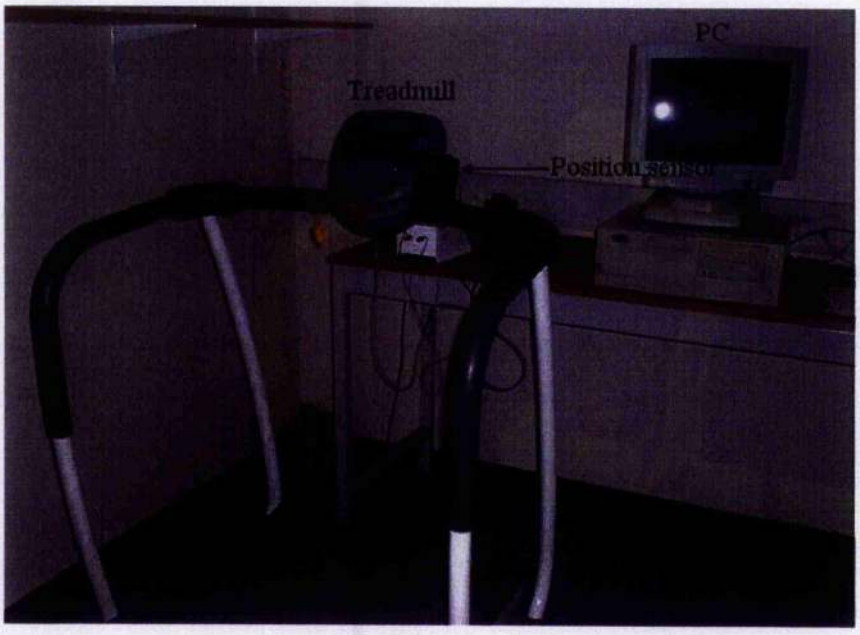

Figure 3.1: Apparatus set-up

3.1.2 Position Measuring Techniques

There are various commercially available non-contact position measuring systems ranging from optical sensors to magnetic sensors etc. In addition, there are different advantages and disadvantages of using one method over the other in terms of cost, application, measurement speed and accuracy, ease of use, durability etc. Table 3.1 shows a brief summary of the limitations of using different positioning sensors for tracking purposes.

Table 3.1: Limitations of position tracking sensors

Sensors	Limitations
mechanical tracking	encumbrance (obstruction) of the device and its restriction of motion
ultrasonic (acoustic)	low resolution, long delay times, line of sight problem, and interference/noises
optical	limited work space, lack of complete rotation motions, processing time problem
magnetic	high time delay for the measurement and processing, range limitations, and interference
inertial	only provides rotational measurements and may be inaccurate for slow position changes

Furthermore, there are potential health hazards when subjects wear head mounted devices.

Polaroid Ultrasonic Sensor :

An ultrasonic sensor (Polaroid 6500 series sonar unit)[2] was built and used to measure the relative distance of a subject from a fixed position, because movement of an object is always relative to a reference point.

The measuring principle of this Polaroid sensor is based on travel time measurement of an emitted sound burst (of 40 kHz from a piezoelectric transducer) to return back (to another piezoelectric transducer, the detector) after reflection as an echo from the measured object in front of the device. The flight time is then converted into distance using the speed of sound in air (345 m/s) in the computer via a micro-controller which synchronises the time of the echoes with the computer clock to determine the object's distance. The measurement range of operation is between 0.15 - 10.67 m with accuracy/resolution of 1 %, sampling time capacity of 20 ms and beam angle of 15 degrees

[2]http://www.acroname.com/robotics/parts/R11-6500.html

(detection cone of 30 degrees).

The ranging sensor is integrated to the digital input and output (I/O) board (using Amplicon 200 series, PCI 215 card) connected to the PC via a connection cord. It is powered by 6 V (2.5 A) which is obtained by step-down of the mains power.

3.1.3 Polar Heart Rate Monitor

HR was measured using a polar belt (T61 Polar HR transmitter belt)[3]. The subject straps this elastic belt around his/her chest or upper abdominal region. The belt consists of a transmitter sensor and a battery which communicates telemetrically to the built-in Polar receiver of the computer-controlled treadmill. The HR obtained from the receiver is an average calculated from a certain time period based on the manufacturer's algorithm.

3.1.4 MetaMax 3B Cardiopulmonary Monitoring System

Pulmonary gas exchange and ventilation were monitored breath-by-breath utilizing a portable metabolic cart (MetaMax 3B, Cortex Biophysik)[4]. A turbine transducer was used to continuously monitor inspired and expired airflow while independent O_2 and CO_2 sensors measured respired gas concentrations. The raw signals were time aligned and processed using algorithms based on those of [13] by the MetaMax system. This system is integrated to the computer controlled system via a serial link thus enabling data transmission, monitoring and control. The MetaMax device is battery operated. The subject wears a face mask connected to the Cortex device via plastic sampling lines. The device stores many types of information; however, we are primarily concerned with $\dot{V}O_2$, $\dot{V}CO_2$, $\dot{V}_E$ and respiratory exchange ratio, RER. We monitored RER, HR and $\dot{V}_E$ throughout the experiments. Prior to usage, the device is calibrated with both calibrated gas and ambient air.

[3] http://www.polarusa.com/
[4] http://www.cortex-medical.de/index-sports.html

The subject wears a facemask secured tightly so that air is drawn through it from the room, and exhaled air flows through it via a volume transducer that is fixed to the face mask and the transducer whilst also connected to MetaMax base. The gas sampled for analysis is drawn off through a sample line inserted into a small hole on top of the volume transducer (drawn by a vacuum pump) which is also connected to the base of the MetaMax system. The base system is connected to the PC via a serial cable. Accuracy of the volume transducers is 2 % with a resolution of 7 ml and a response time of 100 ms.

3.1.5 Computer and Software

A PC was used to interface with all the apparatus discussed earlier for a computer controlled system. Matlab and Simulink a standard computer software is used for analysis, design and simulation. Humusoft real-time toolbox[5] is used in conjunction with Matlab/Simulink to achieve real-time data acquisition and implementation during experiments.

3.2 Methods

The approach adopted throughout this research is the system identification and pole placement methods for modelling and control respectively under the assumption of linearity. The previous sections have discussed the basis of this assumption and the apparatus utilised. Here, the focus of discussion is on these methods involving identification of the plant model in open loop operation, and using the model to design a controller. Subsequent chapters will apply these general methods to each group of experiments while also discussing the protocol, subjects and experiments. Furthermore, the system is treated as a Single Input Single Output (SISO) system throughout this thesis.

[5] http://www.humusoft.cz/rt/index.htm

3.2.1 Modelling Techniques

Models are essential for controller design and it gives the relationship between a plant input and output. Models can be obtained mathematically using physical laws and principles. Similarly, models can be obtained experimentally. Furthermore, models can be obtained by a combination of physical laws/principles and experiments. In this section and throughout this thesis, models will be obtained from experiments. In addition, the purpose of the model will affect the choice and selection of a model. Thus, the model is intended to be used to design a controller that achieves a certain closed-loop performance using the pole-placement method.

The method implemented is based on a well-known parametric ARX (Auto Regressive with eXogenuous input) model. The procedure involves identifying the transfer function by computing the parameters via least squares algorithm [70]. Apart from the least square method, there are other methods of estimating model parameters (for example, instrumental variable method, maximum likelihood, spectral analysis, etc).

Figure 3.2 shows the generic open loop system for a plant with input, u and output, y.

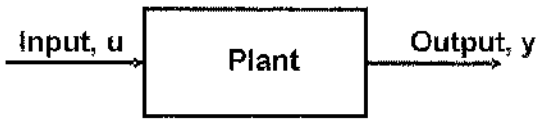

Figure 3.2: Block diagram of a generic open loop system

An input signal, u is sent to the plant and the output signal, y is received, and this input-output data are processed offline using Matlab identification toolbox. This principle of system identification [70] is called black box modelling technique [63]. In this technique, the input is known while the output information is obtained experimentally even though there is inadequate and insufficient knowledge of what is happening within

the system. The process enables one to estimate the mathematical relationship that exists between the excited input signal and the measured response outputs (i.e., obtain the transfer function that consists of the plant order, time constants and time delays). The empirical data obtained are then processed, estimated and validated to obtain various models which are thereafter compared for goodness of fit to the data.

Input/Experiment design

For each experiment a decision is made on which signal is to be controlled. For the treadmill, you can either control the speed or gradient, thus, the speed was used while maintaining the gradient fixed/constant.

An input design is based on input-output data gathered from random excitation so as to excite all modes. Thus, various step inputs are used to excite the plant in-order to determine a time of response of the system to the input, and to obtain other open loop parameters. Once a satisfactory level is achieved, we used the data set gathered from both input and output responses to estimate the rise-time which is subsequently used to determine the sampling time for the system.

We also determined the intended operating range for the system so as to excite the system (to cover all the frequency range and with suitable sample interval) within those ranges in order to capture all the modes (frequency of operation) and the data record length (duration of the experimental tests). Subsequently, a step, ramp, constant and Pseudo Random Binary Sequence, PRBS, signal could be used for exciting the system; however, as previously stated that the system must be excited in all frequencies of operation, the PRBS is thus ideal.

Open-loop identification

Experimental input-output (I/O) data are obtained using pseudo-random binary sequence, PRBS, input excitation with different sampling time, duration and amplitude.

This PRBS input signal is designed offline and then sent to the plant through the computer-controlled system while the corresponding output is then obtained. Consequently, the raw input-output data are collected and recorded and then used offline for system identification. Thus the identification results are obtained off-line.

Data processing

The I/O data are first processed by removing the determined deviations from the physical equilibrium (by subtracting the physical level that corresponds to a constant, close to the desired operating condition/points, i.e. the static constant values and its resulting steady state value to make the data zero-mean) since we have already established that linearity assumption concept is used in this research. Thereafter, the transient period data segments are removed.

Model structure

A model structure is selected from ARX and ARMAX [70]. For the purpose of this research ARX model structure is selected based on its simplicity and its structure which is based on least squares methods [70]. Nevertheless, other suitable model structures were searched for by testing a number of different structures and then comparing/evaluating the resulting models. Equation (3.1) describes the dynamic properties and also represents the standard linear model representation for single input variable, u, and measured output, y and measurement noise, e.

The ARX structure is given by:

$y(t) + a_1 y(t-1) + ... + a_{n_a} y(t-n_a) = b_1 u(t-nk) + b_2 u(t-nk-1) + ... + b_{n_b} u(t-nk-n_b+1) + e(t)$

this can be re-written as:

$$A(q^{-1})y(t) = B(q^{-1})u(t-nk) + e(t) \tag{3.1}$$

where $q^{-1}y(t) = y(t-1)$

Equation (3.1) can be expressed in this generic form:

$$y(t) = q^{-nk}\frac{B(q^{-1})}{A(q^{-1})}u(t) + \frac{1}{A(q^{-1})}e(t) \tag{3.2}$$

$A(q^{-1}) = 1 + a_1 q^{-1} + ... + a_{n_a} q^{-n_a}$
$B(q^{-1}) = b_1 + b_2 q^{-1} + ... + b_{n_b} q^{-n_b+1}$

and generally written in this generic form: ARX(n_a,n_b,nk).

Here,
$A(q^{-1})$ = Auto-Regressive (AR) polynomial in the backward shift operator, q^{-1}

$B(q^{-1})$ = polynomial for external input, $u(t)$ in the backward shift operator, q^{-1}

n_a = order of $A(q^{-1})$

n_b = order of $B(q^{-1})$

nk = number of delays from input to output

$e(t)$ = white noise

q^{-1} = unit delay operator.

Parametric estimation

The data set (after removing physical equilibrium and transient period) is then divided into two data set segments (one is used as the working/estimation data while the other as the validation data). The estimation data is validated with the validation data to

obtain the parameters of various models for the ARX model structure. It involves choosing the size of the model set in terms of selecting the order of the model (degrees of the polynomials in the model) and the delay time.

Since the noise disturbance, e is assumed to be uncorrelated zero-mean stochastic signal, the best 1-step-ahead moment prediction given by [70] is:

$\hat{y}(t) = \theta^T \phi(t-1)$

where,

the parameter vector θ and regression vector ϕ are defined as

$\theta = (a_1 .....a_{n_a}; b_1 .....b_{n_b})^T$

$\phi(t-1) = (-y(t-1) .... - y(t-n_a); u(t-nk) .....u(t-nk-n_b+1))^T$

A measure of model accuracy is provided by the least-square criterion expressed as:

$$J_N(\theta) = \frac{1}{N} \sum_{t=1}^{N} (y(t) - \hat{y}(t))^2 \tag{3.3}$$

where

N is the number of data points. The analytical solution for the optimal parameter estimate is derived by [70] as:

$$\hat{\theta} = \left(\sum_{t=1}^{N} (\phi(t-1)\phi^T(t-1) \right)^{-1} \left(\sum_{t=1}^{N} (\phi(t-1)y(t) \right) \tag{3.4}$$

This is the equation used for parameter estimation which is incorporated in the Matlab System Identification Toolbox used throughout this research.

The fitness (expressed in %) is given by:

$$R^2 = 1 - \frac{J_N(\theta)}{\frac{1}{N}\sum_{t=1}^{N}|y(t)|^2} \tag{3.5}$$

Model validation

Finally, the various models are compared for quality of the fit, and the model with the best fitness is chosen using:

- simulation (by computing the fit),
- cross-validation (for a number of different model and model structure, we plot the loss function and select the minimum, having simulated on a different data set),
- correlation analysis (on the predictor errors to ensure the scatter plots resemble white noise), and
- examining step, impulse and frequency responses (by comparing these with physical insight regarding the process) for determination of adequacy of the estimated models.

The model is then accepted and used for the intended purpose and if not suitable the whole process is repeated depending on the level of attention needed. The design of a pole-placement controller using a model obtained from this system identification method is discussed in the next section.

3.2.2 Control Design Methodology

Generally, a closed-loop system is preferred to open loop systems because of the advantages of closed-loop systems which include faster transient response time, reduction of steady state errors and sensitivity to load uncertainties or variations. Closed-loop systems can be a feed-forward or feed-back system or combination of the two. Here we will focus on feed-back closed-loop systems. To develop such systems, we require a controller to regulate the open-loop system and attenuate noise and disturbances. A feedback controller can be designed using several different approaches, such as linear

quadratic gaussian (LQG) method, pole assignment approach, etc. In this section, the description of a pole placement approach for controller designs is discussed.

Controller design

The controller designed method described here is the pole placement design of a discrete-time RST controller (a two-degree-of-freedom controller) using the polynomial technique [7]. Consider a closed-loop structure of Figure 3.3 with reference signal, Uc, control signal, u and measured signal, y.

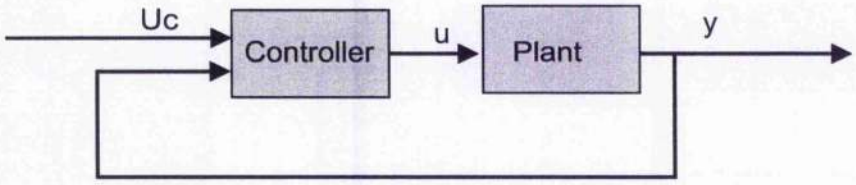

Figure 3.3: Block diagram of a generic closed-loop control system

The controller in Figure 3.3 can be represented by the structure in Figure 3.4.

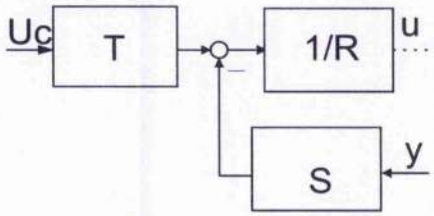

Figure 3.4: Block diagram of a generic RST controller structure

where,

R, S and T are controller polynomials in the backward-shift operator, q^{-1}.

This implies that,

$$R(q^{-1})u(t) = T(q^{-1})Uc(t) - S(q^{-1})y(t) \tag{3.6}$$

Then,

Solving equations (3.6) & (3.1) and omitting the arguments of the polynomial for simplicity, and assuming e to be uncorrelated zero-mean stochastic signal to have:

$$\frac{y}{Uc} = \frac{q^{-nk}BT}{AR + q^{\ nk}BS} \tag{3.7}$$

Therefore,

The feedback design equation is:

$$A_{cl} = AR + q^{\ nk}BS \tag{3.8}$$

where $A_{cl} = A_o\, A_c$

A_{cl} is specified designed closed loop system

with A_o as the observer polynomial

and A_c as the controller polynomial

Equation (3.8) is also called Diophantine Equation.

The polynomials A_c and A_o are chosen using a time-domain method to correspond to the poles of second-order transfer functions having a desired rise-time and damping (zeta). The polynomial characteristics equation (Diophantine Equation) is solved for R and S by employing the Polynomial toolbox[6].

[6]http://www.polyx.com/

A further possibility is to allow the cancellation of faster poles (plant pole) by including such a cancelled pole factor (A^+) in the closed-loop characteristic equation. For solvability, the polynomial S must also contain this factor. Thus having the feedback design equation as:

$$A_o\, A_c' = A^- R + q^{-nk} B S' \tag{3.9}$$

The structure R is determined by the choice of the polynomial Δ in the noise model. When a piecewise-constant offset is present as disturbances, then integral action ($\Delta = 1 - q^{-1}$) must be included in the controller to achieve zero steady-state tracking error [51], [50]. Thus eqn. (3.9) becomes:

$$A_o\, A_c' = A^- \Delta R^- + q^{-nk} B S' \tag{3.10}$$

This equation is solved for R^- and S' subject to a strict proper condition

$$\text{i.e., } deg(S') < deg(A^-) + deg(\Delta)$$

The polynomial T is designed to achieve a suitable command tracking by ensuring unity steady-state gain in eqn. (3.7) and by appropriate definition of T as:

$$T = \lambda A_o\, A^+ \tag{3.11}$$

where the scalar $\lambda = \frac{A_c'(1)}{B(1)}$ and T, A^+ and A_o are polynomials in the backward-shift operator, q^{-1}.

This results in the left hand-side of the eqn. (3.7) becoming:

$$\frac{q^{-nk}\, B\, A_c'(1)}{A_c'\, B(1)} \tag{3.12}$$

as desired.

Note that $B(1) \neq 0$ and that B and A_c' are polynomials in the backward-shift operator, q^{-1}.

Furthermore, the tracking performance can be decoupled from the disturbance rejection response through the introduction of a reference pre-filter. This filter, F will appear outside the feedback loop, thus the closed loop is arbitrarily shaped by cancelling the stable poles in A_c' and replacing these with an alternative set of tracking poles (i.e., introducing the desired closed-loop reference transfer function) [51], [50].

The pre-filter, F is given by:

$$\frac{\lambda_r \, A_c'}{A_r} \tag{3.13}$$

then the numerator of the prefilter cancel the remaining part of the characteristic closed-loop polynomial; i.e., A_c' while the denominator A_r specifies the desired reference tracking behavior. The constant λ_r ensures a steady-state gain of 1 for reference tracking.

$$\lambda_r = \frac{A_r(1)}{A_c'(1)} \tag{3.14}$$

Therefore, the transfer function for reference tracking in eqn. (3.12) taking the prefilter to account becomes:

$$\frac{q^{-nk} \, B \, A_r(1)}{A_r \, B(1)} \tag{3.15}$$

The polynomials A_r is specified by choosing pre-filter rise-time and pre-filter damping factor (pre-filter zeta) of the corresponding polynomials in continuous time.

Note that A_r is also a polynomial in the backward-shift operator, q^{-1}.

The sensitivity function, S_f is given by:

$$S_f = \frac{A(q^{-1})R(q^{-1})}{A_{cl}} \tag{3.16}$$

and the complementary sensitivity function, T_f is expressed as:

$$T_f = q^{-nk}\frac{B(q^{-1})S(q^{-1})}{A_{cl}} \tag{3.17}$$

4 TREADMILL AUTOMATION

This section examines the feasibility of a low-cost non-contact treadmill positioning system (referred to in this thesis as treadmill automation). The purpose is to maintain any subject at a prescribed position or distance relative to a fixed reference point (for safety purposes). To achieve treadmill automation, the speed of a treadmill is controlled by feedback of a subject's current position which is obtained from an ultrasonic measurement.

First, an automatic treadmill speed control system was developed based on analytical feedback control and subsequently an automatic treadmill position system. This section discusses the concept, development, testing and results of experiments on treadmill automation.

4.1 Conceptual Design/Experimental Setup

The general principle is based on a non-contact measurement of subject position using a low-cost ultrasonic sensor which was integrated to the treadmill. This device was mounted on the front of the treadmill as shown in Figure 3.1 (on page 33).

The block diagram in Figure 4.1 illustrates the concept. The concept is based on the fact that a subject's current position relative to a fixed point can be described dynamically as the integral of the difference between the treadmill speed and the subject's speed relative to the treadmill speed. Thus, the measured position is assumed to be the integral of speed error (i.e., the differences between the subject's speed, Vsubject, and the treadmill speed, Vbelt). This measured position is fed back and compared with a preset position (often set to be at the centre of the treadmill surface), and the differences, or error, is

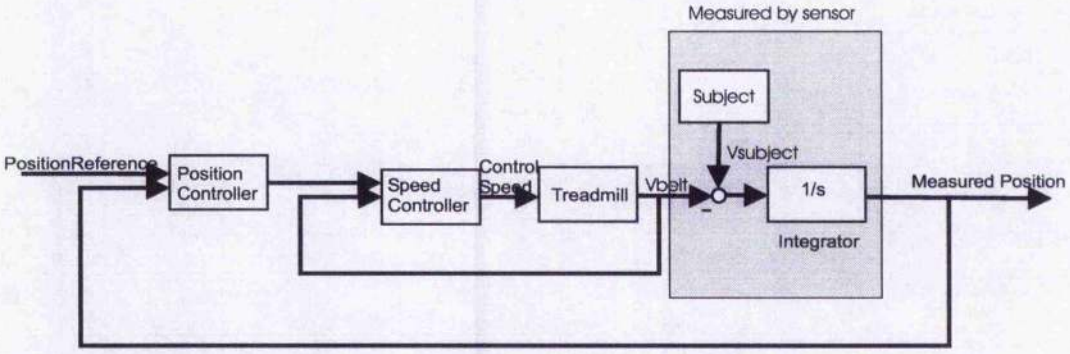

Figure 4.1: Treadmill automation conceptual block diagram

compensated for by the position controller.

For example, if the subject is at the desired position and the treadmill speed is equal and opposite to the subject's speed then the subject would be kept in that position assuming there is no delay. However, it is difficult to measure the subject's speed but easier to measure the subject's position. It is assumed that the delays are negligible. In addition, the inherent delay was incorporated into the system model. It is also assumed that the direction of the subject while walking/running on the treadmill surface is linear, horizontal and lateral to the treadmill. This is the concept used to autonomously control a subject's position. The feasibility of this concept will be tested which forms the tenet of our treadmill automation.

4.2 Identification and Modelling of Treadmill Dynamics

Figure 4.2 shows the generic open loop system for the treadmill in which input (control speed or inclination) can be sent to the system while outputs (treadmill Vbelt speed, inclination/grade and heart rate) are received from the treadmill system. This implies that adjusting either the control speed or inclination can be used to automatically control the treadmill, but we used the control speed for the purpose of this research.

Here the identification approach is based on determining the open-loop response of the plant output (measured treadmill speed, Vbelt) to a Pseudo Random Binary Sequence (PRBS) forcing function plant input (control speed). The linear input-output speed model transfer function is determined from this measured data. The procedure is based on system identification method described in section 3.2.1 on page 37. Two steps are carried out in order to determine the transfer function.

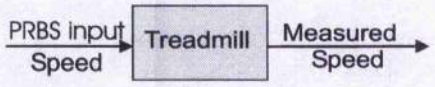

Figure 4.2: Open loop treadmill system block diagram

Step 1: Open-loop test

The speed input is varied around a specified mean level according to a PRBS forcing function. During this test, the input-output data are recorded. Five different but similar data sets are collected using the same PRBS input signals. The PRBS used to generate these data sets were kept the same so as to ensure that the differences obtained were due to treadmill dynamics and not to change in input signals. Figure 4.3 shows a typical open-loop test result.

The PRBS input signal has a mean of approximately 50% of the maximum treadmill speed (2200mm/s) and amplitude of approximately 10% of the mean (200mm/s) at sampling rate of 0.5sec for a duration of 200sec. This PRBS signal was designed offline to excite all the range of frequency in which the treadmill will operate. It is worth noting that the sampling time is obtained by various test experiments using a step input to determine the open loop rise time (2sec).

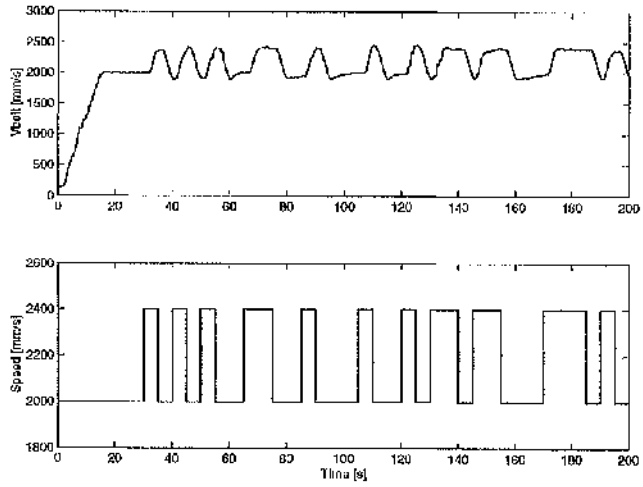

Figure 4.3: Time plot of open-loop input - output data set from PRBS signal (the upper plot shows the output signal, Vbelt while the bottom plot shows the input signal)

Step 2: Model identification and validation

A linear model (ARX structure) is fitted to one of the input-output data obtained from the open-loop test using least squares, LS. A range of model orders are tested, and the models compared and validated using one of the data sets from those obtained in step 1. The data set was processed by first removing the operating condition offset. Then, the first 17.5 s was removed from the data set representing the transient period, thereafter the remaining data set was divided into two portions and one data segment/portion was used for estimation and the other segment/portion was used for validation. Thus, a satisfactory model is obtained from this selection. The structure of the model selected consists of the transfer function order n_a, the numerator polynomial n_b, and the time-delay nk, discussed earlier. Table 4.1 compares some of the resulting models while Figure 4.4 compares the performance of model arx225 in an open-loop situation. Note that the fitness in the table is computed using eqn. (3.5) on page 42.

Table 4.1: Comparisons between several different models

Model	Transfer function	Rise-time	Fitness
arx441	$\frac{-0.01036z^3+0.01278z^2+0.002092z+0.1208}{z^4-1.166z^3-0.00522z^2+0.342z-0.02318}$	2.5s	76.44%
arx225	$\frac{0.05658z+0.0877}{z^6-1.538z^5+0.6843z^4}$	2s	77.27%
arx443	$\frac{-0.003504z^3+0.08002z^2+0.0589z+0.0896}{z^6-0.8632z^5-0.1478z^4+0.1634z^3+0.1044z^2}$	2s	78.82%

The estimated model in form of transfer function is used to analytically design a closed-loop treadmill speed controller. Thereafter, a closed-loop treadmill positioning controller is designed by cascading the speed controller.

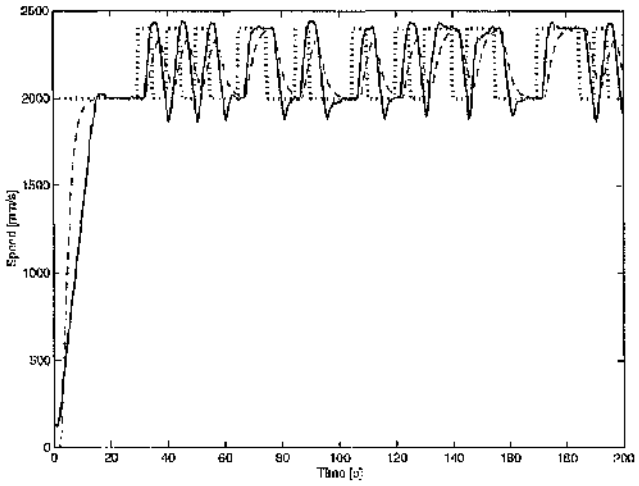

Figure 4.4: Model comparison plot (the dotted line is the input control speed a PRBS signal, the solid line is the measured open-loop treadmill speed output, Vbelt and the dashed-line is the simulated arx225 model output)

4.3 Treadmill Speed Control

Here the treadmill speed controller design, tests and results are described. The goal of the speed controller is to stabilise the system, achieve a desired performance without overshoot. The sensitivities functions were computed using eqn. 3.16 and 3.17 on page 47.

4.3.1 Speed Controller Design

Three steps are carried out to design and test the treadmill speed controller using a sample interval of 2Hz. All tests carried out here are closed loop tests. The configuration of this test is shown in Figure 4.5 (which is the inner loop diagram of Figure 4.1).

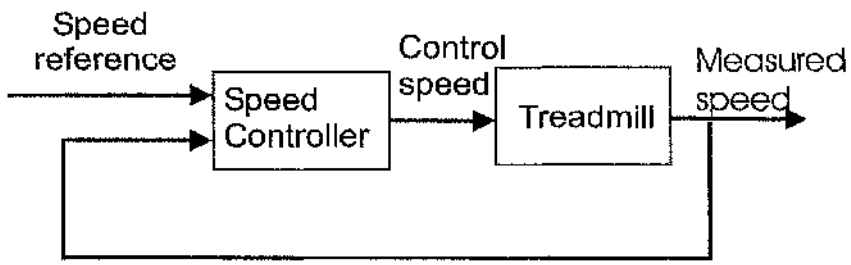

Figure 4.5: Schematic block diagram of the speed closed-loop control system

Step 1: Speed control design

The selected model (from step 2 in section 4.2) is used to design a feedback controller based on pole assignment method (discussed in section 3.2.2 on page 42). The specified desired closed-loop rise-time and damping (zeta) parameters are converted to a pair of dominant closed-loop poles for the design using the controller approach described in section 3.2.2. The results are simulated on the computer before real-time implementation.

Step 2: Speed tracking test

To ascertain the performance of the speed controller, two sets of tests were carried out with load (a subject on treadmill) and without load. With load test is termed "on load" while the without load test is termed "no load" test. Typically, a square wave reference

speed of a given amplitude and frequency is applied and reported here. This speed tracking test was also tested with a constant reference speed.

Step 3: Disturbance rejection test

In this test, the reference speed is held at a constant level while a disturbance was applied by asking a subject to jump on and off the moving treadmill at arbitrary times. The controller is expected to reject the disturbance in order to maintain the constant speed reference. A constant reference and square wave speed references are used for this test.

4.3.2 Speed Controller Results

Typical results of the closed-loop speed tests are presented in this section.

Figure 4.6 shows the performance of model arx225 used for the controller design. The controller is implemented with a subject running on the treadmill and the results presented in the Figure. This Figure also compares a computer simulation of the speed controller with the result from the experimental test.

In Table 4.2, the speed controller design parameters are shown with both observer zeta and zeta critically damped.

Table 4.2: Speed controller design parameters

Parameter	Values
rise time	10s
observer rise-time	0.01s
zeta	0.999
observer zeta	0.999

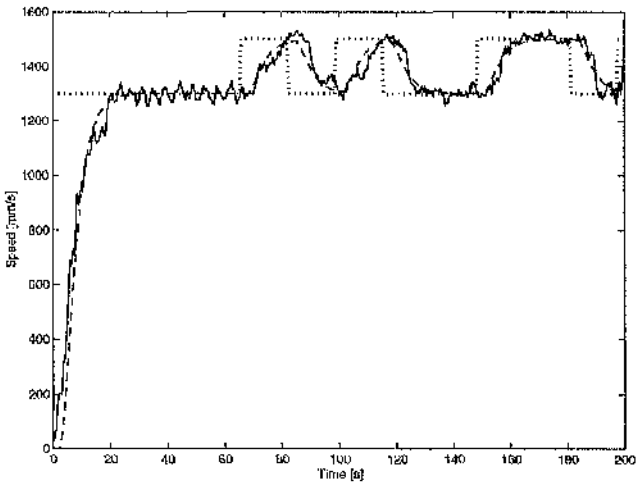

Figure 4.6: Comparisons between the speed controller simulation output and the implementation of the controller with a subject running on the treadmill (the dotted line are the reference signal, the solid line is the closed-loop treadmill speed tracking response while the dashed-line is the simulated controller tracking response).

Figures 4.7, 4.8 and 4.9 show the closed-loop tracking test for no load, on load and disturbance rejection tests respectively.

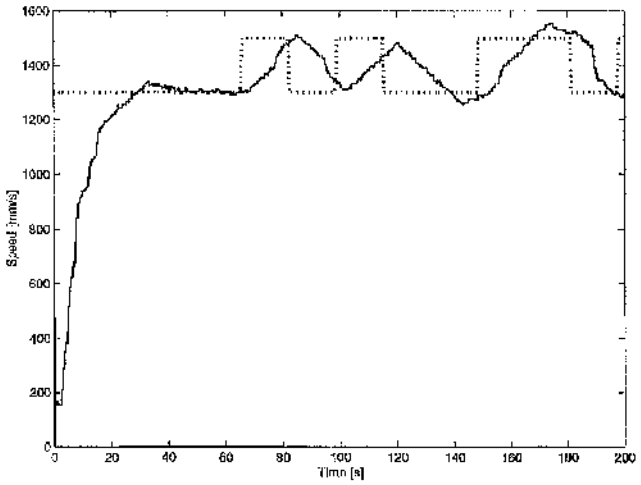

Figure 4.7: No load closed-loop speed tracking test results (dotted line is the reference speed while the solid line is the measured speed)

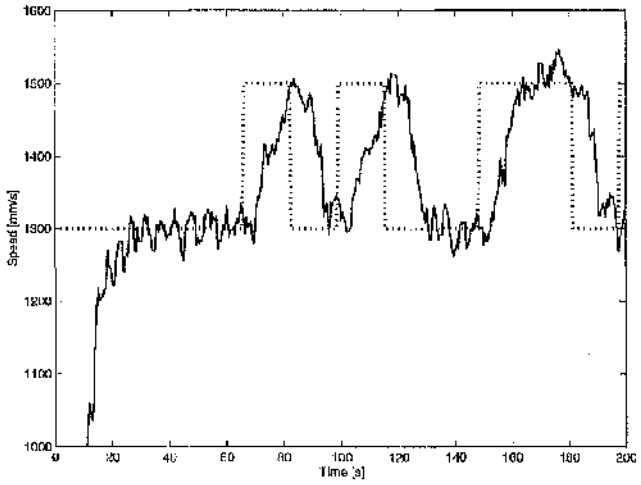

Figure 4.8: On load closed-loop speed tracking test results (dotted line is the reference speed while the solid line is the measured speed)

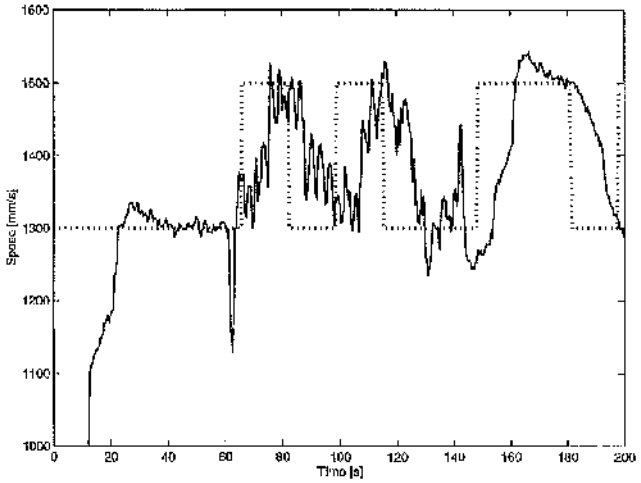

Figure 4.9: Closed-loop speed disturbance rejection test results (dotted line is the reference speed while the solid line is the measured speed, a subject jumped on the treadmill at approximately 62s and jumped off at approximately 140s)

4.3.3 Discussion on Speed Control

Figure 4.3 shows a typical open-loop test result while Table 4.1 compares some of the resulting models. The table shows that high order models, with a high delay, capture the dynamics of the model better; however, the differences between models arx443 and arx225 is not significant to warrant the complexities of developing a controller with a higher model order. Thus, the treadmill dynamics is described by the transfer function given in Table 4.1 for arx225. This transfer function relates the speed input (control speed) to the measured treadmill speed output (Vbelt). Figure 4.4 and Figure 4.6 further compare the performance of model arx225 in open-loop and closed-loop situations.

The controller incorporates an integral action that provides for any offset that may arise during tracking. The closed loop speed controller was designed with a rise time of 10s. Figures 4.6, 4.7, 4.8 and 4.9 show that the speed controller performance was good. Thus, the speed controller copes well with the highly non-linear and time-varying parameters of the plant, and is robust enough to manage both running and walking on the treadmill. Throughout these experiments, a fixed controller with stationary parameters is used (Table 4.2).

For the disturbance rejection test, the treadmill was started without a subject on the treadmill (i.e., no load) and at 62s, a person jumped on to the treadmill. The person jumped off the treadmill at 140s. The treadmill then continued to operate in the no-load situation until the end of the experiment. The purpose of this test was to represent abrupt changes, thus simulating disturbances. Figure 4.9 shows spikes at those periods (62s and 140s) which are successfully rejected by the controller thereafter. This result demonstrates that the treadmill speed controller can adjust reasonably well to these changes and situations.

4.4 Treadmill Automation (Treadmill Position Control)

In this section the steps to design and test the position controller are discussed. The results of position control tests are also presented. The section ends with discussions on treadmill position control.

4.4.1 Position Controller Design

This section describes the work carried out in achieving a treadmill positioning control system. The treadmill model and the speed controller without integral action are further used. The goal here is to stabilise the system and to track the desired input without overshoot.

Two steps are carried out to design and test the treadmill position controller using a sample interval of 2Hz for the inner loop while the sampling time for the outer loop was tested at different sampling time. In addition, the inner loop did not include an integral action. The inner loop is incorporated to include the speed controller. We report in this thesis a sampling interval of 2Hz for both the inner and outer loops.

Step 1: Position control design

Similarly to the speed controller, the desired closed-loop rise-time and damping (zeta) parameters are chosen based on our desired response of the position controller to changes in a subject's position. The inner closed loop rise time is designed to be 5s while the outer closed loop rise time is to be 8s, since the inner loop should be as fast as possible. The results are simulated on the computer, before implementation.

Step 2: Closed-loop position tracking test

To ascertain the performance of this controller a closed-loop tracking test was performed by setting a constant distance/position reference. Subjects are tested with the controller developed (from section 4.4.1 step 1) for the purpose of investigating the possibility of maintaining a certain position relative to the treadmill. The subject's current position

automatically determines what the speed of the treadmill should be to maintain a desired position on the treadmill.

4.4.2 Position Controller Results

Typical results of the position controllers are presented in this section. Firstly, the position controller design parameters are presented. This is followed by sample results from computer simulations of the closed-loop situations. Lastly, the result of closed-loop position tracking test are presented.

The controller parameters for the position control system are shown in Table 4.3.

Table 4.3: Position controller design parameters

Parameter	Values
rise time	8s
observer rise time	6s
zeta	0.999
observer zeta	0.999

Figures 4.10, 4.11 and 4.12 show the computer simulation results in a Matlab/Simulink environment. The computer simulation depicts the model of a runner on the treadmill with an initial speed of 1100mm/s at the start of the experiment, which started increasing at 100s and reached 1150mm/s at 150s, and this final speed was maintained throughout the experiment which lasted 300s (Figure 4.11).

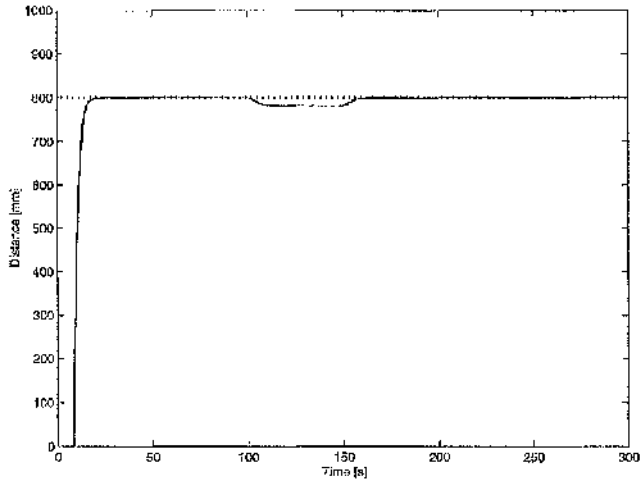

Figure 4.10: Sample simulation results from SIMULINK implementation of the position control system (dotted line is the reference position while the solid line is the measured position)

In addition, Figure 4.10 shows the computer simulation tracking result of the position controller while its corresponding inner and outer-loop control signals are depicted in Figure 4.12. Between 100s and 150s the position of the reference point decreases as the speed of the runner increases (Figure 4.10) compared to the targeted position of 800mm, but was compensated for by the designed positioning feedback control system.

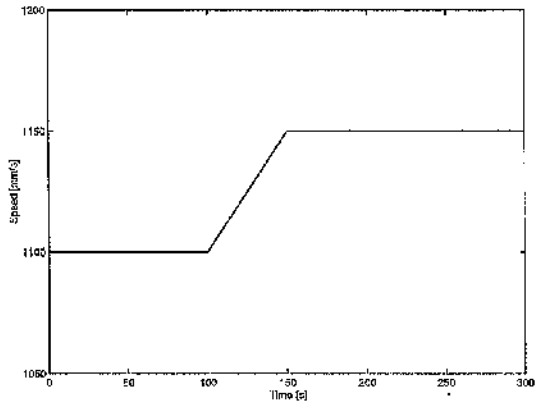

Figure 4.11: Computer simulation with a model of a subject with a relative speed of 1.1m/s at the start of the simulation to 100s was ramped to 1.15m/s at 150s and maintained at that speed for the duration of the experiment

The controller was used in a real-time implementation with a subject on the treadmill that had an ultrasonic device incorporated (as in Figure 3.1) to investigate the feasibility of the approach. Figure 4.13 shows the result of one of the experiments during this investigation. The corresponding inner loop and outer loop control signals are shown in Figure 4.15 and Figure 4.16 respectively. In addition, Figure 4.14 shows the actual measured distance and the filtered (Butterworth low-pass filter) distance. The filtered distance was the distance fed back to the position controller system shown in Figure 4.13.

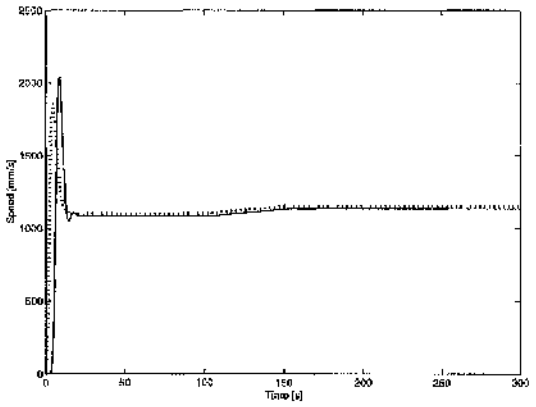

Figure 4.12: Controller signals results obtained from the computer simulation of the position control system (dotted line is the command speed signal from the outer loop position controller while the solid line is the control speed signal from the inner loop speed controller)

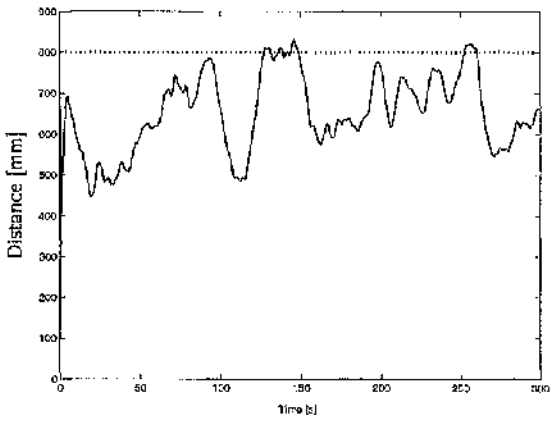

Figure 4.13: Closed-loop feedback position tracking test results (dotted line is the reference position while the solid line is the filtered position obtained from measurement)

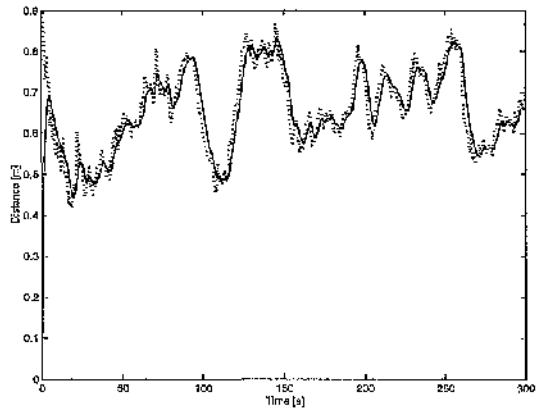

Figure 4.14: Actual (dotted line) and filtered position (solid line) during the treadmill automation implementation

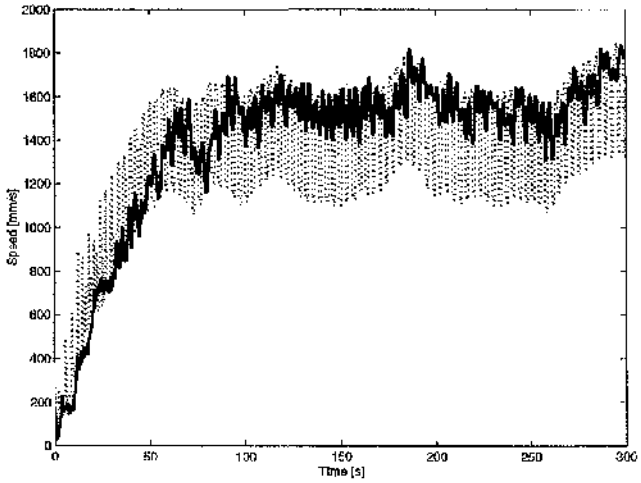

Figure 4.15: Inner loop control signal results (dotted line is the control signal to the treadmill while the solid line is the measured speed from the treadmill)

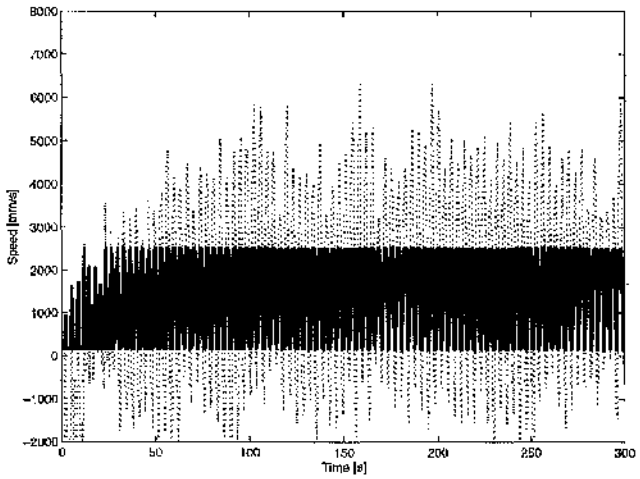

Figure 4.16: Outer loop control signal results (dotted line is the control signal before speed limiter while the solid line is the control signal, a reference speed to the inner loop)

4.4.3 Discussion on Position Control

In our treadmill automation (feedback position control system), the treadmill speed is controlled through a computer-controlled system via feedback of a subject's relative position. As the subject moves backwards the controller decreases the treadmill speed and vice versa.

The results presented here did not meet the acceptable performance standard required by the system, even though the speed controller result was satisfactory. It can be seen that the speed controller is limited by the treadmill bandwidth which thus affected the positioning control system. This is a primary and fundamental limitation of the treadmill. In addition, there is a major problem in sensing a subject due to the low fidelity of the low-cost sensor (sensing limitations). This degrades how the treadmill positioning system responds to the subject's changes/movement. In addition, magnetic, mechanical, optical, and inertial sensors all have major drawbacks when the requirement is for high accuracy and low latency (Table 3.1). A suitable solution is required before a successful

treadmill automation system can be developed. Furthermore, body motion is not as fast as leg motion, so the assumption of using a body position measurement incorporates a delay which is significant in the controller design.

The long delay in the treadmill's response could lead to the subject falling off the back of the treadmill or hitting the front of the treadmill and causing injury.

In the computer simulation, a constant situation was assumed; however, it is difficult for a human to maintain a constant speed while running or walking on the treadmill. This is due to the uncertainty of body movement and also to the inertial force caused by the acceleration/deceleration of the subjects during the treadmill exercise. This could not be rectified during implementation with real subjects. Thus, the rate of acceleration/deceleration is critical and must be sufficiently addressed so that it does not degrade the performance of the positioning control system. This effect could also be crucial during transition between walking and running, making the nonlinear dynamics of movement more pronounced.

Furthermore, during transients, there are dynamic interactions between the treadmill position control and the natural human controller, and this affects the controller performance significantly. This dynamic interaction can result in instability. For the position control system to become practical, these problems need to be solved. In addition, there is a need to develop control laws that can result in a stable coupled system with the capacity to accelerate/decelerate as the subjects react to the inertia of motion on the treadmill.

The treadmill automation experimental results complement the recent paper of Minetti et al, 2003 [75], which discusses the limitation of the treadmill feedback position system. In their study, a similar experimental set-up to the one reported in this thesis is used. The paper further discusses the potential application of this methodology in physiology, biomechanics and pathology of locomotion. The paper also focusses on the

spontaneous speed of walking and running in man. Thus, the feedback-controlled treadmill setup is then use to determine the speed range at which human neither walk nor run.

4.5 Discussion and Conclusions

The feasibility of treadmill automation using a low-cost non-contact position sensor was investigated. Based on the results of the experiments with this set-up, it is concluded that treadmill automation is not feasible and practicable. It could be possible with a high performance (faster) treadmill which may improve accuracy and safety which is unavailable on the treadmill tested. This is because the treadmill used in this study cannot achieve a faster performance in terms of response time, and is therefore inaccurate and imprecise. The findings also show that the system is dependent on initial operating conditions (initial speed of both the treadmill and of the subject). We also observed the following complex dynamic behaviour during treadmill automation:

- Spontaneous variability arising from non-linearity in the system (caused by the effect of chaos and bifurcations due to the subject's spontaneous movement/motion and mode confusion - walking, transition between walking and running, and running - leading to oscillation and body position changes thus introducing noise).
- Interactions between different control systems (human control and our developed position control system) causing confusion.

Other major limitations include:

- Bandwidth limitation (the physical limitation of the hardware, i.e. the treadmill has a communication bandwidth capacity of 0.05s while the ultrasonic device has a capacity of 0.1s).
- Delay in the system (which is of the order of 5 samples), results in a deadtime of approximately 0.25 s which is significant in human motion control. The long delay between changes in the controlled variable and the reaction of the measured variable greatly limits the controller performance. Thus, the time delay is one of the

main factors that compromise the timing accuracy of the controller. Furthermore, the delay time is highly time dependent and could result in a stability problem.

5 CONTROL OF HEART RATE

This section focuses on developing, testing and evaluating a controller that will control the heart rate of subjects. The input to the treadmill system (comprising of the subject running on the treadmill) will be the speed while the output from the system will be the heart rate. This approach is a single input-single output HR closed-loop control system. The controller is then further tested by comparing it with the available in-built HR controller of the treadmill.

5.1 Experiment Design and Protocol

This section will describe the experimental setup, subjects and experimental tests (identification and HR control tests).

5.1.1 Experimental Set-up

The experimental set-up is shown in Figure 3.1 on page 33. In this section, the treadmill, HR polar belt and computer are used.

5.1.2 Subjects

Six volunteer subjects participated in the experiments. None of the subjects had any history of neurological disorder or disease. Consent was obtained from all participants. Tests took place in the Rehabilitation Engineering laboratory in the James Watt Building (south), Mechanical Engineering Department University of Glasgow. The Faculty of

Biomedical and Life Sciences ethics committee reviewed and approved this study.

5.1.3 Identification Tests

Subjects performed a series of PRBS load exercise tests lasting for 20 minutes per visit per day on three different visits. The subject ran on the treadmill while the treadmill speed follows a pre-specified PRBS pattern which is pre-programmed on the PC. Thus, the treadmill speed changes between two levels at preset times. Heart rate was measured telemetrically from a Polar heart rate belt monitor worn round the subject's chest. This test was conducted to obtain data sets for system identification.

Figures 5.1 – 5.3 show the results of the open-loop test using the same PRBS input signal designed offline to excite three of the subjects for three different days. In the reproduced Figures, the solid line is for day 1, the dashed-dot line is for day 2 and the dotted line is for day 3 of the experiments.

Subject A

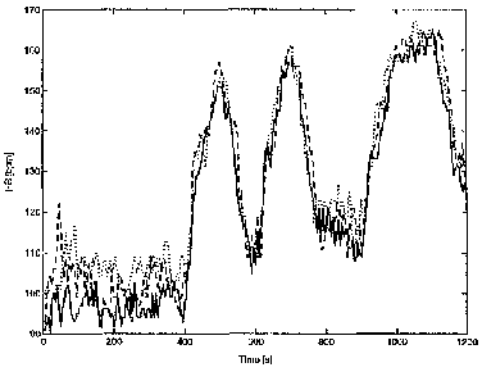

Figure 5.1: Results of open-loop HR test on subject A

Subject B

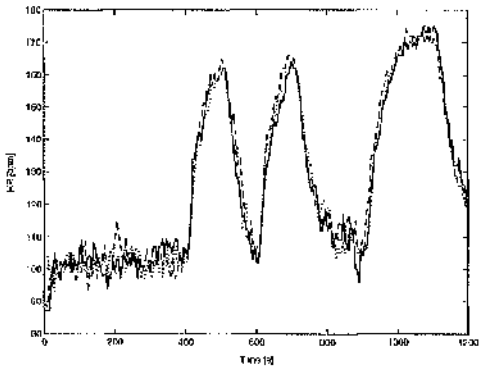

Figure 5.2: Results of open-loop HR test on subject B

Subject C

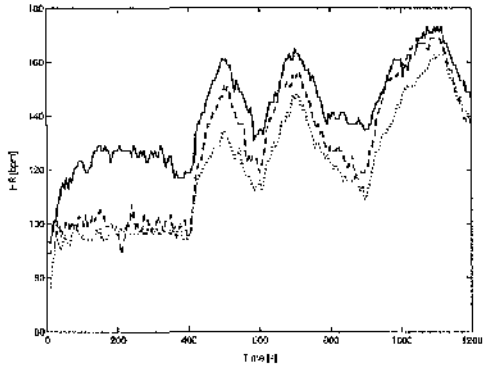

Figure 5.3: Results of open-loop HR test on subject C

5.1.4 HR Control Tests

Subjects performed HR control tests with a time duration ranging from 300s - 1200s depending on the type of HR reference signal. The subjects ran on the treadmill while a desired heart rate profile (reference signal) is sent to the treadmill via an HR feedback controller implemented in the computer. The treadmill speed is then automatically determined by the controller, whose parameters have been designed from a specification of closed-loop parameters using a model obtained from the identification tests. The reference signal consists of either a constant reference test, or a step test or a sequence of step tests for both the designed controller and the in-built HR controller. For HR controller comparisons, the tests were conducted in a randomised order with the controller tested first taken as test 1 and the controller tested second taken as test 2.

5.2 Open-loop Identification and Modelling of HR

The development of a HR feedback closed loop controller requires a HR model. Different trial and error tests were carried out to determine the speed range that would initiate

the kind of heart rate range one wants while obtaining all other necessary parameter (sampling rate, open loop rise time, etc.) All the three subjects use a PRBS signal with a mean speed of 1600mm/s, and amplitude of 800mm/s for 1200s at a sampling interval of 5s.

The data sets obtained from the three subjects that participated in the identification tests were averaged over the number of experiments. Figure 5.4 shows the averaged data results for the three subjects. These averaged data sets were compared, and one of the averaged data set was selected for system identification in order to obtain a linear model. The selection was made because the averaged HR data for the three subjects were identical. Thus, the data sets from the other subjects were discarded. A possible alternative is to use the averaged data of one of the subject to cross-validate the other two subjects.

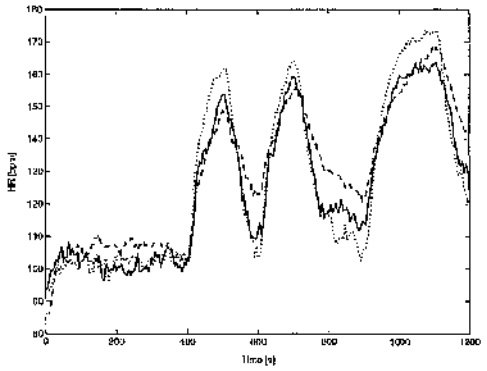

Figure 5.4: Plot showing the average of all the identification experiments for each subject (solid line is Subject A, dotted line is Subject B, and dashed line is Subject C)

Figure 5.5 depict the time plot of the data set (Subject A in Figure 5.4) which is used for model identification results.

The data set was first normalised by removing the initial values (HR at rest and initial

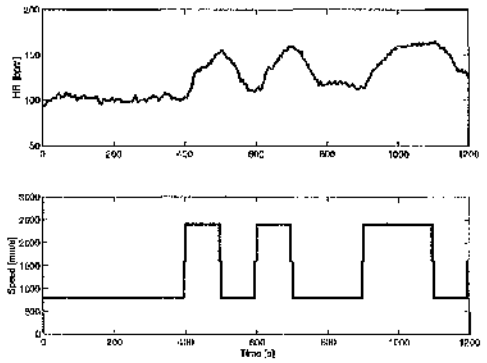

Figure 5.5: Time plot of open-loop input and output data set from PRBS signal (the upper plot shows the output signal while the bottom plot shows the input signal)

speed). Then, the first 275s of the data set was discarded. The data set from 276s to 795s was used as the working data and the data set from 796s to 1200s was used as the validation data. Section 3.2.1 discusses the procedure for modelling estimation and validation to determine a suitable model.

Table 5.1 illustrates the performance characteristics of different models obtained during model identification process using the averaged HR data set of Subject A. Note that the fitness is defined by eqn. (3.5) on page 42.

Table 5.1: Comparisons between several different HR models

Model	Rise-time (s)	Fitness (%)
arx211	200	75.10
arx311	165	72.99
arx441	145	67.51
arx411	175	74.49
arx111	195	74.23

From Table 5.1, arx111 model is chosen because the magnitude of change in higher order (arx211 or arx411) does not justify the complexity of using this order in controller design. The generic arx(n_a,n_b,nk) model structure is given in Eqn. (3.2).

The model is a first order model with delay and has the following parameters at a sampling interval of 5s.

$$A(q^{-1}) = 1 - 0.9451\ q^{-1}$$
$$B(q^{-1}) = 0.002794\ q^{-1}$$

5.3 Controller Design and Implementation

After thorough examination of the various appropriate models, a first-order model (identified in section 5.2) was selected and used for controller design based on the algorithm developed using the controller approach (see page 43). The HR controller in Figure 5.6 has the design specification shown in Table 5.2. The values of 0.999 for both zeta and observed zeta in that table indicates that the controller was critically damped.

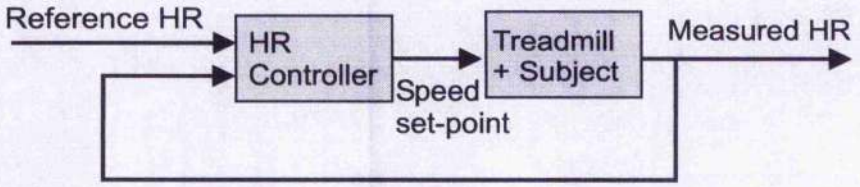

Figure 5.6: Block diagram of the HR closed-loop feedback control system

Table 5.2: HR controller design parameters

Parameter	Values
rise time	100s
observer rise time	80s
zeta	0.999
observer zeta	0.999

5.4 Controller Comparison

The following statistical equation (standard deviation) is used to compare our HR controller with inbuilt treadmill HR controller.

$$\mathrm{Std}(HR_{error}) = \sqrt{\sum_{i=1}^{N} \frac{(HR_{ref} - HR_{act})_i^2}{N-1}} \tag{5.1}$$

where i (is an integer multiple of sampling intervals Ts, 5s) at every sampling interval and N is the test duration/sample interval (i.e., the data set has N samples). HR_{ref} is the reference HR and HR_{act} is the measured HR.

5.5 HR Closed-loop Control Results

Here the results of the fixed controller implemented on subjects during a series of tests performed on the treadmill are presented. The series of tests include constant load reference test, step test and a sequence of step tests. For each test on each subject, the order of the test was randomize in order to compare our HR controller with inbuilt controller, i.e. the controller tested first is taken as test 1 and the controller tested second is referred to as test 2. The controller was tested with three subjects (these subjects did not take part in previous experiments to identify the HR model).

Tables 5.3 – 5.10 show the summary of the HR comparison tests performed on the subjects which correspond with Figures 5.7 – 5.14 closed-loop tracking results plot respectively.

Subject D

Figure 5.7 shows the result of a sequence of IIR step tests performed by subject D.

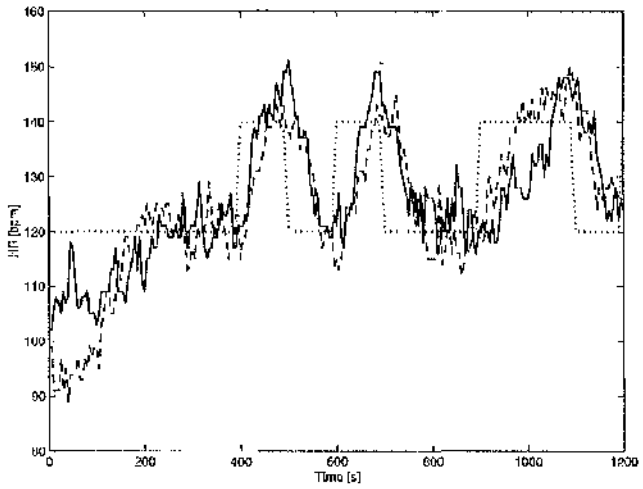

Figure 5.7: Results of a series of square HR load tests for subject D (reference HR is dotted line, inbuilt HR is dashed line and designed controller is solid line)

Table 5.3: Results of a series of square HR load tests for subject D

Caption	in-built	designed controller
Standard deviation of HR error	12.6089 bpm	11.3741 bpm
Minimum HR	89 bpm	102 bpm
Maximum HR	150 bpm	151 bpm
Test order	test 1	test 2

The designed HR controller is better than the in-built treadmill HR controller based on the results of the standard deviation of HR error shown in Table 5.3. In this experiment, the inbuilt controller was the first test performed (test 1) while the designed controller was test 2 (the controller tested second).

Figure 5.8 is a closed-loop IIR step test result. The result shows that the designed IIR control is significantly better than the in-built treadmill HR controller (see Table 5.4).

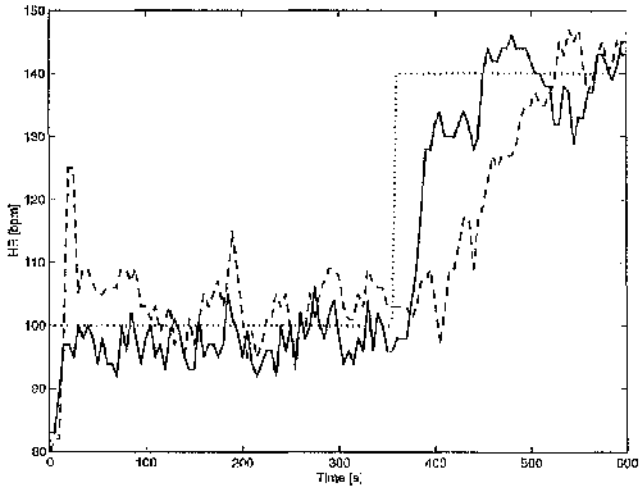

Figure 5.8: Results of the step HR load test for subject D (reference HR is dotted line, inbuilt HR is dashed line and designed controller is solid line)

Table 5.4: Results of the step HR load test for subject D

Caption	in-built	designed controller
Standard deviation of HR error	14.8313 bpm	9.8552 bpm
Minimum HR	80 bpm	83 bpm
Maximum HR	147 bpm	146 bpm
Test order	2	1

However, this subject did not participate in a constant HR test.

Subject E

Figure 5.9 presents the result of a closed-loop HR control test for Subject E.

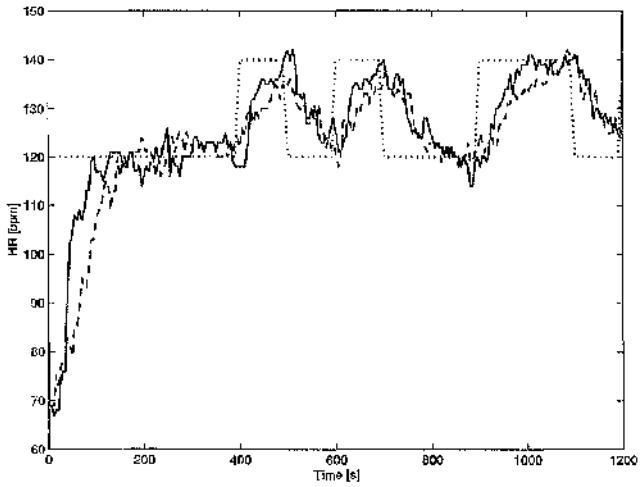

Figure 5.9: Results of a series of square HR load tests for subject E (reference HR is dotted line, inbuilt HR is dashed line and designed controller is solid line)

Table 5.5: Results of a series of square HR load tests for subject E

Caption	in-built	designed controller
Standard deviation of HR error	13.8666 bpm	12.7645 bpm
Minimum HR	69 bpm	67 bpm
Maximum HR	142 bpm	142 bpm
Test order	2	1

The results show that the designed HR controller is moderately better than the inbuilt HR controller (Table 5.5).

Figure 5.10 shows Subject E's feedback control test results for a step HR load test.

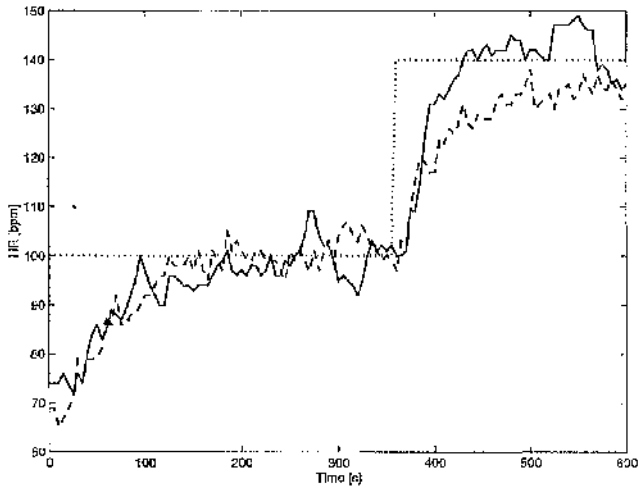

Figure 5.10: Results of the step HR load test for subject E (reference HR is dotted line, inbuilt HR is dashed line and designed controller is solid line)

Table 5.6: Results of the step HR load test for subject E

Caption	in-built	designed controller
Standard deviation of HR error	13.5324 bpm	11.8950 bpm
Minimum HR	65 bpm	72 bpm
Maximum HR	138 bpm	149 bpm
Test order	1	2

These results show that the designed HR controller performed better than inbuilt treadmill HR controller.

Subject E performed a closed-loop constant HR load test and the results of the experiment is shown in Figure 5.11, which is also summarised in Table 5.7.

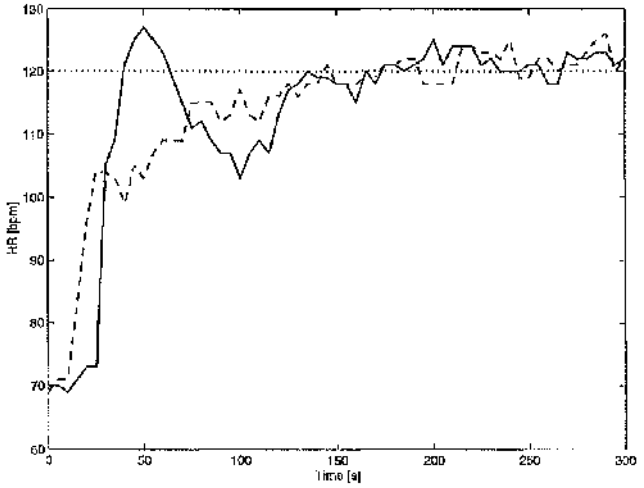

Figure 5.11: Results of the constant HR load test for subject E (reference HR is dotted line, inbuilt HR is dashed line and designed controller is solid line)

Table 5.7: Results of the constant HR load test for subject E

Caption	in-built	designed controller
Standard deviation of HR error	13.0336 bpm	15.1580 bpm
Minimum HR	69 bpm	69 bpm
Maximum HR	126 bpm	127 bpm
Test order	2	1

The results show that the treadmill in-built HR controller is moderately better than the designed HR controller based on the standard deviation of HR error. However, the minimum HR for both controllers is 69bpm while the maximum HR for both controllers' differs by 1bpm.

Subject F

A closed-loop test using a series of square HR loads profile is tested on Subject F and the results of this test is presented in Figure 5.12, and then summarised in Table 5.8.

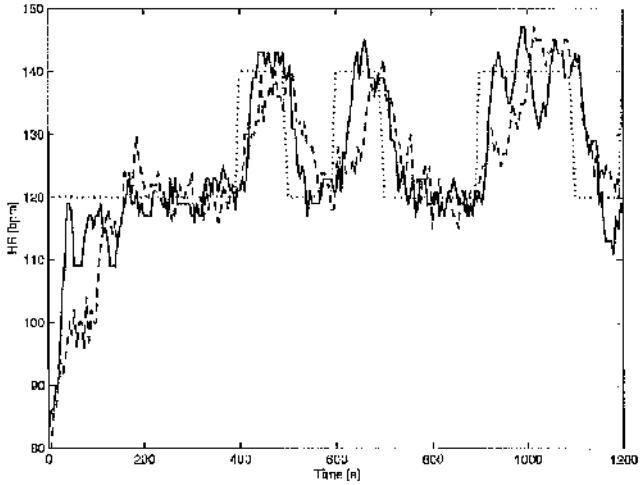

Figure 5.12: Results of a series of square HR load tests on subject F (reference HR is dotted line, inbuilt HR is dashed line and designed controller is solid line)

Table 5.8: Results of a series of square HR load tests on subject F

Caption	in-built	designed controller
Standard deviation of HR error	11.1518 bpm	8.8176 bpm
Minimum HR	80 bpm	83 bpm
Maximum HR	147 bpm	147 bpm
Test order	2	1

The results show that the designed HR controller is significantly better than the in-built treadmill HR controller.

Figure 5.13 and Table 5.9 show a closed-loop test result for Subject F.

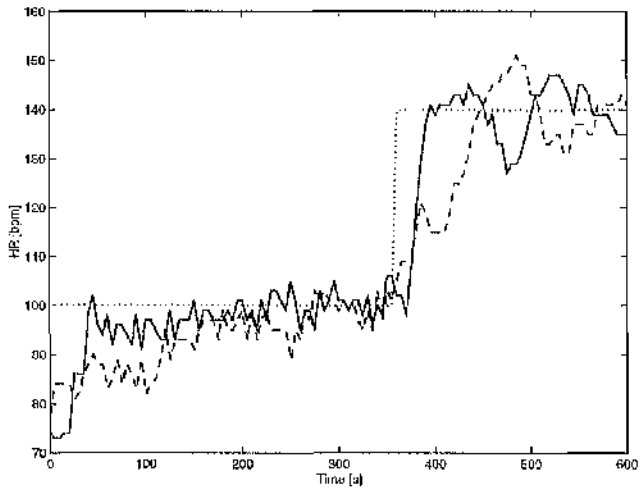

Figure 5.13: Results of the step HR load test for subject F (reference HR is dotted line, inbuilt HR is dashed line and designed controller is solid line)

Table 5.9: Results of the step HR load test for subject F

Caption	in-built	designed controller
Standard deviation of HR error	11.8071 bpm	10.1246 bpm
Minimum HR	78 bpm	73 bpm
Maximum HR	151 bpm	147 bpm
Test order	1	2

The designed HR controller performs better than the treadmill in-built HR controller based on these results.

The HR feedback control test results for Subject F using a constant HR load as reference HR is depicted in Figure 5.14.

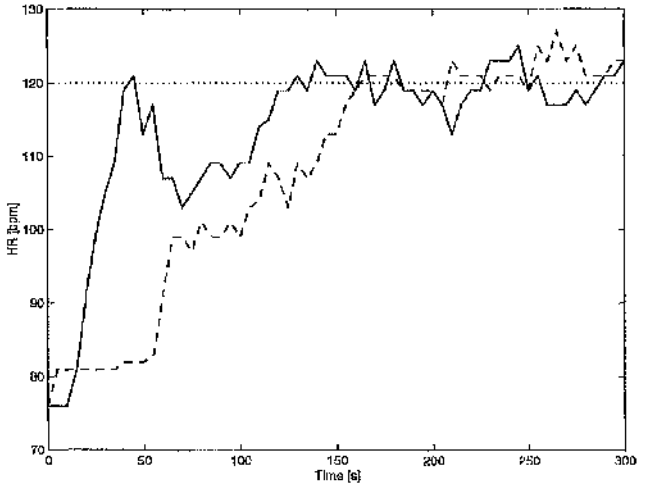

Figure 5.14: Results of the constant HR load test for subject F (reference HR is dotted line, inbuilt HR is dashed line and designed controller is solid line)

Table 5.10: Results of the constant HR load test for subject F

Caption	in-built	designed controller
Standard deviation of HR error	18.4602 bpm	12.3699 bpm
Minimum HR	76 bpm	76 bpm
Minimum HR	127 bpm	125 bpm
Test order	1	2

The results of this constant load test show that the designed controller performed significantly better than the inbuilt controller.

From all these series of results, only the result from Figure 5.11 (Table 5.7) shows that the treadmill in-built HR controller performs better than the designed HR controller.

Figures 5.15 – 5.17 show the average of each set of similar tests for all the subjects while Tables 5.11 – 5.13 show the corresponding summary of the results respectively.

Average of each set of similar tests for all the subjects

Figure 5.15 shows the average of the combination of the series of square load tests performed by Subjects D, E and F. This Figure is based on the average of the closed-loop results plotted in Figures 5.7, 5.9 and 5.12.

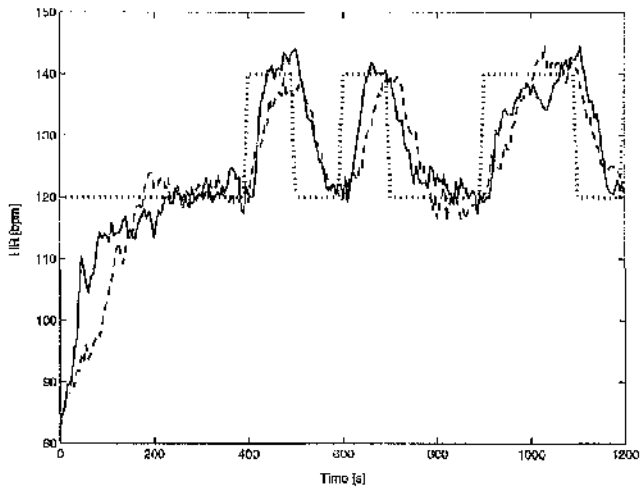

Figure 5.15: Results for the series of square HR load tests (reference HR is dotted line, inbuilt HR is dashed line and designed controller is solid line)

Table 5.11: Results for the series of square HR load tests

Caption	in-built	designed controller
Standard deviation of HR error	11.8114 bpm	10.1762 bpm
Minimum HR	82.75 bpm	84 bpm
Maximum HR	144.75 bpm	144.5 bpm

Based on this averaged, the designed HR controller performs better than the treadmill

inbuilt HR controller.

The average of all the step HR load control tests for all the three subjects is plotted in Figure 5.16.

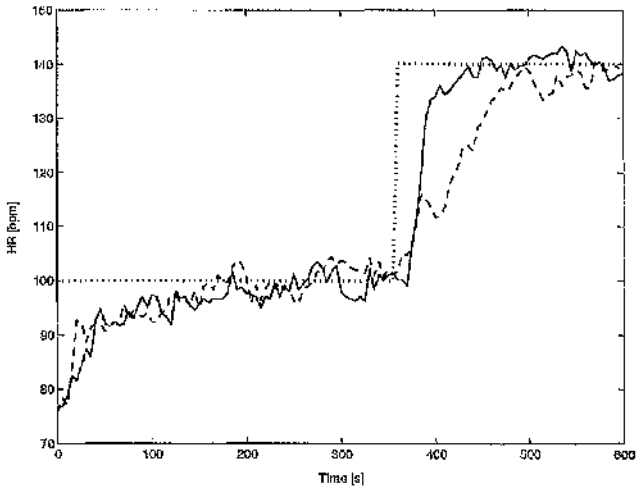

Figure 5.16: Results for the step HR load test (reference HR is dotted line, inbuilt HR is dashed line and designed controller is solid line)

Table 5.12: Results for the step HR load test

Caption	in-built	designed controller
Standard deviation of HR error	11.5549 bpm	9.7203 bpm
Minimum HR	75.7 bpm	76.7 bpm
Maximum HR	140.3 bpm	143.3 bpm

The results support the fact that the designed HR controller performs better than the inbuilt treadmill HR controller.

Similarly, the results of all the constant HR load control tests are averaged and then presented in Figure 5.17. Table 5.13 summarises and compares the result.

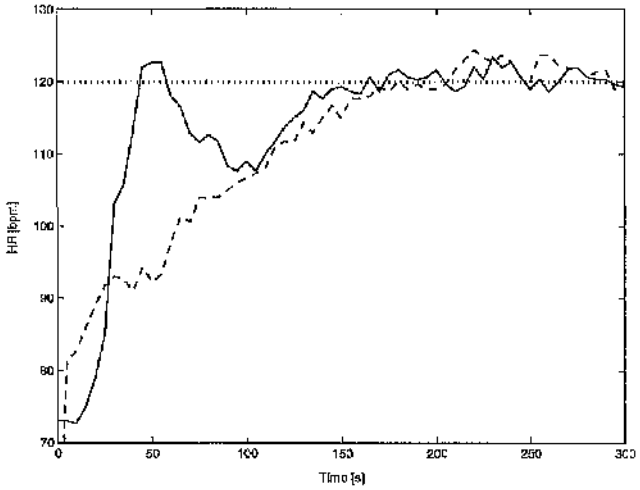

Figure 5.17: Results for the constant HR load test (reference HR is dotted line, inbuilt HR is dashed line and designed controller is solid line)

Table 5.13: Results for the constant HR load test

Caption	in-built	designed controller
Standard deviation of HR error	17.6885 bpm	14.8790 bpm
Minimum HR	70.3 bpm	72.3 bpm
Maximum HR	124.3 bpm	123.3 bpm

The results also confirm that the designed HR controller performs better than the treadmill inbuilt HR controller.

A bar chart showing the summary of HR results as a function of the standard deviation of HR error is displayed in Figure 5.18. This Table shows that the designed HR controller is generally better that the in-built HR controller.

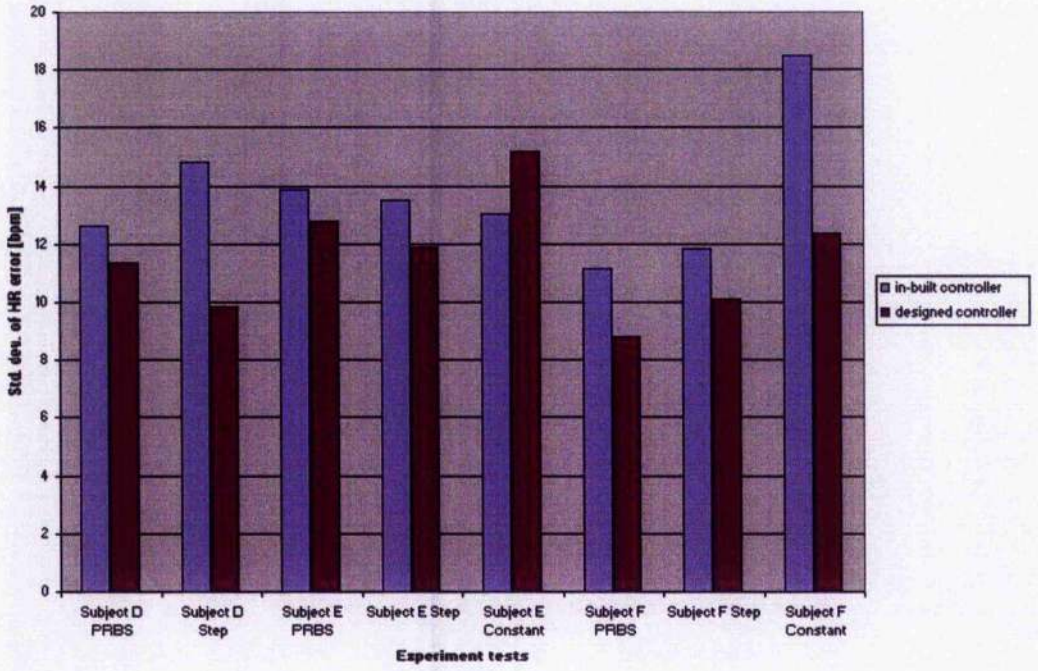

Figure 5.18: Summary of HR tests

5.6 Discussion

The results of the model identification tests show that a simple linear first order transfer function is able to accurately model the HR dynamics. In addition, the closed-loop HR controller based on this model provided accurate tracking of various HR reference set-points. The slight overshoot after a steady-state HR level is reached (after approximately 100s from the start of the experiment) shows the effect of HR variability (HRV).

All the results were from the same fixed controller and protocol except that the reference inputs were different. The fixed controller is designed for one of the subjects (Subject A) and implemented on other subjects (Subjects D, E, F) to test for the robustness of the controller. The tests confirm that the controller is sufficiently robust and caters for individual (inter/intra individual) differences.

The evaluation of the designed HR controller's performance was made by comparing with the treadmill in-built HR controller using a constant HR level, step HR level and a series of step HR levels. From the results of these tests, the HR standard deviation from the reference set-point was computed. In addition, minimum and maximum HR were calculated. To remove bias from the results, the tests were randomised in the order which the control tests were performed (i.e., the test performed first as test 1 and the test performed second as test 2). The results confirm that the designed controller is robust to cater for individual differences without the need to specifically alter the controller for each subject.

The ability to achieve a specified exercise intensity can therefore be achieved by using this automatic HR controller. However, automatic HR controllers may have limitation when used for disabled subjects because the subject's HR may be impaired, or because of irregular heart beats which can be inaccurately measured by the HR monitor. Hence, the reasons why we excluded hypertensive, diabetic, heart failure subjects, etc., from our experiments. Thus, the HR controller limitation is governed by our inclusion criteria.

In addition, the polar HR monitor has limitations when used for certain measurements because it is not designed to detect arrhythmia or irregular rhythms, and will interpret them as noise or interference. The HR monitor may not work for subjects with a medical condition such as bundle branch blocks[1] or atrial fibrillation[2], etc. It could also produce

[1] occurs when transmission of the heart's electrical impulse is delayed or fails to conduct along the bundle branch (a specialised conducting tissue in the ventricles) and can be detected by electrocardiogram, ECG.

[2] is a rhythm disturbance of the atrial that results in irregular and chaotic heart beat.

abnormal readings due to poor contact between the skin and the electrodes of the transmitter, or due to a loose strap around the chest of the subject leading to movement of the strapped belt. It could also pick up a signal from all other transmitters (such as radio signals, ultrasonic waves, etc.) within its range resulting in abnormally high readings. Furthermore, erratic readings on the receiver can be caused by electromagnetic disturbances from computers, cell phones, etc. Therefore, $\dot{V}O_2$ control may be more appropriate for controlling exercise intensity.

The effect of fatigue is shown by the non-linear HR results which is evident in the last session of the test (i.e. from 800 -1200s) in Figures 5.1 – 5.3. Similarly, there could be a physical conditioning effect within individuals due to health and fitness, or a training effect which can change a subject's HR level. Furthermore, the effect of increase in temperature (i.e. changes in body temperature during exercise) or changes in blood volume can alter HR. However, the robustness of the HR controller compensates for these effects.

From various experiments carried out, it is evident that transition between walking and running is not a critical factor to be considered. However, this may be crucial during the control of $\dot{V}O_2$.

5.7 Conclusions

A fixed controller for the control of HR during treadmill exercise/training has been presented. Comparisons of the results from experiments of the HR controller with an in-built treadmill HR controller indicate that the developed controller is superior, i.e., it exhibits a faster response and also maintains HR stability except for normal fluctuations, which is a common phenomenon of HR often referred to as heart rate variability. These fluctuations also occur with the in-built HR controller.

The main contributions of this chapter are:

1. Estimated the transfer function from speed to HR useful for the design and development of a HR control system.

2. Designed and developed a HR controller from the linear HR model.

3. Examined the performance of the HR controller, which was found satisfactory.

4. Evaluated and compared the designed HR controller with the in-built treadmill HR controller.

5. Observed that the designed and developed HR controller is superior to the in-built HR controller in terms of speed of response and steady state errors (based on the standard deviation of the difference between the reference HR and the measured HR).

6 CONTROL OF OXYGEN UPTAKE

The experiment on the control of HR presented in chapter 5 provided a background insight into the control of oxygen uptake. The results also show that HR could be used to control exercise intensity. Furthermore, the control of HR has become a widely used means to assess cardiovascular function in lieu of $\dot{V}O_2$ and thus control exercise intensity. However, if the HR is blunted due to disease (as discussed in section 5.6 on page 90), then control of HR will be an inappropriate means to prescribe exercise intensity that is important for increasing fitness and improving health. Thus, this chapter describes the experimental work to investigate the feasibility of a more effective means of controlling exercise intensity, i.e., investigating the control of $\dot{V}O_2$ during moderate treadmill exercise.

Therefore, the primary aim of the investigation carried out and discussed in this chapter is to investigate the possibility of controlling $\dot{V}O_2$ in real-time via the development of a controller. This will enable an understanding of $\dot{V}O_2$ in the realms of real-time control.

A $\dot{V}O_2$ feedback control has several potential advantages over HR feedback control and also over using ACSM[1] published data, since the controller will adjust to adapt to $\dot{V}O_2$ responses measured from individual subjects. In addition, when HR is impaired or if there is an irregular heart beat (arrhythmia), as may be common with disabled people, the $\dot{V}O_2$ controller compensates for these (false heart beat since $\dot{V}O_2$ is not affected by these premature heart beat) changes (while in this case of an HR controller, it will be ineffective, inappropriate and dangerous).

Other benefits envisaged of $\dot{V}O_2$ feedback controllers in exercise and rehabilitation are:

[1] American College of Sports Medicine

1. To remove the routine task of manually monitoring $\dot{V}O_2$ (this will be carried out by an automatic controller that is hoped to be developed).

2. To accurately and precisely control exercise intensity through $\dot{V}O_2$ which will be more beneficial in clinical setting and rehabilitation therapy. Moreover, the advantage of using a model for automatic control will be verified.

3. Advantageous because automatic controllers have abilities to be robust and thus able to cope with inter-individual and intra-individual variability or changes.

4. Serve as a means for determining $\dot{V}O_{2_{max}}$ (this can be achieved by ramping $\dot{V}O_2$).

Another advantage of controlling $\dot{V}O_2$ is that it allows exercise intensity to be constrained within a domain in which fat may be preferentially oxidised and thus using a $\dot{V}O_2$ control system will be beneficial.

However, the experimental apparatus (MetaMax 3B) is expensive and may be complex to use on a daily basis. Thus, for a given subject, the relationship between HR and $\dot{V}O_2$ may be periodically recalibrated with this system in order to maximise sustainable exercise intensity. This is because the HR control provides a proxy for $\dot{V}O_2$ in the regions where HR and $\dot{V}O_2$ are linear.

In this thesis, the control of $\dot{V}O_2$ is to be achieved by varying the treadmill speed whilst maintaining the treadmill gradient at a constant level.

6.1 Experimental Procedures

6.1.1 Subjects

Nine healthy active males who undertake regular aerobic exercise participated in the study. All subjects were free of cardiac and pulmonary disease and had no medical history of cardio-respiratory or neurological disease, nor acute upper respiratory tract infection. Before participation, each subject was familiarised with the experimental procedure and was informed of the possible risk associated with the experiments and the

safety procedures in place. Subjects were provided with a consent form, health questionnaire and experiment procedure before taking part in the experiments. All the subjects gave their voluntary informed consent. The experimental study was reviewed and approved by the Faculty of Biomedical and Life Sciences ethics committee. The exclusion and inclusion criteria applied in this study are:

Exclusion Criteria

Subjects with the following were excluded from the study:

1. Asthma, diabetes, epilepsy, heart disease, a family history of sudden death at a young age, fainting bouts, high blood pressure, anaemia and muscle or joint injury.
2. Taking any medication that may adversely affect performance or health.
3. Taking recreational drugs.
4. Who have ingested alcoholic drinks in the previous 48 hours, were not allowed to take part in the study.

Inclusion Criteria

Subjects with the following were included in the study:

1. Male or female subject aged at least 18 years and normally no more than 35 years.
2. In good health at the time of testing.

6.1.2 Apparatus

Figure 6.1 shows a typical setup of the equipment during one of the experiments. The description of the apparatus was discussed earlier (section 3.1 on page 32). A Matlab interfaced for the MetaMax device was developed to enable a real-time implementation. Colleagues at the centre for rehabilitation engineering assisted in setting-up and calibrating the MetaMax during every experimental session. Data for the experiments were saved and simultaneously displayed (on-line) on Matlab/Simulink environment.

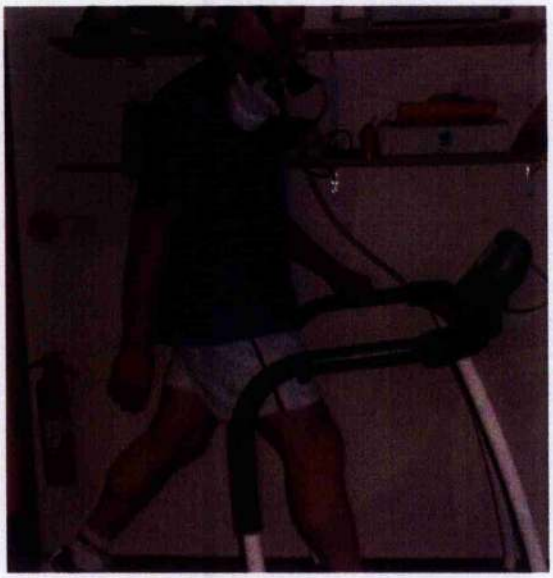

Figure 6.1: A subject during one of the experiment sessions

6.1.3 Experiment Protocols

Prior to each experimental session with subjects, the resting (HR, $\dot{V}_E$, $\dot{V}O_2$, RER, etc.,) values are obtained for 5 minutes.

Familiarisation Trials

This is an open-loop speed test that consists of two steps lasting for between 15 - 30 minutes:

Step 1: A subject determines a "minimum comfortable" running speed (the lowest running speed) and run on the treadmill wearing the mask at that speed. The steady-state $\dot{V}O_2$ corresponding to this speed was acquired. The subject ran at this speed for five minutes.

Step 2: A subject sets speed to a "moderate-sustainable" running speed level and run on

the treadmill wearing the mask at that speed level. The steady-state $\dot{V}O_2$ corresponding to this speed was acquired. The subject ran at this speed for five minutes.

A typical familiarisation trial result for a subject under open-loop conditions is presented in Figure 6.2.

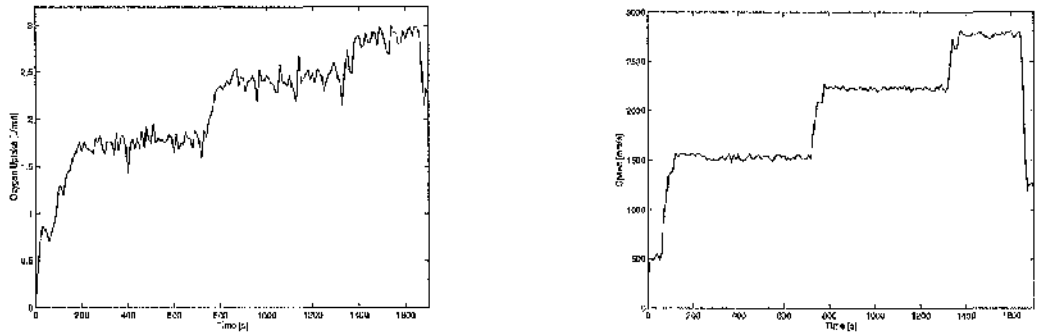

(a) $\dot{V}O_2$ response

(b) Treadmill Speed

Figure 6.2: Familiarisation results for a subject

Identification Tests

The subject ran on the treadmill while the treadmill speed follows a pre-specified PRBS pattern which is pre-programmed on the PC. Thus, the treadmill speed changes between two levels at preset times. $\dot{V}O_2$ and other variables are measured during this test. The experimental session lasted for approximately 40 minutes and was repeated for five days using the same protocol.

Following the tests, dynamic models describing oxygen uptake responses to the PRBS forcing function (treadmill speed) were computed off-line using systems identification approach. A model is then selected and used to compute feedback controller parameters for subsequent $\dot{V}O_2$ feedback control tests.

Feedback Control Tests

This is a closed-loop $\dot{V}O_2$ test lasting 40 minutes, and consists of the following stages:

Stage 1: First 10 minutes at 2.0L/min

Stage 2: Next 5 minutes at 2.5L/min

Stage 3: Next 5 minutes at 2.0L/min

Stage 4: Next 5 minutes at 2.5L/min

Stage 5: Next 15 minutes at 2L/min (with subjects having an option to stop after 5 minutes at this level if he/she so desire)

For subjects that could not run at these two levels, the levels were raised to 2.5L/min and 3.0L/min respectively or reduced to 1.5L/min and 2.0L/min. The level of 2.0L/min (or 2.5L/min or 1.5 L/min as the lower limit steady-state $\dot{V}O_2$) was chosen in order to be able to compare results between subjects.

6.1.4 Data Processing

In this study, the $\dot{V}O_2$ data were obtained from breath-by-breath data which were sampled and recorded at every second. The data at every second were processed with an algorithm that time-averaged this data over every 10 seconds which is the fixed control sampling interval (10 sec.).

Figure 6.3 shows breath-by-breath raw data and the algorithm processed data plotted on the same graph. In this Figure, the variability and noise effect are evident in the raw breath-by-breath data.

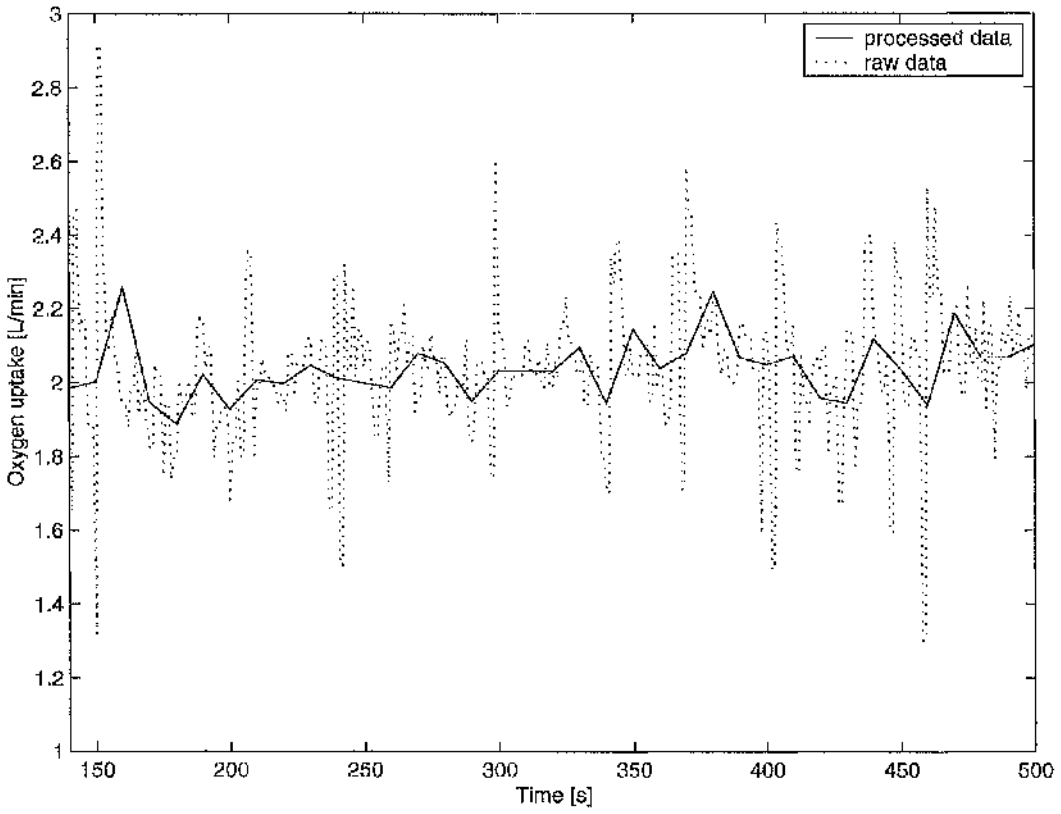

Figure 6.3: Raw data set and algorithm process data set

This averaging algorithm utilised for processing the raw breath-by-breath $\dot{V}O_2$ data recorded at every second is given by:

$$\dot{V}O_2(k) = \frac{1}{10}\sum_{i=0}^{9}\dot{V}O_2(k-i) \tag{6.1}$$

where k is an integer multiple of the sampling interval Ts = 10s.

The frequency response was checked and it did not affect the $\dot{V}O_2$ response of interest.

6.2 Oxygen Uptake Model Identification

In this section a system identification technique was used to obtain a $\dot{V}O_2$ model from input-output data. This approach has been extensively discussed in section 3.2.1 on page 37. The input to the plant (treadmill and subject) is treated as speed and the output from the plant is $\dot{V}O_2$. The input-output data used for system identification were collected from a series of repeat tests using the same protocol over five different days with the same subject. The experimental session lasted 40 minutes and only one experiment test was conducted on each day. Initially, three of the subjects performed a preliminary experiment using a similar protocol in order to determine which subject's data will be more repeatable, relatively consistent and less noisy. From the basis of this preliminary experiment, one of the subjects was selected to undergo that battery of tests for five times on separate days (see Identification Tests in section 6.1.3). The purpose of repeating the test for five times on separate days is to ensure repeatability of the data and to remove the daily variation effects.

The model identification and controller design has a sample time, Ts of 10s.

The procedure used for model selection are as follows:

Step 1: Firstly, the operating condition offsets (initial values) were removed from each data set since a linear model is to be obtained.

Step 2: Secondly, a range was selected for each data set covering a time span of 391 - 2400s (i.e., the samples for first 390s were removed because they represented the transient period).

Step 3: Next, each data set is used in turn as working data while the other data sets were used as validating data set and the following two iteration process (in Step 4) was performed.

Step 4: A model structure was obtained by varying a model order, n_a from 1 to 4, and

time-delay, nk from 1 to 4 while n_b was fixed at 1 in each case.

Step 5: The average fit for each model structure across all the data-sets is calculated and then compared.

Step 6: From this analysis, the best time-delay, nk is determined, so also the best model order.

Step 7: A model structure is chosen based on the best time-delay, nk with the simplest model order as the appropriate or best model even though higher model order with similar time-delay, nk may be marginally better.

Step 8: Since this model structure has five possible parameter sets depending on the dataset used for estimation, then the average fit for this selected model structure is estimated for each dataset.

Step 9: Finally, a model which has the best average model fit (based on Step 8) is selected and used as the nominal model.

The results of the Identification Tests (on page 98) conducted for 5 days are reproduced in Figure 6.4. The results are for Subject 3.

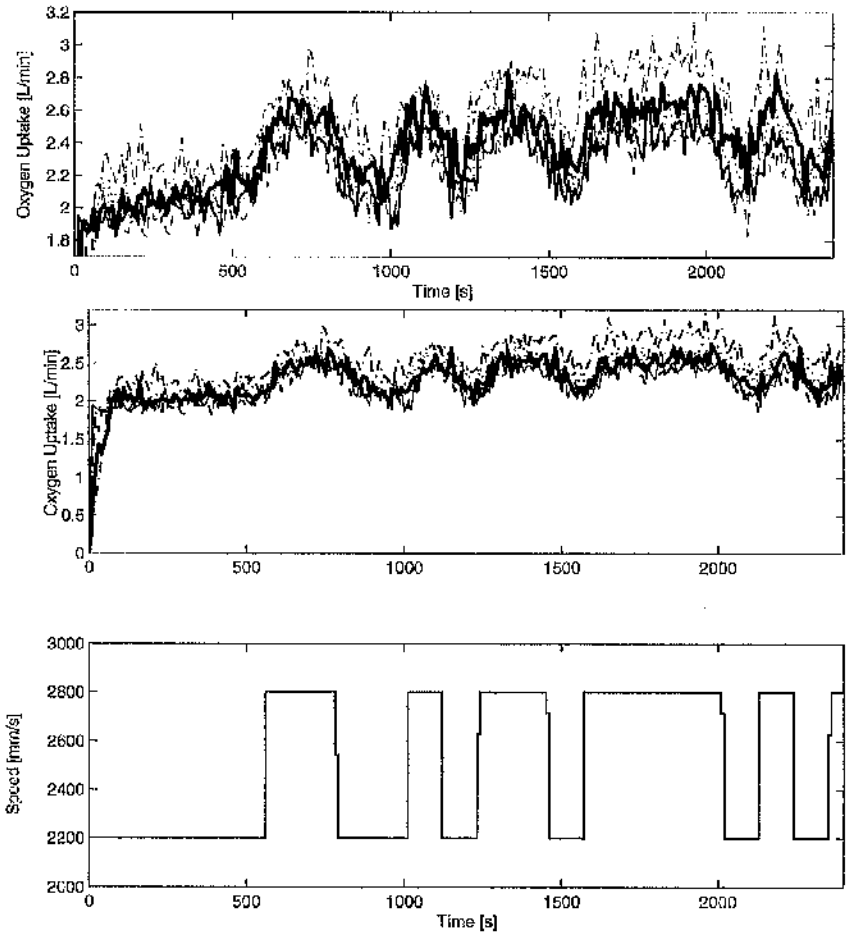

Figure 6.4: Results from the identification tests showing five different data set results obtained over five different experiments conducted on Subject 3.

Figure 6.5 shows a sample of a working and validation data using certain data-sets from Figure 6.4. It should be noted that the operating condition offsets (initial values) and the transient period samples have been removed from the data based on the procedure described in section 6.2, Step 1. The bottom plot in Figure 6.5 shows the speed forcing function as the input data (in PRBS form) while the upper plot (in Figure 6.5) shows the working data (dataset 5) and the validation data in this case dataset 3.

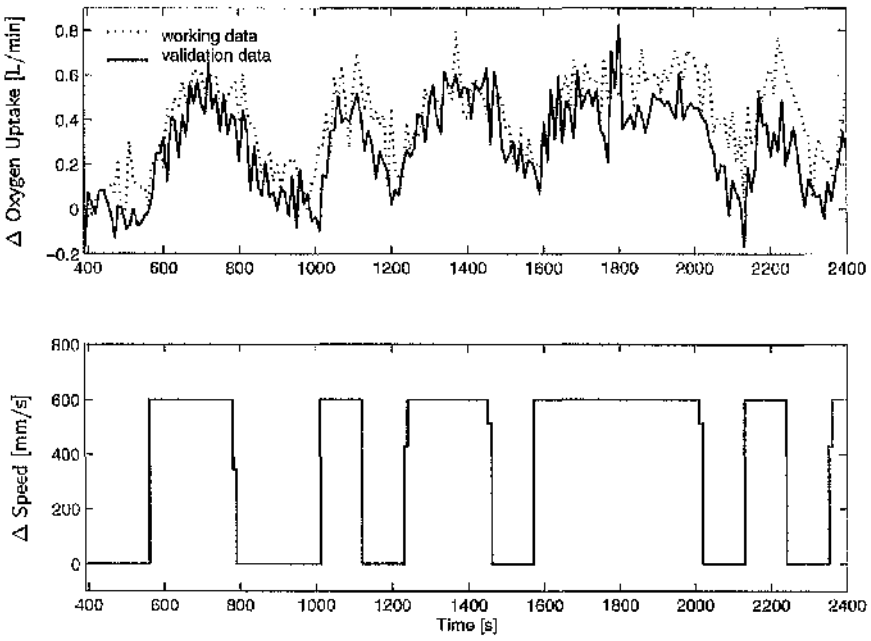

Figure 6.5: A measured validation data set output together with a working data set

Table 6.1 displays the computation results of the average fit for each model structure across all the data sets, i.e., the average of the 20 validation fitness values for each model structure as described in Step 5 of section 6.2.

Table 6.1: The average fit for each model structure

Model Structure	Validation fitness average (%)
arx411	31.87542
arx311	31.20177
arx211	30.57192
arx112	29.75688
arx111	29.11408
arx312	29.01054
arx113	28.66231
arx413	28.56549
arx412	28.06044
arx114	27.81300
arx313	27.57544
arx212	27.34543
arx213	27.21140
arx214	25.27757
arx414	23.58428
arx314	22.52385

A further analysis showing the average fit for the four entries for each nk =1, nk =2, nk =3 and nk =4 from Table 6.1 is present in Table 6.2.

Table 6.2: Average fit for model structures arranged by model order and time-delay

Model	Fit (%)	Model	Fit (%)	Model	Fit (%)	Model	Fit (%)
arx411	31.87542	arx412	28.06044	arx413	28.56549	arx414	23.58428
arx311	31.20177	arx312	29.01053	arx313	27.57544	arx314	22.52386
arx211	30.57192	arx212	27.34543	arx213	27.21140	arx214	25.27757
arx111	29.11408	arx112	29.75688	arx113	28.66232	arx114	27.81300

The average fit for the four entries for delay, nk =1, 2, 3, and 4 is shown in Table 6.3. This Table depicts that as time-delay increases the average fitness decreases.

Table 6.3: The average fit for the model structures as a function of time-delay

Time-delay, nk	Average fitness (%)
1	30.6908
2	28.5433
3	28.0037
4	24.7997

From Table 6.1, the following can be deduced:

- that time-delay, nk =1 delay is the best, since three of the top four models have this delay (see also Table 6.3).
- for the models with delay, nk =1, the fit goes up directly with model order (Table 6.2).

Thus, among the four nk=1 models the choice of arx111 is justified by the fact that it is the simplest (thus leading to the simplest controller order) and by the fact that the fit of the higher order model is no more than 2.8%, which is only a small improvement (i.e. arx411 fitness 31.88% compared with arx111 whose fitness is 29.11%).

Having selected the arx111 structure (a first order model), there remain five possible parameter sets for this model structure depending on the dataset that is used for estimation (see Step 8, section 6.2).

Table 6.4 displays the average fit for each arx111 model estimated from each dataset (each average model fit is the mean of the four validation fit values).

Table 6.4: Comparisons between the different estimation datasets based on the average model fit for arx111

Estimation Dataset	arx111 model average fitness (%)
Dataset 5	34.8288
Dataset 2	34.1303
Dataset 1	28.3831
Dataset 3	25.7574
Dataset 4	22.4708

From Table 6.4 the arx111 estimated from datasets 5 has the best fit (i.e., the arx111 is estimated from dataset 5 and validated on datasets 1, 2, 3, and 4), and was used for the nominal model (section 6.2, Step 9). It has the following parameters:

$A(q^{-1}) = 1 - 0.8097\ q^{-1}$
$B(q^{-1}) = 0.0002019\ q^{-1}$

open-loop rise time = 100s
open-loop settling time = 190s
time-delay = 10s

This model is the only model used throughout the $\dot{V}O_2$ controller designs. Thus, the designed controllers are obtained from the identification with only one subject, and are used unchanged with all subjects in closed-loop tests.

6.3 Oxygen Uptake Control

Here the feasibility of $\dot{V}O_2$ control is investigated by first designing a controller, which was tested on eight subjects. The results of the closed-loop test are then presented.

6.3.1 Controller Design

In this section we adopted the controller design method described in section 3.2.2 on page 43. The $\dot{V}O_2$ closed-loop structure is represented schematically by the block diagram shown in Figure 6.6. The controller is computed by specifying the following design parameters:

rise time = 100s

zeta = 0.999

observer rise-time = 30s

observer zeta = 1

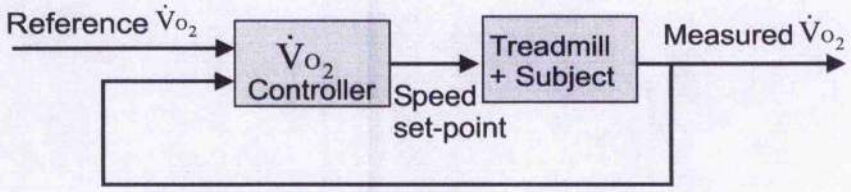

Figure 6.6: $\dot{V}O_2$ Closed-Loop Structure

6.3.2 Feedback Control Results

The RST controller parameters obtained from the specifications (section 6.3.1) using our controller algorithm described in section 3.2.2 are:

$$R(q^{-1}) = 1.0000 - 1.2243\ q^{-1} + 0.2243\ q^{-2}$$

$$S(q^{-1}) = 1174.8 - 931.1\ q^{-1}$$

$$T(q^{-1}) = 371.5493 - 127.8701\ q^{-1}$$

The result of the control was simulated on the computer before real-time implementation. In addition, the sensitivities functions (given by eqns. 3.16 and 3.17 on page 47) were also plotted.

Furthermore, the results of the Feedback Control Tests (on page 99) with this controller for each subject using a sequence of square wave profile are presented in Figures 6.7 - 6.14.

In these Figures, the $\dot{V}O_2$ response profile plot has the reference $\dot{V}O_2$ signal in dotted line, the nominal closed-loop $\dot{V}O_2$ response in dashed line and the measured $\dot{V}O_2$ in solid line, while the plot of the Treadmill Speed has the measured speed in solid line and the controller output in dotted line.

Subject 1

The result of closed-loop tracking test is presented in Figure 6.7. In this Figure, a square-wave reference profile described in section 6.1.3 is used as reference signal (represented as dotted line), the designed controller (is the dashed line) and the $\dot{V}O_2$ closed-loop response (solid line) tracks this reference signal, and follows the designed controller closely. The corresponding treadmill speed (actual speed in solid line) as computed automatically by the controller using measurement of $\dot{V}O_2$ is shown in Figure 6.7(b).

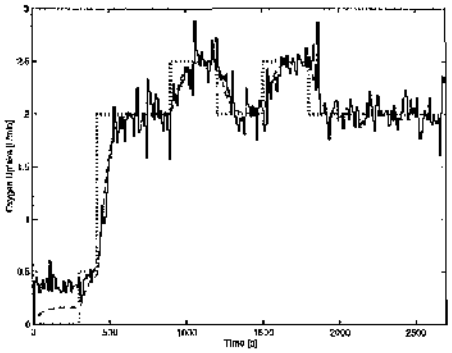

(a) $\dot{V}O_2$ response profile

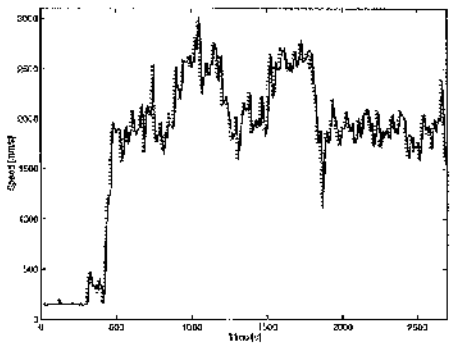

(b) Treadmill Speed

Figure 6.7: Control results for subject 1

Subsequent Figures show similar results reproduced in other subjects using the same controller during closed-loop tests.

Subject 2

The tracking result of the desired $\dot{V}O_2$ by the measured $\dot{V}O_2$ is displayed in Figure 6.8.

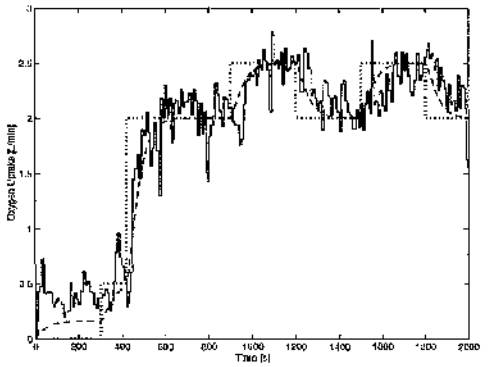

(a) $\dot{V}O_2$ response profile (reference $\dot{V}O_2$ signal in dotted line, nominal closed-loop $\dot{V}O_2$ response in dashed line and measured $\dot{V}O_2$ in solid line)

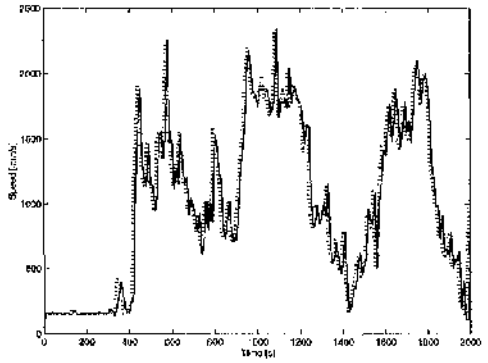

(b) Treadmill Speed (measured speed in solid line and the controller output in dotted line)

Figure 6.8: Control results for subject 2

The treadmill speed measured in Figure 6.8(b) corresponds to the measured $\dot{V}O_2$ response in Figure 6.8(a). This subject was at some point jogging on the spot as is evidence in Figure 6.8(b). This occurs at approximately 1000mm/s (3.6Km/hr) and below.

Subject 3

The model for the controller is based on this subject (Subject 3). Thus, the closed-loop result (Figure 6.9) is expected to be very good for the subject (i.e., tracks the reference $\dot{V}O_2$ profile closely).

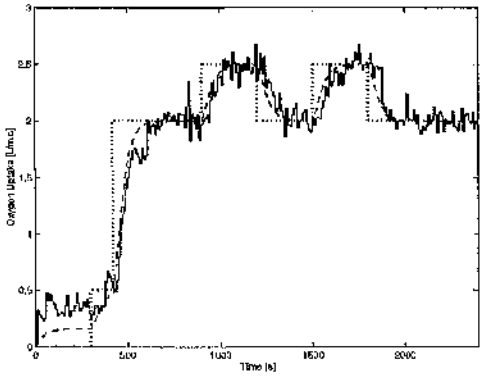

(a) $\dot{V}O_2$ response profile

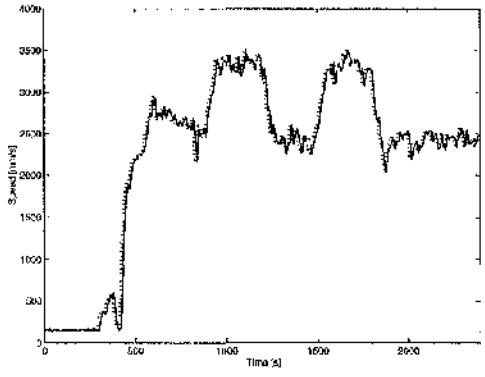

(b) Treadmill Speed

Figure 6.9: Control results for subject 3

With this subject, the treadmill speed (control signal) is smoother than Subjects 1 and 2 (Figures 6.7(b) and 6.8(b)) all with the same $\dot{V}O_2$ reference level profile. These three subjects have different running speed.

Subject 4

The feedback control test result for Subject 4 is shown in Figure 6.10. This subject occasionally sprint at certain periods, which is evident at approximately 910s, 1100s and 1500s (see Figure 6.10(b)).

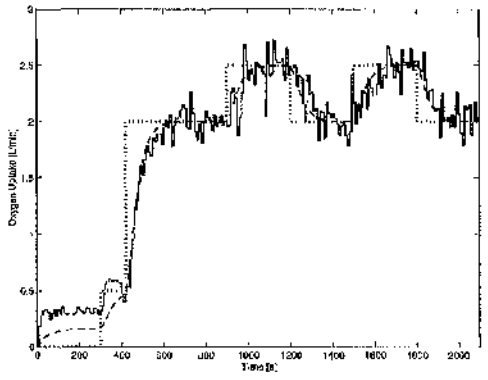

(a) $\dot{V}O_2$ response profile

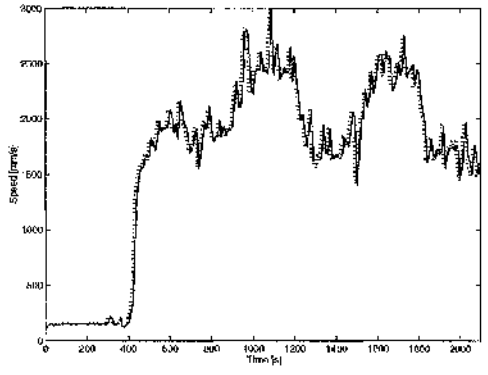

(b) Treadmill Speed

Figure 6.10: Control results for subject 4

Subject 5

This subject ran at speeds corresponding to $\dot{V}O_2$ levels which ranges from 2.5L/min - 3.0L/min as compared with previous subjects (Subjects 1, 2, 3 and 4). Nevertheless, the controller still tracked the $\dot{V}O_2$ reference profile satisfactorily as it can be seen in Figure 6.11.

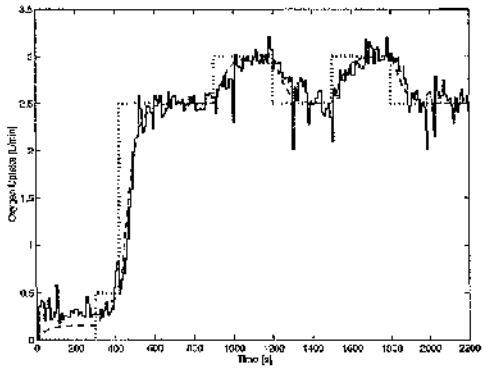

(a) $\dot{V}O_2$ response profile

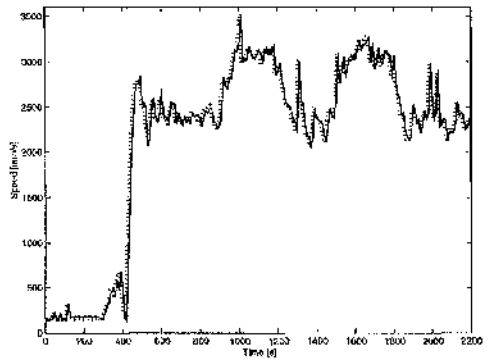

(b) Treadmill Speed

Figure 6.11: Control results for subject 5

Subject 6

At 840s the sampling line became disconnected and was immediately fixed hence the sharp fall in $\dot{V}O_2$ at that point. Furthermore, at 1380s the $\dot{V}O_2$ response became faulty hence the sharp drop in $\dot{V}O_2$ which continues for some few seconds and resulted in stopping the experiment at 1500s for the safety of the subject (Figure 6.12(a)). During the period the device was communicating properly, the feasibility of the controller was proven (see Figure 6.12). The $\dot{V}O_2$ levels are set at 1.5L/min and 2.0L/min because the subject's fitness and health cannot sustain $\dot{V}O_2$ levels higher than this for moderate exercise.

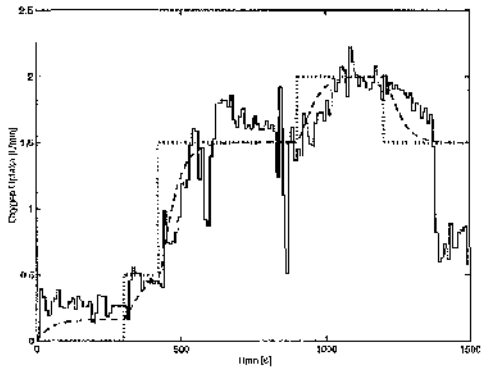

(a) $\dot{V}O_2$ response profile

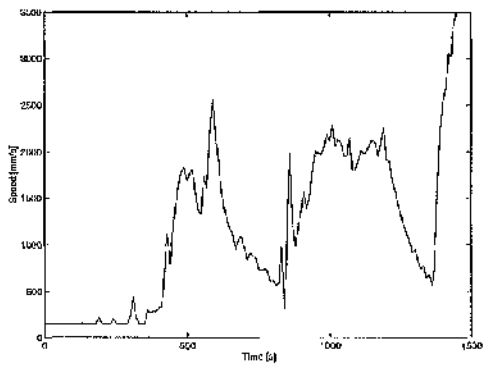

(b) Treadmill Speed

Figure 6.12: Control results for subject 6

Subject 7

This subject's $\dot{V}O_2$ reference level is between 2.5L/min and 3.0L/min. Even at this level, the feasibility of $\dot{V}O_2$ control was achieved as illustrated in Figure 6.13.

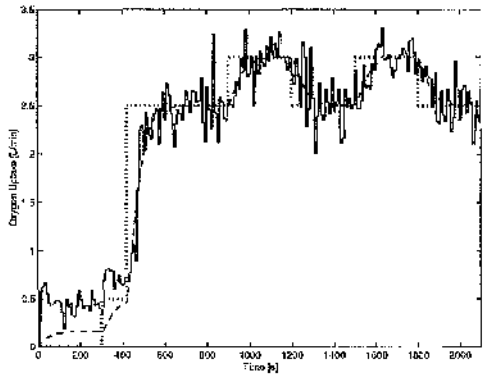

(a) $\dot{V}O_2$ response profile

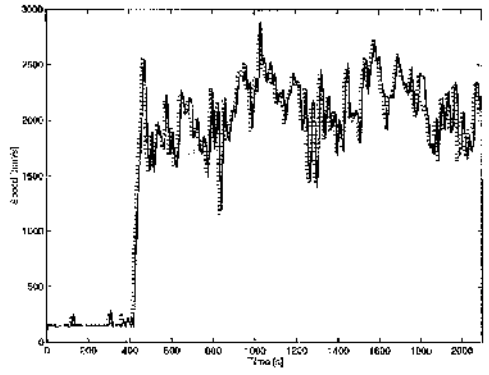

(b) Treadmill Speed

Figure 6.13: Control results for subject 7

This subject at every level of $\dot{V}O_2$ walked and ran intermittently (see Figure 6.13(b)) despite our asking him to jog when it is inconvenient for him to run. However, the $\dot{V}O_2$ response Figure 6.13(a) was not compromised.

Subject 8

This experiment was stopped due to increasing HR which exceeded 165bpm (85% of subject's maximal HR). For the HR to continue to increase and exceed 165bpm, the exercise level for this subject might not be moderate. Thus, the result for this subject (shown in Figure 6.14) is inconclusive, and deductions on the performance of the control on this subject cannot be concluded.

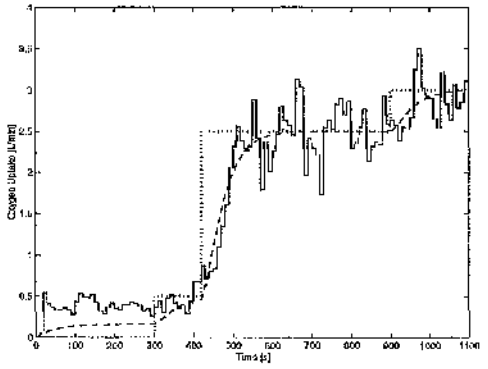

(a) $\dot{V}O_2$ response profile

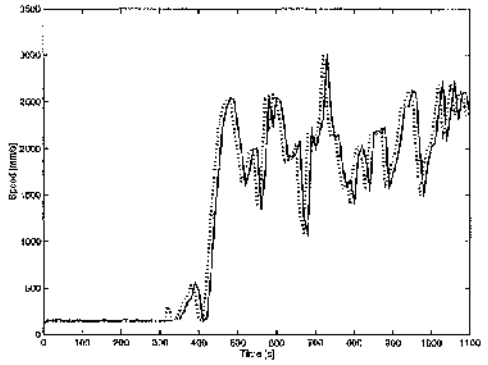

(b) Treadmill Speed

Figure 6.14: Control results for subject 8

From the open loop familiarization test for this subject, there was no stability of $\dot{V}O_2$ at the two speed levels (2400m/s = 8.6Km/hr and 2550mm/s = 9.2Km/hr) which the

subject feels comfortable to run. This two levels were also very close based on the subject's fitness, and thus the signal to noise ratio is affected. Hence, lowering the $\dot{V}O_2$ levels may not solve this situation. Thus for this subject, the most probable way to test the controller is by using a constant $\dot{V}O_2$ level as reference signal.

6.3.3 Discussion

These results demonstrate that $\dot{V}O_2$ control is feasible. Examining all these results, it can be observed that the control signal is "too aggressive", i.e. speed command too active/noisy. Possible improvement includes tuning the closed-loop rise time, increasing the sampling time from 10s to say 20s, changing the observer rise-time or introducing a pre-filter in the control system.

6.4 Effects of Slower Closed-loop Rise-time

Here we examined the effect of tuning the closed-loop rise-time by changing the rise time from 100s in the previous controller to 200s.

6.4.1 Controller Design

The effects of slower closed-loop rise-time will be considered by using the following closed-loop parameters:

rise time = 200s

zeta = 0.999

observer rise-time = 30s

observer zeta = 1

6.4.2 Feedback Control Results

The following are the RST controller parameters for the specification given in section 6.4.1:

$$R(q^{-1}) = 1.0000 - 1.3087\ q^{-1} + 0.3087\ q^{-2}$$

$$S(q^{-1}) = 345.5657 - 274.5408\ q^{-1}$$

$$T(q^{-1}) = 108.2951 - 37.2702\ q^{-1}$$

The experiments on the effect of slow closed-loop rise-time controller is reported in this section. Figures 6.15 and 6.16 show the results of the closed-loop reference tests performed by two of the previous subjects.

In these Figures, the $\dot{V}O_2$ response profile plot has the $\dot{V}O_2$ reference signal in dotted line, the nominal closed-loop $\dot{V}O_2$ response in dashed line and the measured $\dot{V}O_2$ in solid line, while the plot of the Treadmill Speed has the measured speed in solid line and the controller output in dotted line.

Subject 1

The result in Figure 6.15 shows improvement on the previous result for this subject (Figure 6.7) when we compare the treadmill speed (control signal) results. As expected, the response time for the $\dot{V}O_2$ closed-loop tracking is slower. In Figure 6.15(a) the dotted line is the reference profile, the dashed line is the designed $\dot{V}O_2$ response and the solid line is the $\dot{V}O_2$ closed-loop response.

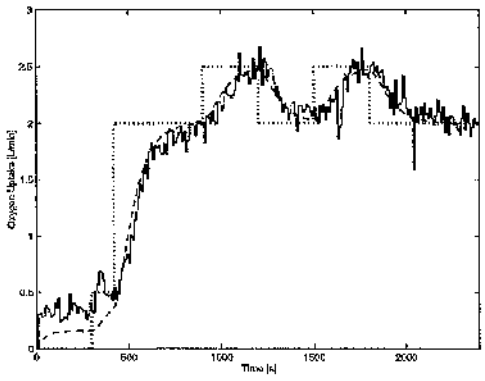

(a) $\dot{V}O_2$ response profile

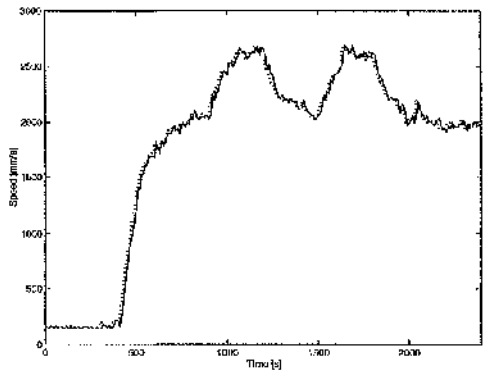

(b) Treadmill Speed

Figure 6.15: Control results for subject 1 using a slower controller

At approximately 2040s, the subject lost concentration and slipped slightly, hence the $\dot{V}O_2$ spike at that point.

Subject 3

Similar result in terms of a smoother treadmill speed achieved for Subject 1 in Figure 6.15 is confirmed by the result for Subject 3 and is shown in Figure 6.16.

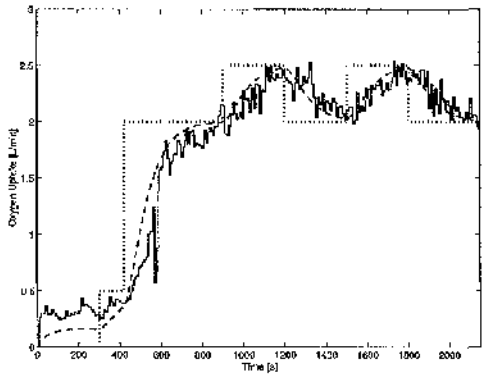

(a) $\dot{V}O_2$ response profile

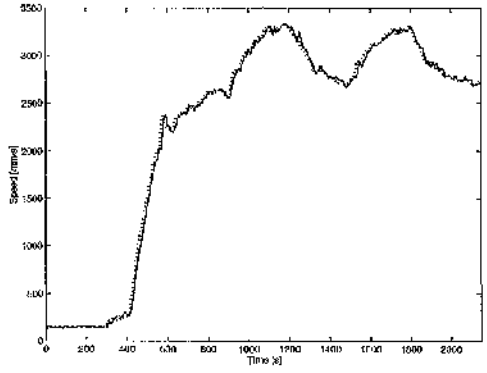

(b) Treadmill Speed

Figure 6.16: Control results for subject 3 using a slower controller

At approximately 540s, the sampling line became disconnected and was immediately fixed, hence the $\dot{V}O_2$ outlier at that time.

6.4.3 Discussion

The results in this section show a good speed command and slow $\dot{V}O_2$ response when compared with the controller results in section 6.3. Note that the number of subjects that took part in this experiment was limited to two so as to prove the feasibility of the approach. Thereafter, it was decided to extend the improvement on the control results by making further modifications.

To further improve on the results in this section, a pre-filter will be designed and incorporated in the reference signal in addition to using the closed-loop rise time of 200s. The aim of this is to improve the slow $\dot{V}O_2$ response while taking advantage of the good speed command.

6.5 Effects of using Pre-filter on Reference Signal

This section investigates the effect of using a controller with a pre-filter (section 3.2.2 on page 46). The section consists of the controller design specifications and parameters, and the results of using the controller. A brief discussion on the results of this controller follows the presentation of the feedback control results.

6.5.1 Controller Design

The effects of using pre-filter (a discrete filter described by eqns. 3.13, 3.14 and 3.15 on page 46) will be investigated with the following specified design parameters:

rise time = 200s

zeta = 0.999

observer rise-time = 30s

observer zeta = 1

pre-filter rise time = 100s

pre-filter zeta = 0.999

6.5.2 Feedback Control Results

The following are the RST controller parameters for the specification given in section 6.5.1:

$R(q^{-1}) = 1.0000 - 1.3087\ q^{-1} + 0.3087\ q^{-2}$

$S(q^{-1}) = 345.5657 - 274.5408\ q^{-1}$

$T(q^{-1}) = 108.2951 - 37.2702\ q^{-1}$

$dF(q^{-1}) = 1 - 1.4526\ q^{-1} + 0.5276\ q^{-2}$

$nF(q^{-1}) = 3.4309 - 5.8480\ q^{-1} + 2.4921\ q^{-2}$

where nF is the numerator and dF is the denominator of the digital filter.

In Figures 6.17 - 6.22, we present the results of the closed-loop feedback control tests using a pre-filter to improve the performance of $\dot{V}O_2$ response time while also maintaining the good speed command (as in section 6.4.2). This approach is tested with six subjects.

In these Figures, the $\dot{V}O_2$ response profile plot has the reference $\dot{V}O_2$ signal in dotted line, the nominal closed-loop $\dot{V}O_2$ response in dashed line and the measured $\dot{V}O_2$ in solid line, while the plot of the Treadmill Speed has the measured speed in solid line and the controller output in dotted line.

Subject 1

Figure 6.17 shows that a good response time and smooth treadmill speed signal can be achieved by using a prefilter incorporated into the $\dot{V}O_2$ control system. In the Figure, the dotted line is the reference $\dot{V}O_2$ profile, the dashed line is the designed $\dot{V}O_2$ response while the solid lines is the closed-loop $\dot{V}O_2$ response.

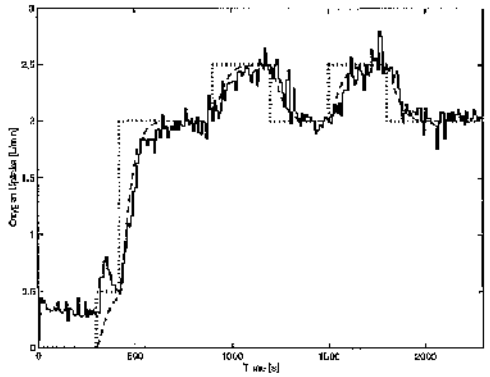

(a) $\dot{V}O_2$ response profile

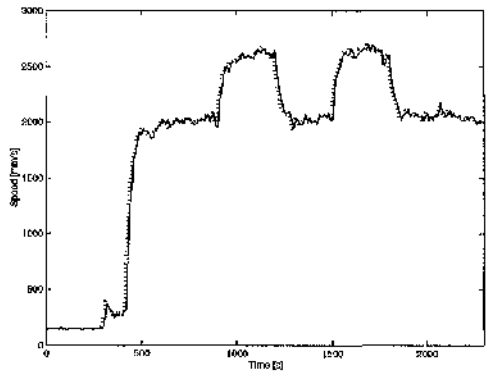

(b) Treadmill Speed

Figure 6.17: Results of a controller with a pre-filter tested on subject 1

Subject 2

For Subject 2, the results of the controller with a prefilter control test is reproduced in Figure 6.18 (dotted line represents the reference signal, solid line is the $\dot{V}O_2$ response, while the dashed line is the designed controller response).

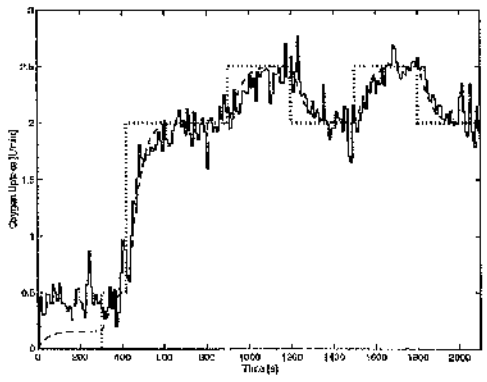

(a) $\dot{V}O_2$ response profile

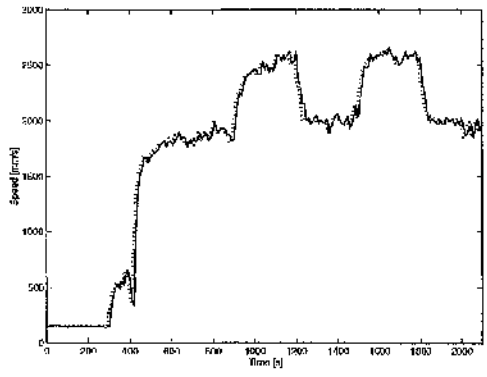

(b) Treadmill Speed

Figure 6.18: Results of a controller with a pre-filter tested on subject 2

The treadmill speed signal result shows a significant improvement when compared with a similar test with the same subject but using a different controller (i.e. compared with Figure 6.8).

Subject 3

As in previous experimental results, the result shown in Figure 6.19 is for Subject 3, using the same controller and set-up as previously.

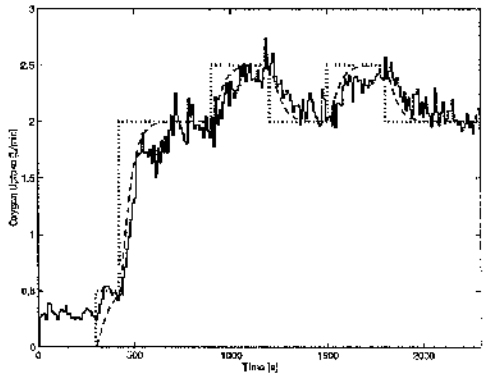

(a) $\dot{V}O_2$ response profile

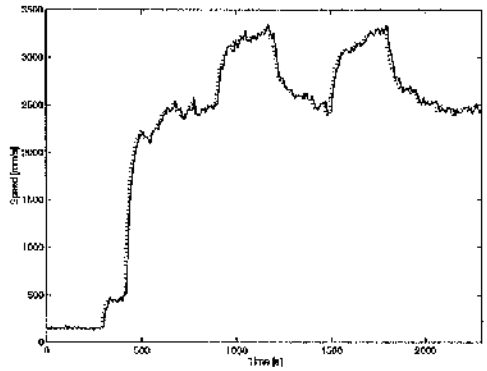

(b) Treadmill Speed

Figure 6.19: Results of a controller with a pre-filter tested on subject 3

Subject 4

The result of $\dot{V}O_2$ closed-loop experiment for Subject 4 is presented in Figure 6.20.

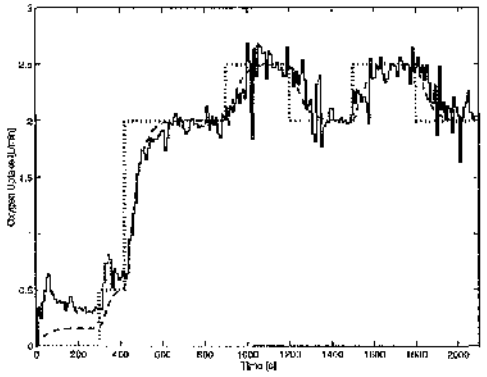

(a) $\dot{V}O_2$ response profile

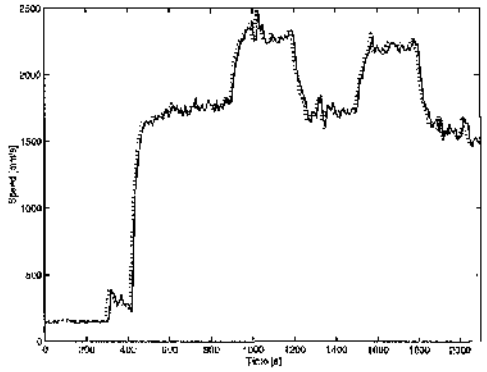

(b) Treadmill Speed

Figure 6.20: Results of a controller with a pre-filter tested on subject 4

The subject informed us that at a point in time he felt like blowing his nose because of a blockage. This may have resulted in one of the spikes during the experiment.

Subject 5 could not perform this test because he was not available in the country. Subject 6 was excluded from this set of $\dot{V}O_2$ control test in order to ensure the safety of the subject.

Subject 7

Figure 6.21 shows the $\dot{V}O_2$ closed-loop test tracking results for Subject 7. This subject was jogging throughout the experiment.

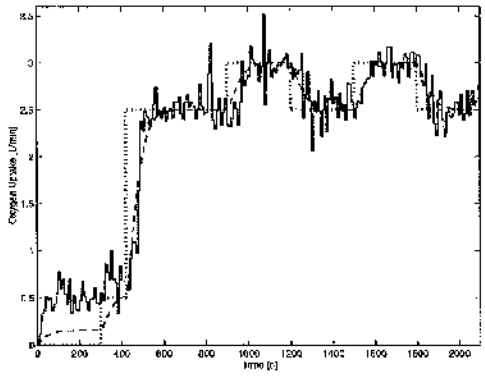

(a) $\dot{V}O_2$ response profile

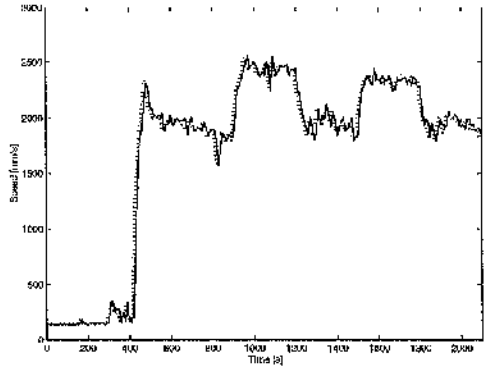

(b) Treadmill Speed

Figure 6.21: Results of a controller with a pre-filter tested on subject 7

Subject 8 was excluded from this set of $\dot{V}O_2$ control test in order to ensure the safety of the subject.

Subject 9

Figure 6.22 is the result of the $\dot{V}O_2$ closed-loop test for Subject 9. Unfortunately, the subject did not participate in the previous closed-loop tests. However, the $\dot{V}O_2$ tracking response and the command signal (treadmill speed) are very good. The results also compares favourably with other subjects' results presented in this section.

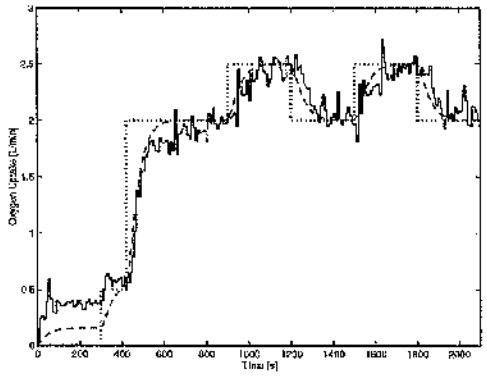

(a) $\dot{V}O_2$ response profile

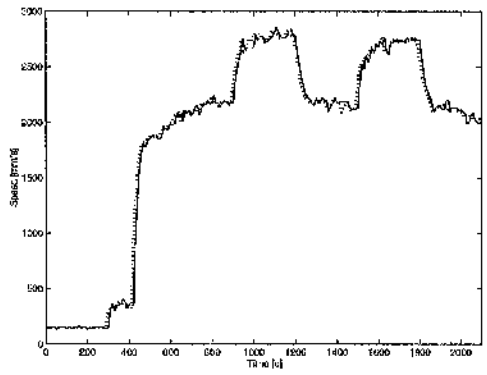

(b) Treadmill Speed

Figure 6.22: Results of a controller with a pre-filter tested on subject 9

6.5.3 Discussion

The results presented here are consistent with the results presented in sections 6.3.2 and 6.4.2 which showed that controlling $\dot{V}O_2$ during exercise can be achieved.

The results in this section confirm the expectation that introducing a pre-filter (with a rise-time of 100s) in the reference signal in addition to using previous slow closed-loop rise-time (of 200s) will improve the performance of the $\dot{V}O_2$ response time and also give a good speed command.

Subject 5 could not take part in this experiment because he was out of the country. Subjects 6 and 8 were excluded from participating in this experiment because we had to stop the previous experiment they participated in (see Figure 6.12 and Figure 6.14) due to health and safety reasons (i.e., exceeding 85% of subject's maximal HR). However, the two subjects still wanted to participate in the experiment. Subject 9 did not take part in any of the previous control experiments because of personal reasons, although he enrolled to participate in all the experiments.

The summary of feedback control tests performed by each subject is depicted in Table 6.5. Here Test 1, Test 2 and Test 3 results are presented in sections 6.3.2, 6.4.2 and 6.5.2 respectively.

Table 6.5: Summary of feedback control tests by subjects

Subjects	Test 1	Test 2	Test 3	$\dot{V}O_2$ range (L/min)
1	x	x	x	2.0 - 2.5
2	x		x	2.0 - 2.5
3	x	x	x	2.0 - 2.5
4	x		x	2.0 - 2.5
5	x			2.5 - 3.0
6	x			1.5 - 2.0
7	x		x	2.5 - 3.0
8	x			2.5 - 3.0
9			x	2.0 - 2.5

6.6 Discussion on Control of Oxygen Uptake

Most of the computerised gas exchange and monitoring devices measure the physiological variables (including $\dot{V}O_2$) on a breath-by-breath basis [11]. The use of the breath-by-breath method introduces noise into the measurement due to the coupling effects of each breath. Cautero et al [17] in their study identified the sources of such errors and tested some algorithms for estimating breath-by-breath alveolar gas exchange. It is worth mentioning that most physiologists process B-by-B data off-line. However, for a real-time control of $\dot{V}O_2$ a discrete sampling time is required, and to achieve this, the breath-by-breath data must be obtained in a fixed sampling interval.

Furthermore, a B-by-B method introduces random errors because of the variability of each breath. Subsequently, a conversion of B-by-B data to a fixed sampling time increases these errors because of the inherent difficulty to decouple and isolate each breath accurately in a fixed interval. To reduce the effect of noise and these errors, and the effect of variability of breath, an algorithm that processes data in real-term is utilised.

The feedback control tracking results presented in this chapter (sections 6.3.2, 6.4.2 and 6.5.2) are processed using the mean filter algorithm discussed in section 6.1.4. In the closed-loop results presented in this chapter, it could be observed that in the first 300s, the actual $\dot{V}O_2$ value is approximately the resting value, while between 300s to 420s represents the warm-up $\dot{V}O_2$ values which we preset as 0.5L/min and which the controller uses to automatically determine which speed the subject should run. For the resting value, the desired $\dot{V}O_2$ is at 0L/min, i.e. the controller is passive during this period. Since $\dot{V}O_2$ is measured in real-time, the effect of irregularity of each breath and the noise from the system, even though these signals have been processed by an algorithm, is still evident as the spikes in the results. A more complex algorithm could be used to deal with these spikes/outliers.

Preliminary observation indicates that when a fraction of inspired O_2, dry F_IO_2 becomes 0% and F_ICO_2 becomes 30% or when the preceding and subsequent breathing frequency is significantly different the spike occurs. Ideally, F_IO_2 should be 20.93% and F_ICO_2 should be 0.03%. Thus at some breaths, F_IO_2 becomes 0% and F_ICO_2 becomes 30% which is a misnomer. Furthermore, $\dot{V}O_2$ is obtained from the subtraction of F_IO_2 and $\dot{V}_I$ components from F_EO_2 and $\dot{V}_E$ components. Thus, if both F_IO_2 and $\dot{V}_I$ components are erroneous, then the spike will be substantial, assuming the other components (such as F_EO_2 and $\dot{V}_E$) are normal and correct.

More thorough investigation shows that if either F_IO_2 or F_EO_2 or $\dot{V}_I$ or $\dot{V}_T$ or breathing frequency are incorrectly measured then the spikes in $\dot{V}O_2$ become significant. In addition, if these measurements are within a tolerable magnitude when compared with the preceding and subsequent breaths, then the changes are insignificant. Moreover, a great variance in breathing frequency can also lead to problems. Similarly, if the time inspired is greater than time expired, then this shows that the subject coughed, which the MetaMax device may not take into consideration. Hence, these problems represent limitations of the hardware (MetaMax device), and the fact that operations are in real time.

The possible limitations in using $\dot{V}O_2$ for real time control include the inherent delay in sampling from the exhaled breath and transient time of blood from the locomotor muscle to the lungs. Wasserman et al [106] estimated a delay of approximately 15 seconds (depending on the step magnitude of the exercise) for a normal $\dot{V}O_2$ response to exercise work-rate at moderate exercise, and that $\dot{V}O_2$ reaches a steady state at 180s (which compares with the open-loop settling time reported on page 107). However, these limitations did not present a fundamental limitation for the control of $\dot{V}O_2$ as presented in this investigation. This is because our model explicitly includes dynamic delay and thus captures accurately the $\dot{V}O_2$ dynamics. Furthermore, the $\dot{V}O_2$ controller results are not affected by changes in blood volume or body temperature during exercise which can alter heart rate. In addition, stress and anxiety cannot influence $\dot{V}O_2$ although this is more important for heart rate when at a low work rate (below 120bpm) [56]. Therefore, the $\dot{V}O_2$ feedback control results (sections 6.3.2, 6.4.2 and 6.5.2) demonstrate that automatic control of $\dot{V}O_2$ during moderate treadmill exercise is achievable.

It is important to state that during treadmill exercise, it is always difficult to impose a far greater accuracy on a work rate profile than can be achieved on a cycle ergometer because of the effect of mode changes and runner's strategy. To this end each subject was asked to run throughout the experiment to avoid the transition speed between walking and running. In addition, the subjects participated in familiarisation trials for about 15 - 30 minutes. This allows the subjects to get used to the mask and the treadmill, and to obtain the elicited $\dot{V}O_2$ at those running speeds with which the subjects are comfortable. The familiarisation trials also provided the $\dot{V}O_2$ within which the subjects will be able to run and not walk, and thus avoid mode changes. This method is adopted instead of subjecting our subjects to experiments that will determine their Running Speed Lactate Threshold and $\dot{V}O_{2_{max}}$. Nevertheless, this did not eliminate the subject's instinct to change his/her running style because we cannot constrain his/her running.

The effect of increasing the rise time (to 200s) is evident in Figure 6.15(b) and Figure 6.16(b). These Figures show smoother speed signals than the experiments when the rise time is 100s. However, as expected, it compromises the responses of the closed-loop

$\dot{V}O_2$ results (Figures 6.15(a) and 6.16(a)).

The effect of using a pre-filter is apparent in the results presented in section 6.5.2. The Figures in that section show that the smoother control signals in section 6.4.2 are still maintained, while also achieving the $\dot{V}O_2$ response results of using a rise-time of 100s presented in Figures 6.7 - Figures 6.14 for the subjects. The results also show that the controller with this pre-filter has the advantage of producing a smoother control action with less fluctuation in the change of speed of subjects.

The effect of breath variability and noise can be seen in Table 6.1, where the percentage of model fitness is generally low. Nevertheless, the results of model identification show that a first order transfer function (in Table 6.4) is able to accurately model the $\dot{V}O_2$ – speed dynamics. This confirms earlier publications which demonstrated that a linear model can be appropriate for modelling cardio-respiratory dynamics [67], [112].

Furthermore, the closed-loop controller based on the identified linear model provides a good tracking performance for $\dot{V}O_2$ even though random B-by-B spikes are still evident in the closed-loop response (Figures 6.7 - Figures 6.14) despite the use of our algorithm. Similarly, the Figures show that the designed controller result (in dashed-line) and the real-time controller result implemented on our subject (and shown in solid line) is very good. In addition, the treadmill actual speed signal follows closely the control speed. Although the Figures still show that the effect of B-by-B has been significantly reduced, it has not been eliminated.

It was also observed that as the sampling time is increased, the effect of variability and noise on $\dot{V}O_2$ measurements is reduced. This confirms other publications on the effect of sampling time on B-by-B measurements [82], [46], [58]. However, no conclusion has been reached on an optimum sampling time when using commercially available B-by-B systems.

Throughout each test reported in sections 6.3.2, 6.4.2 and 6.5.2, a single fixed controller

is tested in each section with healthy subjects. That is, the model and controller is tuned for only one subject, yet control is good for all subjects. The results of each controller used for each section validates the robustness of the controller. For both Sections 6.3.2 and 6.5.2 the controllers were tested with at least five subjects.

Some subjects could not complete the specified $\dot{V}O_2$ profile because the amplitude changes on $\dot{V}O_2$ for such subjects are limited (i.e., for the subjects to run comfortably at the two different $\dot{V}O_2$ levels). For such subjects, their transition from walking/fast walking to running occurs at very close speed (i.e., 8.6 km/hr (2.40m/s) and 9.2 km/hr (2.55m/s)). Thus, the second $\dot{V}O_2$ level (which should be at least 0.5L/min above the first level) may be above the subject's lactate threshold. This could be seen in a subject's HR response which continuously increased to above 85% of the subject's maximal HR. It can be postulated that this may be due to the subject's long stride length and weight. Hence the changes in amplitude between 8.6 km/hr and 9.2 km/hr may not elicit a reasonable $\dot{V}O_2$ change that may be significant enough for a controller test using a step profile $\dot{V}O_2$ load. However, a constant $\dot{V}O_2$ load can be tested for such a subject. If the first $\dot{V}O_2$ level was lowered, the subject may be in the vicinity of walking which would affect the performance of the controller. In addition, running skills, economy and efficiency based on the person's weight, stride length, stride cadence and fitness might be important.

The idea that the differences between the two sets of $\dot{V}O_2$ levels should be at least 0.5L/min is to avoid the effect of signal-to-noise ratio based on the variability and noise corruption caused by B-by-B effects in $\dot{V}O_2$ measurements.

Further evidence of a strong coupling between control of $\dot{V}O_2$ and control of HR was observed as expected (i.e., HR response pattern follows $\dot{V}O_2$ response profile during all the experiments on the control of $\dot{V}O_2$). In addition, it was found that during automatic control of $\dot{V}O_2$, $\dot{V}_E$ follows the same pattern as the reference tracking profile. This suggests that $\dot{V}_E$ can be automatically controlled during exercise (treadmill exercise).

The identification of a suitable $\dot{V}O_2$ model requires considerable effort and time. The most plausible explanation for this is the complex nature of the dynamics of $\dot{V}O_2$ (non-linearity and variability of $\dot{V}O_2$). However, in this study, it was impossible to use a first order model to capture the dynamics of $\dot{V}O_2$ during moderate treadmill exercise.

The control of $\dot{V}O_2$ brings a novel ideal that exercise intensity can be specified as percentages of LT (which has an associated $\dot{V}O_2$) or $\dot{V}O_{2_{max}}$, since LT or $\dot{V}O_{2_{max}}$ are descriptor of exercise tolerance. In addition, LT is regularly used to guide exercise prescription.

Another application of this $\dot{V}O_2$ control system is that it could be used for prescribing work rates for elite athletes who may be required to train at a very specific exercise intensity.

The control of $\dot{V}O_2$ using real-time B-by-B measurement may not always be practicable. The alternative is to use open-loop control, i.e., pre-specifying the map from speed – $\dot{V}O_2$ profile obtained from open-loop testing, and implementing this as a look-up table with interpolation. However, this alternative method will not be robust enough to cater for the effect of disturbances.

It is possible to use the results to control exercise intensity without regular need to use the real-time B-by-B apparatus during every exercise session. This could be achieved for a given subject by using the HR and $\dot{V}O_2$ relationship in the regions where this relationship is linear for the subject. However, a routine re-calibration using this apparatus and control set-up would be needed from time to time so as to calibrate this relationship due to changes that may have occurred because of the subject's fitness level or detraining effects.

Furthermore, the $\dot{V}O_2$ is limited to running at moderate treadmill exercise levels (exercising below the lactate threshold). Notwithstanding, this method could be conceptually applied to other exercise modes, i.e., cycle ergometry (where the control signal will be the work-rate/load at a given cadence).

6.7 Conclusions

Tracking performance for $\dot{V}O_2$ is accurate and satisfactory, and the results of the experimental tests for the first time proved that controlling $\dot{V}O_2$ during a treadmill exercise and indeed any exercise, is feasible and possible. It can be concluded that the controller incorporating a pre-filter is the most appropriate to achieve a smooth control signal without degrading the response time based on our results.

These controllers reported in this chapter are obtained from identification with only one subject (Subject 3), and the identified model is used unchanged with all subjects in closed-loop tests.

Furthermore, the various control tests performed by normal healthy subjects have established the robustness of the controller to inter-subject variability, and have shown that a precise and unambiguous $\dot{V}O_2$ control can be achieved.

Based on the success of this work, this approach is being developed to be incorporated and implemented within our research programme which is investigating exercise, fitness and health benefits of FES cycling with paraplegic subjects [52].

The findings in this chapter may also provide a conceptual frame-work for understanding $\dot{V}O_2$ control in real-time domain.

Thus, the major contributions of this chapter are:

1. Contribution to the description of linear models for $\dot{V}O_2$.
2. The use of a system identification method to obtain a model useful for $\dot{V}O_2$ control.
3. The model identification and validation approach is novel in comparison to the treatment of $\dot{V}O_2$ kinetics/dynamics in the exercise physiology literature.

4. Finally, the developed $\dot{V}O_2$ controller can precisely regulate $\dot{V}O_2$ and thus exercise intensity.

Future application of the $\dot{V}O_2$ feedback control system may:

1. Open the possibility of the development of optimal exercise and therapy regimes during primary rehabilitation and in long-term exercise usage for fitness and health.
2. Be beneficial for human performance training (to prescribe optimal exercise regimes for elite athletes who may be required to train at a very specific exercise intensity).
3. Serve as a means for determining $\dot{V}O_{2_{max}}$ (by ramping $\dot{V}O_2$ input in a pre-specified fashion).

7 GENERAL DISCUSSION, CONCLUSIONS AND OUTLOOK

In this chapter, the general overview of the research work carried out and the contribution of this work are discussed. An outlook of possible researches in the light of the experimental results and findings presented in preceding chapters are highlighted.

7.1 General Discussion

This thesis focuses on a new approach to treadmill automation and physiological control systems. It will serve as a platform for enhanced rehabilitation therapy.

Firstly, the idea that a low-cost non-contact treadmill positioning system can be used as a platform to improve safety, enhance a patient's feeling of well-being, and reduce the load on staff during treadmill rehabilitation therapy are explored. The investigation study was carried out using healthy subjects, and the results of this study reveal fundamental limitations (time delays, bandwidth limitation, etc.) which could not be resolved. This could be improved by using a faster (higher performance) treadmill. These technical limitations affect the speed of response and also the accuracy of the system in real-time experiments. However, the tracking result of the speed controller implemented with subjects running on the treadmill was satisfactory. Furthermore, the robustness and disturbance rejection of the speed controller was good.

Due to the close interplay between mobility training and a subject's physiological status,

and because treadmill training may also provide secondary beneficial effects on cardiopulmonary fitness, investigation into a new approach to control physiological variables, HR and $\dot{V}O_2$, during treadmill exercise training was studied. Empirically determined linear models for the dynamics of these variables were obtained for normal healthy subjects. The models proved to be a simple representation of the variables considered and was useful for controlling these variables.

The results obtained from HR control indicate that our controller can provide a fixed level of HR that is independent of respiration rate. This HR controller is versatile and could be used for routine exercise. Furthermore, the designed and developed HR controller is an improvement on the in-built treadmill HR controller. One shortcoming of HR control is that a subject with an irregular heart beat may be overloaded during exercise, and this may be dangerous to the health of the subject.

The results of $\dot{V}O_2$ feedback control tests demonstrate that exercise intensity can be controlled below the lactate threshold level (moderate or comfortable exercise level) which is very significant for maximizing the work rate that disabled and impaired subjects (and even normal subjects) can perform, and thus prolong the exercise period. Exercising at this level is regarded as a safe and effective level for exercise training. Furthermore, the results of the study with healthy subjects are very compelling and consistent. The controller with a pre-filter (and a slower closed-loop rise-time) enables the comfortability of subjects during exercise, as compared with the controller with a faster closed-loop rise-time (and without a pre-filter) that occasionally resulted in the subject sprinting at certain times.

It was observed that posture changes can alter $\dot{V}O_2$ and HR sharply. It was also noticed that $\dot{V}O_2$ variability at rest is lower than during walking. Furthermore, $\dot{V}O_2$ variability depends on individual subject's movement on the moving treadmill, and probably on the subject's cadence.

The main reason for the development of an averaging algorithm which is used in the

control of $\dot{V}O_2$ study is that control requires regularly-spaced samples in real-time. In addition to this, the variability in B-by-B measurement is also a factor. The $\dot{V}O_2$ data was averaged every 10s and then used for control purposes. However, the data averaging approach did not significantly alter $\dot{V}O_2$ control. Nevertheless, this could be a weakness of the present study since other averaging intervals may produce different values that can prove superior. However, the 10s averaging is a reasonable compromise to achieve a good speed of controller response. In addition, sample time is largely dictated by response dynamics, and desired closed-loop response time. Furthermore, large averaging intervals may produce too a long delay in $\dot{V}O_2$ response time.

7.2 Conclusions

The conclusion is listed in the form of contributions to knowledge, and it follows the order of the chapters in this thesis.

- In chapter 1 the primary contribution is the introduction of the research work and the scope of work, while chapter 2 discusses the background to the work and relevant literature.
- Chapter 3 describes the materials and methods. Based on the experimental set-up described in section 3.1 and the general methodology described in section 3.2, we investigated treadmill automation and physiological control systems.
- Chapter 4 provides an understanding of treadmill position control and its limitations. While a satisfactory automatic speed control was achieved, the effects of low bandwidth and high time delays affected the performance of the treadmill automation system. A higher performance treadmill could change this. Furthermore, there is interaction between natural human control and our position controller during experiments.
- The contribution of chapter 5 includes designing an HR controller, improving on HR control by increasing the speed/time of response while maintaining small tracking and steady state errors when compared with an in-built treadmill HR control.

- Chapter 6 presents a novel study which demonstrates that accurate control of $\dot{V}O_2$ during treadmill exercise is achievable. The results of this work provide significant original contributions in the control of $\dot{V}O_2$, thus extending the application of control theory into physiological systems.

- Finally, this research work is a translational feasibility study that could be deployed, applied and developed into potential therapies in rehabilitation and clinical sciences, and also in advanced physiological control studies.

7.3 Outlook

A brief list of recommendations for further study based on ideas generated from the result of this thesis are presented here.

The limitations in achieving treadmill automation may provide directions for future research in this area.

The focus has been only on adjusting the treadmill speed alone, and it is hoped that future work could consider/focus on investigating $\dot{V}O_2$ and IIR control using both treadmill speed and elevation (gradient).

Further research is also needed to remove and eliminate spikes or outliers in $\dot{V}O_2$ such that it will filter out coughs and abnormal breaths in real-time to remove this problem which is common with B-by-B measurement. One possible suggestion which could be useful is an adaptive filter or algorithm that predicts subsequent breaths and thus identifies breath and other outliers.

The possibility of using local linear models (multiple model approach) could be used such that different linear models can be developed for walking, transition between walking to running, and running such that a fully automated $\dot{V}O_2$ system can be developed that will switch control for different movement modes.

A control of $\dot{V}O_2$ using breath-by-breath time course in lieu of a fixed sampling time would be an interesting study. This implies that the control will be dynamic to follow the time course of breath variability.

Finally, an isolation and accumulation detector that applies appropriate algorithm should be incorporated into the system so as to cut-off the input to the system when there is danger (i.e. a failure of the devise to measure the desired variable correctly) is required for safety purpose.

Bibliography

[1] R. Abel, M. Schablowski, R. Rupp, and H. J. Gerner. Gait analysis on the treadmill - Monitoring exercise in the treatment of paraplegia. *Spinal Cord*, 40(1):17–22, 2002.

[2] O. O. Ajayi, L. Jamieson, K. J. Hunt, and H. Gollee. Treadmill automation and physiological control systems. In *Proc IEEE EMBSS PC Conf.*, pages 39–40, 2004.

[3] R. M. Alexander. *Exploring Biomechanics: Animals in Motion.* Scientific American Library, New York, 1992.

[4] C. D. Ashley, P. Bishop, J. F. Smith, P. Reneau, and C. Perkins. Menstrual phase effects on fat and carbohydrate oxidation during prolonged exercise in active females. *J. Exerc. Physiol.*, 3(4):67 – 73, 2000.

[5] T. A. Astorino, R. A. Robergs, F. Ghiasvand, D. Marks, and S. Burns. Incidence of the oxygen plateau at $\dot{V}O_{2_{max}}$ during exercise testing to volitional fatigue. *J. Exerc. Physiol. online*, 3(4):1–12, 2000.

[6] P-O. Astrand and K. Rodahl. *Textbook of work physiology: Physiological bases of exercise.* McGraw-Hill, New York, 1977.

[7] K. J. Åström and B. Wittenmark. *Computer-Controlled Systems: Theory and Design.* Prentice Hall, London, 1997.

[8] H. Barbeau, M. Ladouceur, K. E. Norman, A. Pepin, and A. Leroux. Walking after spinal cord injury: Evaluation, treatment, and functional recovery. *Arch. Phys. Med. Rehabil.*, 80(2):225–235, 1999.

[9] T. J. Barstow and P. A. Mole. Linear and nonlinear characteristics of oxygen uptake kinetics during heavy exercise. *J. Appl. Physiol.*, 71(6):2099–2106, 1991.

[10] D. R. Bassett and E. T. Howley. Limiting factors for maximum oxygen uptake and determinants of endurance performance. *Med. Sci. Sports Exerc.*, 32(1):70–84, 2000.

[11] W. L. Beaver, K. Wasserman, and B. J. Whipp. On-line computer analysis and breath-by-breath graphical display of exercise function tests. *J. Appl. Physiol.*, 34(1):128–132, 1973.

[12] W. L. Beaver, K. Wasserman, and B. J. Whipp. Improved detection of lactate threshold during exercise using a log-log transformation. *J. Appl. Physiol.*, 59(6):1936–1940, 1985.

[13] W. L. Beaver, K. Wasserman, and B. J. Whipp. A new method for detecting anaerobic threshold by gas exchange. *J. Appl. Physiol.*, 60(6):2020 2027, 1986.

[14] V. L. Billat, L. Mille-Hamard, B. Petit, and J. P. Koralsztein. The role of cadence on the $\dot{V}O_2$ slow component in cycling and running in triatheletes. *Int. J. Sports Med.*, 20(7):429–437, 1999.

[15] T. Busso, P. Liang, and P. A. Robbins. Breath-to-breath relationships between respiratory cycle variables in humans at fixed end-tidal PCO_2 and PO_2. *J. Appl. Physiol.*, 81(5):2287–2296, 1996.

[16] B. Caruana-Montaldo, K. Gleeson, and C. W. Zwillich. The control of breathing in clinical practice. *Chest*, 117(1):205–225, 2000.

[17] M. Cautero, P. E. di Prampero, and C. Capeli. New acquisitions in the assessment of breath-by-breath alveolar gas transfer in humans. *Eur. J. Appl. Physiol.*, 90:231–241, 2003.

[18] S. Cavalcanti and E. Belardinelli. Modeling of cardiovascular variability using a differential delay equation. *IEEE Trans. Biomed. Eng.*, 43(10):982–989, 1996.

[19] P. R. Cavanagh and R. Kram. Stride Length in Distance Running: Velocity, body dimensions, and added mass effects. *Med. Sci. Sports Exerc.*, 21(4):467–479, 1989.

[20] Y. H. Chang, H. W. Huang, C. M. Hamerski, and R. Kram. The independent effects of gravity and inertia on running mechanics. *Journal of Experimental Biology*, 203:229–238, 2000.

[21] R. Christensen, J. M. Hollerbach, Y. Xu, and S. Meek. Inertial force feedback for a locomotion interface. In *Proc. ASME Dynamic Systems and Control Division, DSC-Vol. 64*, pages 119–126, 1998.

[22] R. R. Christensen, J. M. Hollerbach, Y. Xu, and S. G. Meek. Inertial-force feedback for the treadport locomotion interface. *Presence*, 9(1):1–14, 2000.

[23] G. Colombo, M. Joerg, R. Schreier, and V. Dietz. Treadmill training of paraplegic patients using a robotic orthosis. *Journal of Rehabilitation Research and Development*, 37(6):693–700, 2000.

[24] A. Danielsson and K.S. Sunnerhagen. Oxygen consumption during treadmill walking with and without body weight support in patients with hemiparesis after stroke and in healthy subjects. *Arch. Phys. Med. Rehabil.*, 81(7):953–957, 2000.

[25] R. P. Darken, W. R. Cockayne, and D. Carmein. The omni-directional treadmill: A locomotion device for virtual worlds. In *Proc. UIST Conf.*, pages 213–221, Alberta, Canada, 1997.

[26] V. Dietz, G. Colombo, L. Jensen, and L. Baumgartner. Locomotor capacity of spinal cord in paraplegia subjects. *Ann. Neurol.*, 37(5):574–582, 1995.

[27] R. C. Dorf and J. L. Unmack. A comparison of two models of the human heart rate control system. In *Proc. of the 18th Annual Conference on Engineering in Medicine and Biology*, Philadelphia, 1965.

[28] R. C. Dorf and J. L. Unmack. A time domain model of the heart rate control system. In *Proc. of the 5th Annual San Diego Symposium for Biomedical Engineering*, pages 43–47, San Diego, 1965.

[29] F. Cottin F, C. Medigue, P. M. Lepretre, Y. Papelier, J. P. Koralsztein, and V. Billat. Heart rate variability during exercise performed below and above ventilatory threshold. *IEEE Trans. Biomed. Eng.*, 36(4):594–600, 2004.

[30] F. Felici, M. Bernardi, A. Rodio, P. Marchettoni, V. Castellano, and A. Macaluso. Rehabilitation of walking for paraplegic patients by means of a treadmill. *Spinal Cord*, 35(6):383–385, 1997.

[31] E. C. Field-Fote. Combined use of body weight support, functional electric stimulation, and treadmill training to improve walking ability in individuals with chronic incomplete spinal cord injury. *Arch. Phys. Med. Rehabil.*, 82(6):818–824, 2001.

[32] J. L. Fleg, I. L. Pina, G. J. Balady, B. R. Chaitman, C. Lavie B. Fletcher, M. C. Limacher, R. A. Stein, M. Williams, and T. Bazzarre. Assessment of functional capacity in clinical and research applications. *Circulation*, 102(13):1591–1597, 2000.

[33] M. Folke, L. Cernerud, M. Ekstrom, and B. Hok. Critical review of non-invasive respiratory monitoring in medical care. *Med. Biol. Eng. Comput.*, 41(4):377–383, 2003.

[34] Y. Fukuba, K. Hara, Y. Kimura, A. Takahashi, S.A. Ward, and B.J. Whipp. Estimating the parameters of aerobic function during exercise using an exponentially increasing work rate protocol. *Med. Biol. Eng. Comput.*, 38(4):433–437, 2000.

[35] F. Gazzani, M. Bernardi, A. Macaluso, D. Coratella, J. F. Ditunno, V. Castellano, M. Torre, V. Macellari, and M. Marchetti. Rehabilitation of walking for paraplegic patients by means of a treadmill. *Spinal Cord*, 37:336–344, 1999.

[36] D. S. Goldstein, R. S. Ross., and J. V. Brady. Biofeedback heart rate training during exercise. *Biofeedback and self-regulation*, 2(2):107–125, 1977.

[37] L. L. Hamilton and O. Lindan. Development of a servo controlled tiltboard using heart rate or blood pressure as feedback controllers. In *Proc. Annual Clinical Spinal Cord Injury Conf.*, number 15, pages 36–43, 1966.

[38] J. P. Hasler, N. J. Postans, D. J. Maxwell, D. B. Allen, and M. H. Granat. Functional electrical stimulation augmented treadmill training for incomplete spinal cord injured patients - a pilot study. In *Proc. 1st FESnet Conf.*, pages 47–49, 2002.

[39] J. Hayano, F. Yasuma, A. Okada, S. Mukai, and T. Fujinami. Respiratory sinus arrhythmia: A phenomenon improving pulmonary gas exchange and circulatory efficiency. *Circulation*, 94(4):842–847, 1996.

[40] N. C. Heglund and C. R. Taylor. Speed, stride frequency and energy cost per stride: How do they change with body size and gait? *J. Exp. Biol.*, 138:301–318, 1988.

[41] S. Hesse, C. Bernet, M. T. Jahnke, A. Schaffrin, P. Baake, M. Malezic, and K. H. Mauritz. Treadmill training with partial body weight support compared with physiotherapy in nonambulatory patients. *Stroke*, 26:976–981, 1995.

[42] S. Hesse, M. Konrad, and D. Uhlenbrock. Treadmill walking with partial body weight support versus floor walking in hemiparetic subjects. *Arch. Phys Med Rehabil*, 80:421–427, 1999.

[43] S. Hesse, C. Werner, A. Bardeleben, and H. Barbeau. Body weight-supported treadmill training after stroke. *Curr. Atheroscler Rep.*, 3:287–294, 2001.

[44] S. A. Hesse, C. Bertelt, A. Schaffrin, and K. H. Mauritz. Restoration of gait in nonambulatory hemiparetic patient by treadmill training with partial body-weight support. *Arch. Phys. Med. Rehabil.*, 75:1087–1093, 1994.

[45] S. A. Hesse, M. Malezic, A. Schaffrin, and K. H. Mauritz. Restoration of gait by combined treadmill training and multichannel electrical stimulation in non-ambulatory hemiparetic patients. *Scand. J. Rehabilitation Med.*, 27:199–204, 1995.

[46] D. W. Hill, L. P. Stephens, S. A. Blumoff-Ross, D. C. Poole, and J. C. Smith. Effect of sampling strategy on measures of $\dot{V}O_{2peak}$ obtained using commercial breath-by-breath systems. *Eur. J. Appl. Physiol.*, 89(6):564–569, 2003.

[47] J. M. Hollerbach. Locomotion interfaces. In K. M. Stanney, editor, *Handbook of Virtual Environments Technology: Design, Implementation, and Applications*, pages 239–254. Lawrence Erlbaum Associates, 2002.

[48] J. M. Hollerbach, Y. Xu, R.R. Christensen, and S. C. Jacobsen. Design specification for second generation sarcos treadport locomotion interface. In *Proc. ASME Dynamic Systems and Control Division*, volume 69, pages 1293–1298, 2000.

[49] R. W. Hoyt, J. J. Knapik, J. F. Lanza, and B. H. Jones J. S. Staab. Ambulatory foot contact monitor to estimate metabolic cost of human locomotion. *J. Appl. Physiol.*, 76(4):1818– 1822, 1994.

[50] K. J. Hunt, H. Gollee, R. P. Jaime, and N. D. Donaldson. Design of feedback controllers for paraplegic standing. *IEE Proc. Control Theory Appl.*, 148(2):97–108, 2001.

[51] K. J. Hunt, M. Munih, N. D. Donaldson, and F. M. D. Barr. Optimal Control of Ankle Joint Moment: Towards unsupported standing in paraplegia. *IEEE Trans. Automatic Control*, 43(6):819–832, 1998.

[52] K. J. Hunt, B. Stone, N. Negrad, T. Schauer, M. H. Fraser, A. J. Cathcart, C. Ferrario, S. A. Ward, and S. Grant. Control strategies for integration of electric motor assist and functional electrical stimulation in paraplegic cycling: Utility for exercise testing and mobile cycling. *IEEE Transactions on Neural Systems and Rehabilitation Engineering*, 12(1):89–101, 2004.

[53] D. Imbeau, L. Desjardins, P. C. Dessureault, P. Riel, and R. Fraser. Oxygen consumption during scaffold assembling and disassembling work: Comparison between field measurements and estimation from heart rate. *Int. J. of Industrial Ergonomics*, 15(13):247–259, 1995.

[54] G. F. Inbar, R. Heinze, K. S. Hoekstein, H-D. Liess, K. Stangl, and A. Wirtzfeld. Development of a closed-loop pacemaker controller regulating mixed venous oxygen saturation level. *IEEE trans. on Biomedical Eng.*, 35(9):679–690, 1988.

[55] H. Iwata. Locomotion interface for virtual environments. In J. Hollerbach and D. Koditschek, editors, *Robotics Research: the Ninth International Symposium*, pages 275–282. Springer-Verlag, 2000.

[56] S. Jacobsen and O. Johansen. An ergometer bicycle controlled by heart rate. *Medical & Biological Engineering*, 12:675–680, 1974.

[57] S. L. James and C. E. Brubaker. Running mechanics. *J. of the American Medical Association*, 221(9):1041–1016, 1972.

[58] J. S. Johnson, J. J. C. Varlson, R. L. Vanderlaan, and D. E. Langholz. Effect of sampling interval on peak oxygen consumption in patients evaluated for heart transplantation. *Chest*, 113(3):816–819, 1998.

[59] D. J.Reinkensmeyer, L. E. Kahn, M. Averbuch, A. McKenna-Cole, B. D. Schmit, and W. Z. Rymer. Understanding and treating arm movement impairment after chronic brain injury: Progress with arm guide. *Journal of Rehabilitation Research & Development*, 37(6):653–662, 2000.

[60] T. Kawada, Y. Ikeda, H. Takaki, M. Sugimachi, O. Kawaguchi, T. Shishido, T. Sato, W. Matsuura, H. Miyano, and K. Sunagawa. Development of a servo-controller of heart rate using a cycle ergometer. *Heart Vessels*, 14:177–184, 1999.

[61] T. Kawada, G. Sunagawa, H. Takaki, T. Shishido, H. Miyano, H. Miyashita, T. Sato, M. Sugimachi, and K. Sunagawa. Development of a servo-controller of heart rate using a treadmill. *Japanese Circulation Journal*, 63:945–950, 1999.

[62] M. C. K. Khoo. Determinants of ventilatory instability and variability. *Respiration Physiology*, 122:167–182, 2000.

[63] M. C. K. Khoo. *Physiological Control System: Analysis, Simulation, and Estimation*. IEEE Press, New York, 2000.

[64] O. Kwon and J. H. Park. Gait transitions for walking and running of biped robots. In *Proc. of the IEEE Intl' Conf. on Robotics and Automation*, pages 1350–1355, 2003.

[65] H. Kyrolainen, A. Belli, and P. V. Komi. Biomechanical factors affecting running economy. *Med. Sci. Sports Exerc.*, 33(8):1330–1337, 2001.

[66] M. Ladouceur, A. Pepin, K. E. Norman, and H. Barbeau. Recovery of walking after spinal cord injury. In F. J. Seil, editor, *Advances in Neurology, Vol 72: Neural Regeneration, Reorganization, and Repair*, pages 249–255. Lippincott-Raven Publishers, 1997.

[67] N. Lamarra, B. J. Whipp, M Blumenberg, and K. Wasserman. Model-order estimate of cardiorespiratory dynamics during moderate exercise. In B. J. Whipp and D. N. Wiberg, editors, *Modelling and Control of Breathing*, pages 338–345. Elsevier Science Publishers, 1983.

[68] V. J. Leibetseder, C. Ekmekcioglu, and P. Haber. A simple running test to estimate cardiorespiratory fitness. *J. Exerc. Physiol. online*, 5(3):6–13, 2002.

[69] L. Li and X. Liu. Simulating human walking on special terrain: up and down slopes. *Computer and Graphics*, 24:453–463, 2000.

[70] L. Ljung. *System Identification: Theory for the User*. Prentice Hall, New Jersey, 1999.

[71] J. S. Maritz, J. F. Morrison, J. Peter, N. B. Strydom, and C. H. Wyndham. A practical method of estimating an individual's maximal oxygen intake. *Ergonomics*, 4:97–122, 1961.

[72] P. E. Martin and D. W. Morgan. Biomechanical considerations for economical walking and running. *Med. Sci. Sports Exerc.*, 24:467–474, 1992.

[73] W. D. McArdle, F. I. Katch, and V. L. Katch. *Essential of Exercise Physiology*. Lippincott Williams and Wilkins, Philadelphia, 2000.

[74] J. Mead. Control of respiratory frequency. *J. Appl. Physiol.*, 15(3):325–336, 1960.

[75] A. E. Minetti, L. Boldrini, L. Brusamolin, P. Zamparo, and T. McKee. A feedback-controlled treadmill (treadmill-on-demand) and the spontaneous speed of walking and running in humans. *J. Appl. Physiol.*, 95(2):838–843, 2003.

[76] A. E. Minetti, C. Capelli, P. Zamparo, P. E. di Prampero, and F. Saibene. Effects of stride frequency on mechanical power and energy expenditure of walking. *Med. Sci. Sports Exerc.*, 27:1194–1202, 1995.

[77] I. Miyai, Y. Fujimoto, Y. Ueda, H. Yamamoto, S. Nozaki, T. Saito, and J. Kang. Treadmill training with body weight: its effect in parkinson disease. *Arch. Phys. Med. Rehabil.*, 81:849–852, 2000.

[78] M. Modarreszadeh and E. N. Bruce. Ventilatory variability induced by spontaneous variations of $PaCO_2$ in humans. *J. Appl. Physiol.*, 76(6):2765–2775, 1994.

[79] M. Moghaddam and M. Buehler. Control of virtual motion systems. In *Proc. of the IEEE/RSJ Int. Conf. on Intelligent Robots and Systems*, pages 63–67, 1993.

[80] D. Morgan, P. Martin, M. Craib, C. Caruso, R. Clifton, and R. Hopewell. Effect of step length optimization on the aerobic demand of running. *J. Appl. Physiol.*, 77:245–251, 1994.

[81] A. M. Moseley, A. Stark, I. D. Cameron, and A. Pollock. Treadmill training and body weight support for walking after stroke. *Stroke*, 34(12):3006, 2003.

[82] J. Myers, D. Walsh M. Sullivan, and V. Froelicher. Effect of sampling on variability and plateau in oxygen uptake. *J. Appl. Physiol.*, 68(1):404–410, 1990.

[83] T. D. Noakes. *Lore of Running*. Leisure Press, Illinois, 1991.

[84] T. D. Noakes. Maximal oxygen uptake: "classical" versus "contemporary" viewpoints: A rebuttal. *J. Appl. Physiol.*, 30(9):1381–1398, 1998.

[85] H. Noma and T. Miyasato. Design for locomotion interface in a large scale virtual environment. ATLAS: ATR Locomotion Interface for Active Self Motion. In *Proc. ASME Dynamic Systems and Control Division, DSC-Vol. 64*, pages 111–118, 1998.

[86] H. Noma, T. Sugihara, and T. Miyasato. Development of Ground Surface Simulator for Tel-E-Merge System. In *Proc. of IEEE-Virtual Reality 2000 Conference*, pages 217–224, 2000.

[87] T. F. Novacheck. The biomechanics of running. *Gait and Posture*, 7:77–95, 1998.

[88] B. F. Giraldo M. Vallverdu S. Benito G Vazquez P. Caminal, L. Domingo and D Kaplan. Variability analysis of the respiratory volume based on non-linear prediction methods. *Med. Biol. Eng. Comput.*, 42:86 91, 2004.

[89] S. Perrey, R. Candau, J. D. Rouillon, and R. L. Hughson. The effect of prolonged submaximal exercise on gas exchange kinetics and ventilation during heavy exercise in humans. *Eur. J. Appl. Physiol.*, 89:587–594, 2003.

[90] M. Pohl, J. Mehrholz, C. Ritschel, and S. Ruckriem. Speed-dependent treadmill training in ambulatory hemiparetic stroke patients: A randomized controlled trial. *Stroke*, 33:553–558, 2002.

[91] M. L. Pollack, G. A. Gaesser, J. D. Butcher, J. P. Despres, R. K. Dishman, B. A. Franklin, and C. E. Garber. The recommended quantity and quality of exercise for developing and maintaining cardiorespiratory and muscular fitness, and flexibility in healthy adults. *Med. Sci. Sports Exerc.*, 30(6):975–991, 1998.

[92] S. K. Power and E. T. Howley. *Exercise Physiology: Theory & Application to Fitness and Performance*. WCB McGraw-Hill, Boston, 1997.

[93] Daniela Rus and Sanjiv Singh, editors. *Experimental Robotics VII [ISER 2000, Waikiki, Hawaii, USA, December 11-13, 2000]*, volume 271 of *Lecture Notes in Control and Information Sciences*. Springer, 2001.

[94] K. Sada, S. Hamada, Y. Yonezawa, and I. Ninomiya. Self-biofeedback control of heart rate during exercise. *Japanese Journal of Physiology*, 49(6):275–281, 1999.

[95] T. Sasaki, K. Tsunoda, and I. Kato. Method of Estimation of $\dot{V}O_2$ from HR using Mathematical Model. In *Japan Intersociety Conference: The Integrative Biology of Exercise*, 1996.

[96] M. R. Schindl, C. Forstner, H. Kern, and S. Hesse. Treadmill training with partial body weight support in nonambulatory patients with cerebral palsy. *Arch. Phys Med Rehabil*, 81:301–306, 2000.

[97] A. W. Schindler, T. W. L. Scheeren, O. Picker, M. Doehn, and J. Tarnow. Accuracy of feedback-controlled oxygen delivery into a closed anaesthesia circuit for measurement of oxygen consumption. *British Journal of Anaesthesia*, 90(3):281–290, 2003.

[98] T. J. Sieber, C. W. Frei, M. Derighetti, P. Feigenwinter, D. Leibundgut, and A. M. Zbinden. Model-based automatic feedback control versus human control of end-tidal isoflurane concentration using low-flow anaesthesia. *British Journal of Anaesthesia*, 85(6):818–825, 2000.

[99] K. S. Stadler, D. Leibundgut, R. Wessendorf, A. H. Glattfelder, and A. M. Zbinden. Automatic feedback control of mechanical ventilation during general anaesthesia: A model-based approach. In *IFMBE Proc.*, volume 3, pages 1602–1603, 2002.

[100] A. Stefanovska and M. Bracic. Reconstructing cardiovascular dynamics. *Control Engineering Practice*, 7:161–172, 1999.

[101] K. Svedahl and B. R. MacIntosh. Anaerobic threshold: The concept and methods of measurement. *Canadian J. Appl. Physiol.*, 28(2):299–323, 2003.

[102] C. R. Taylor, N. C. Heglund, T. A. McMahon, and T. R. Looney. Energetic cost of generating muscular force during running. *J. Exp. Biol.*, 86:9–18, 1980.

[103] D. F. Treacher and R. M. Leach. ABC of Oxygen: Oxygen transport - Basic principles. *BMJ*, 317(7168):1302–1306, 1998.

[104] E. Varraine, M. Bonnard, and J. Pailhous. Intentional on-line adaptation of stride length in human walking. *Exp. Brain Res.*, 130:248–257, 2000.

[105] M. Visintin, H. Barbeau, N. Korner-Bitensky, and N.E. Mayo. A new approach to retrain gait in stroke patients through body weight support and treadmill stimulation. *Stroke*, 29:1122–1128, 1998.

[106] K. Wasserman, J. E. Hansen, D. Y. Sue, R. Casaburi, and B. J. Whipp. *Principles of exercise testing and interpretation.* Lippincott Williams & Wilkins, Philadelphia, 1999.

[107] K. Wasserman and B. J. Whipp. Exercise physiology in health and disease. *Am. Rev. Respir. Dis.*, 112(2):219–249, 1975.

[108] K. Wasserman, B. J. Whipp, S. N. Koyal, and W. L. Beaver. Anaerobic threshold and respiratory gas exchange during exercise. *J. Appl. Physiol.*, 35:236–243, 1973.

[109] J. P. Weir, S. Koerner, J. Masek, D. Vanderhoff, and B. C. Heiderscheit. Plateau detection in cycle ergometry. *J. Exerc. Physiol.*, 7(2):55–62, 2004.

[110] P. G. Weyand, M. Kelly, T. Blackadar, J. C. Darley, S. R. Oliver, N. E. Ohlenbusch, S. W. Joffe, and R. W. Hoyt. Ambulatory estimates of maximal aerobic power from foot-ground contact times and heart rates in running humans. *J. Appl. Physiol.*, 91:451–458, 2001.

[111] B. J. Whipp. Dynamics of pulmonary gas exchange. *Circulation*, 76:19–28, 1987.

[112] B. J. Whipp and S. A. Ward. Pulmonary gas exchange kinetics during exercise: Physiological inferences of model order and parameters. *Int. Journal of Sport Medicine*, 1:146–159, 1980.

[113] B. J. Whipp, S. A. Ward, N. Lamarra, J. A. Davis, and K. Wasserman. Parameters of ventilatory and gas exchange dynamics during exercise. *J. Appl. Physiol.*, 52:1506–1513, 1982.

[114] B. J. Whipp and K. Wasserman. Oxygen uptake kinetics for various intensities of constant-load work. *J. Appl. Physiol.*, 33:351–356, 1972.

[115] J. E. Whitney and L. Solomon. Respiration-rate signal extraction from heart rate. In *Proc. of SPIE*, pages 104–112, 2001.

[116] S. J. Wickler, D. F. Hoyt, E. A. Cogger, and G. Myers. The energetics of the trot-gallop transition. *Journal of Experimental Biology*, 206:1557–1564, 2003.

[117] C. A. Williams and P. Lopes. The influence of ventilatory control on heart rate variability in children. *J. Sports Sci.*, 20(5):407–415, 2002.

[118] K. Williams and P. Cavanagh. Relationship between distance running mechanics, running economy, and performance. *J. Appl. Physiol.*, 63:1236–1245, 1987.

[119] K. R. Williams. Biomechanics of running. In R. L. Terjung, editor, *Exercise and Sport Science Reviews*, pages 389–442. Mac Millian Publishing, 1985.

[120] M. Yamamoto, K. Tanabe, K. Ohmiya, T. Iwasaki, H. Ito, M. Murayam, J. Sugai, and N. Toyofuku. Development of computer software in ramp slope controller for treadmill ergometer. *Japan of Cardiology*, 22:687, 1992.

[121] H. Yano, H. Noma, H. Iwata, and T. Miyasato. Shared walk environment using locomotion interface. In *Proc. of ACM CSCW 2000*, pages 163–170, 2000.